CHALMERS
UNIVERSITY OF TECHNOLOGY

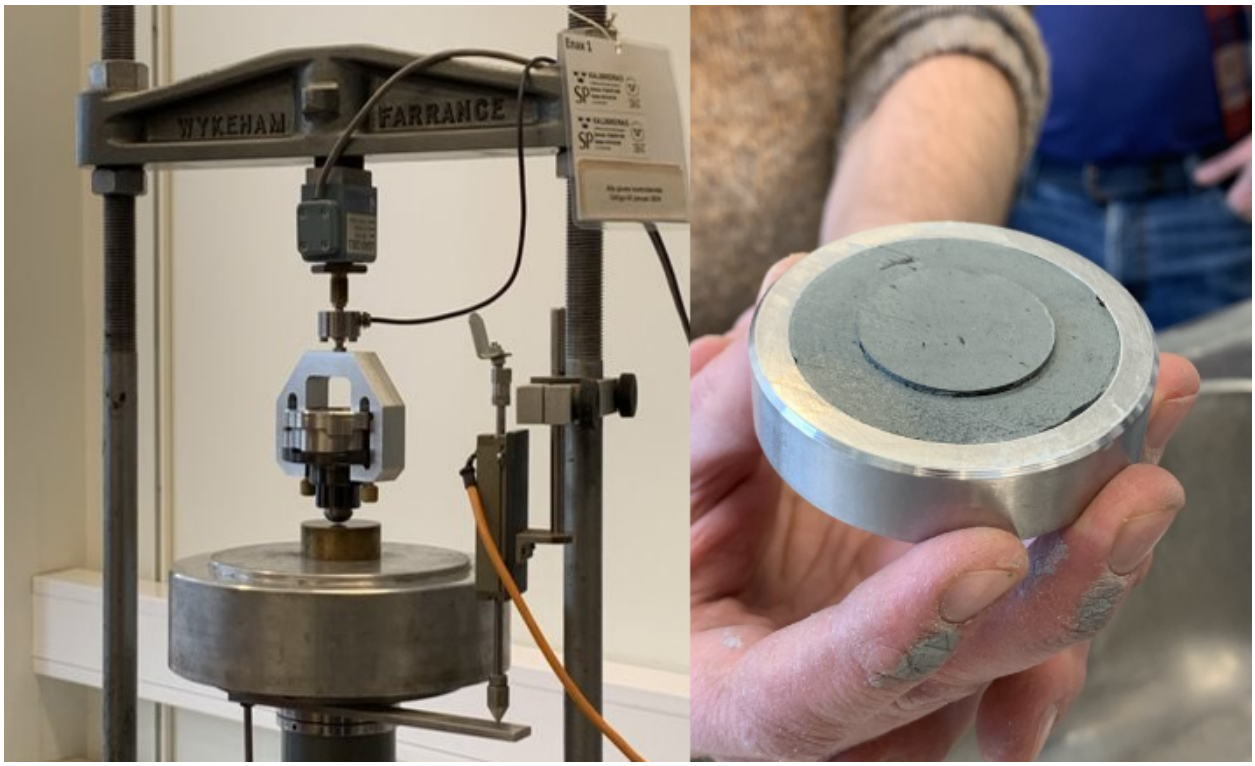

Evaluation of the Shear Punching Test

A comparative analysis with fall-cone and direct simple shear test

Master's thesis in Infrastructure and Environmental Engineering

EVELINA HALL & ELLEN LINDEBY

DEPARTMENT OF ARCHITECTURE AND CIVIL ENGINEERING
CHALMERS UNIVERSITY OF TECHNOLOGY
Gothenburg, Sweden 2024
www.chalmers.se

Master's thesis 2024

Evaluation of the Shear Punching Test

A comparative analysis with the fall-cone and direct simple shear test

EVELINA HALL & ELLEN LINDEBY

CHALMERS
UNIVERSITY OF TECHNOLOGY

Department of Architecture and Civil Engineering
Division of Geology and Geotechnics
Chalmers University of Technology
Gothenburg, Sweden 2024

Evaluation of the Shear Punching Test
A comparative analysis with the fall-cone and direct simple shear test
EVELINA HALL & ELLEN LINDEBY

Supervisor: Arthur Jedenius, Awer Sverige AB
Supervisor: Mats Karlsson, Department of Architecture and Civil Engineering
Examiner: Mats Karlsson, Department of Architecture and Civil Engineering
Laboratory expertise: Martin Holmén & Rickard Kalén, SGI

Master's Thesis 2024
Department of Architecture and Civil Engineering
Division of Gelogy and Geotechnics
Chalmers University of Technology
SE-412 96 Gothenburg
Telephone +46 31 772 1000

Cover: The shear punching apparatus at SGI's laboratory (left) and a recently examined sample (right).

Typeset in LaTeX
Printed by Chalmers Reproservice
Gothenburg, Sweden 2024

Evaluation of the Shear Punching Test
A comparative analysis with the fall-cone and direct simple shear tests
EVELINA HALL & ELLEN LINDEBY
Department of Architecture and Civil Engineering
Chalmers University of Technology

Abstract

Between the years 2019 and 2023, SGI developed a new method to assess the undrained shear strength in cohesive soils. The new test, named the shear punching test, is developed to possibly replace or compliment existing test methods, particularly the fall-cone test. The fall-cone test, which is an index test for evaluating the shear strength of soil, is based on empirical analyses. This makes it challenging to derive mathematically and often underestimates the results. A method similar to the shear punching test was devised by Bror Fellenius 1935. Although the results were considered promising at the time, the method came to nothing.

This thesis aims to investigate the potential of the shear punching test to become a standardized test in geotechnical investigations by analyzing the correlation between the shear punching test, fall-cone test and direct simple shear test (DSS). This is achieved by conducting a literature review and analyzing results from soil samples where all relevant methods have been performed. Furthermore a numerical model of the shear punching apparatus is developed using Plaxis 2D, and an in depth stability analysis is conducted on a section from Gamleby Harbor in Västervik using Geostudio SLOPE/W.

The results show that the shear strength that is calibrated to the DSS test aligns reasonably well with empiricism and naturally in relation to the shear strength obtained from DSS tests. The normalized shear strength however, shows a wide spreading within 2 standard deviations as well as a few outliers. Numerical modeling in Plaxis can to some extent recreate results from the laboratory tests. During evaluation of the shear strength trend for the use in stability analysis, the shear punching test leads to an increase in cases where the DSS test is excluded.

In conclusion, the shear punching test cannot be considered a complete replacement for the fall-cone test as an index test, as the sensitivity of the soil cannot be determined. However, it can be used as a complement to other tests for the evaluation of the undrained shear strength in cohesive soils. Due to the scatter in the normalized shear strength, no specific range for certain parameters can be observed where shear punching is relevant or not. It can be concluded that it is possible to recreate the shear punching numerically and obtain results that reasonably align with laboratory results. Including results from the shear punching test in the evaluation of the shear strength trend will only have an effect if more reliable test methods are not included.

Keywords: Shear punching test, shear strength, numerical FE modelling, data analysis, slope stability

Utvärdering av skjuvstansning
En jämförande analys med fallkon- och direkt skjuvförsök
EVELINA HALL & ELLEN LINDEBY
Institutionen för arkitektur och samhällsbyggnadsteknik
Chalmers tekniska högskola

Sammanfattning

Under åren 2019 till 2023 utvecklade SGI en ny metod för att bestämma den odränerade skjuvhållfastheten i kohesionsjordar. Den nya metoden, benämnd skjuvstansning, utvecklas för att kunna ersätta eller kompletera nuvarande metoder, i synnerhet fallkonsförsöket. Fallkonsförsöket, vilket är ett indexförsök för utvärdering av skjuvhållfastheten i jordprover, baseras på empiriska analyser. Detta gör metoden svår att härleda matematiskt, samtidigt som den ofta underskattar resultatet. En metod liknande skjuvstansningen utvecklades år 1935 av Bror Fellenius. Trots att resultaten vid denna tid verkade lovande, rann metoden ut i sanden.

Examensarbetet syftar till att utreda skjuvstansningens potential att bli en standardiserad metod vid geotekniska utredningar genom att analysera korrelationen mellan skjuvstansning, fallkonsförsök och direkta skjuvförsök. Detta uppnås genom en litteraturstudie följt av analys av resultat från jordprover där samtliga relevanta metoder har utförts. Vidare utvecklas en numerisk modell av skjuvstansen i Plaxis 2D, och en fördjupad stabilitetsanalys för en sektion i Gamleby hamn i Västervik genomförs i Geostudio SLOPE/W.

Resultatet visar att skjuvhållfastheten som har kalibrerats med direkt skjuvförsök stämmer någorlunda väl överens med empiri samt naturligt i förhållande till skjuvhållfastheten erhållen från direkta skjuvförsök. Den normaliserade skjuvhållfastheten visar däremot en stor spridning inom intervallet två standardavvikelser med ett fåtal extremvärden. Den numeriska modelleringen i Plaxis kan till viss del återskapa resultat från skjuvstansen i laboratoriet. Vid utvärdering av en skjuvhållfasthetstrend för användning vid stabilitetsanalyser medför skjuvstansingen en ökning i de fall då direkta skjuvförsök utesluts.

Sammanfattningsvis kan skjuvstansning inte helt ersätta fallkonsförsöket som ett indexförsök, eftersom jordens sensitivitet inte kan bestämmas. Den kan däremot komplettera andra tester för att utvärdera den odränerade skjuvhållfastheten i kohesionsjordar. På grund av spridningen i den normaliserades skjuvhållfastheten kan inget specifikt intervall för utvalda parametrar observeras där skjuvstansningen är relevant eller inte. Det kan även konstateras att det är möjligt att återskapa skjuvstansen numeriskt och erhålla resultat som någorlunda sammanfaller med laboratorieresultat. Att inkludera resultat från skjuvstansning vid utvärdering av skjuvhållfasthetstrenden har enbart en effekt om mer pålitliga testmetoder inte inkluderas.

Nyckleord: Skjuvstansning, skjuvhållfasthet, Numerisk FE-modellering, dataanalys, släntstabilitet

Acknowledgements

We would like to start by thanking our supervisor and examiner Mats Karlsson for guidance, interesting thoughts and endless Plaxis support. We would also like to thank our supervisor at Awer Geoteknik, Arthur Jedenius, along with the rest of Awer for interesting discussions, encouragement, and for making us feel like a part of the team. Many thanks to Martin Holmén and Rikard Kalén at SGI for a much appreciated study visit to the laboratory in Linköping, providing us with laboratory data and their expertise in geotechnical laboratory testing. Additional thanks to David Gahara at LabMind for providing us with even more laboratory data from the shear punching test. Finally, we would like to thank Västervik Municipality for making this thesis possible in the first place by allowing the shear punching test to be conducted at Gamleby Harbor.

Evelina Hall & Ellen Lindeby, Gothenburg, June 2024

List of Acronyms

Below is the list of acronyms that have been used throughout this thesis listed in alphabetical order:

CPT	Cone Penetration Test
CRS	Constant Rate of Strain
DSS	Direct Simple Shear Test
FE	Finite Element
FEM	Finite Element Method
IEG	Implementeringskommission för Europastandarder inom Geoteknik
IL	Incremental Loading
MC	Mohr-Coulomb
OCR	Over Consolidation Ratio
POP	Pre-Overburden Pressure
SHANSEP	Stress History And Normalized Soil Engineering Properties
SIS	Swedish Institute for Standards
SGF	Swedish Geotechnical Society
SGI	Swedish Geotechnical Institute
SGU	Geological Survey of Sweden
SPT	Shear punch test
SS	Soft Soil
TK Geo 13	Trafikverkets tekniska krav för geokonstruktioner 13
TOC	Total Organic Carbon

Nomenclature

Below is the nomenclature of parameters that have been used throughout this thesis.

Roman letters

A	Area
A_p	Surface area of the punch
A_r	Reduced area of the shear surface
A_s	Total shear surface area
c	Cohesion
c'	Effective cohesion
c_u/s_u	Undrained shear strength
c_{u-ds}	Undrained shear strength from the DSS test
c_{u-f}	Undrained shear strength from the fall-cone test
$c_{u-f(corr)}$	Undrained shear strength from the fall-cone test corrected with regard to the liquid limit
$c_{f,v}$	Undrained shear strength obtained from field vane shear test
$c_{u,Hansbo}$	Empirical undrained shear strength, Hansbo's formula
$c_{u,r}$	Remoulded shear strength
c_{u-s}	Undrained shear strength from the shear punching test
$c_{u-s(corr)}$	Undrained shear strength from the shear punching test corrected against undrained shear strength from DSS tests
$c_{u-s(corr2)}$	Undrained shear strength from the shear punching test corrected against undrained shear strength from DSS tests with correction equation 2
$c_{u-s(corr3)}$	Undrained shear strength from the shear punching test corrected against undrained shear strength from DSS tests with correction equation 3
$c_{u,SGI}$	Empirical undrained shear strength, SGI's recommendation
e_{int}	Initial void ratio
E_{ref}	Young's modulus

F	Force
G	Shear modulus
g	Gravitational acceleration
i	Cone penetration depth
K	Cone factor
K_0	Lateral earth pressure at rest
K_0^{nc}	Lateral earth pressure ratio in the NC-region
k	Permeability
k_x/k_y	Permeability in x and y direction
M	Critical state line
M'	Modulus number
M_0	Constant constrained modulus below the effective vertical pre-consolidation pressure
M_L	Constant constrained modulus between the stressed σ'_c and σ'_v
n_{int}	Initial porosity
p'	Mean effective stress
p_{excess}	Excess pore pressure
q	Deviatoric stress
q_t	Tip resistance in CPT
R^2	Coefficient of determination
R_{inter}	Strength reduction factor
s'	Mean effective stress
S_t	Sensitivity
$s_{u,ref}$	Reference undrained shear strength
T_{max}	Maximum torque
w_L	Liquid limit
w_N	Water content

Greek letters

β_k	Coefficient of permeability change
γ	Unit weight
γ_{cu}	Partial coefficient used to convert undrained shear strength
γ_M	Partial coefficient
γ_s	Shear strain
γ_{sat}	Saturated unit weight
γ_{unsat}	Unsaturated unit weight
γ_ϕ	Partial coefficient used to convert the friction angle
γ_{xy}	Total cartesian strain
Δu_l	Excess pore pressure at cone tip in CPT
ε	Vertical deformation in the shear punching test
η	Conversion factor
η_{cu}	Conversion factor applied to cohesion materials
$\eta_{\phi'}$	Conversion factor applied to friction materials
$\kappa*$	Modified swelling index
$\lambda*$	Modified compression index
μ	Correction factor
ν	Poisson's ratio
ν_{ur}	Poisson's ratio for unloading/reloading
ρ	Density
σ_p	Stress in punch
σ'	Effective stress
σ_1	Axial stress in Triaxial test
σ_3	Radial stress in Triaxial test
σ'_c	Pre-consolidation pressure
σ'_L	Effective stress were compression modulus starts to increase
σ_t	Tension cut-off and tensile strength
σ'_v	Vertical effective stress
σ_{v0}	Overburden pressure
σ'_{v0}	In situ vertical effective stress
σ_{xy}	Cartesian shear stress
σ_{yy}	Vertical total cartesian stress
τ	Shear strength

ϕ	Friction angle
ϕ'	Effective friction angle
ψ	Dilatancy angle

Contents

List of Figures

List of Tables

1
Introduction

This chapter contains a summary of the historical shear punching test developed by Bror Fellenius, along with a problem definition that outlines the aim, objectives, and limitations of this thesis.

1.1 Background

Between the years 2019 and 2023, SGI developed a new test method for assessing the undrained shear strength in cohesive soils (Kalén et al., 2023). The newly developed test, called the shear punching test, aims to potentially replace or complement existing test methods, particularly the fall-cone test. In practice, the shear punching test involves inducing a well-defined shear failure by pressing or punching a soil specimen through a fixed circular opening. Simultaneously, the force required to generate the deformation is measured and subsequently converted to the shear strength of the soil.

1.1.1 The beginning of the shear punching test

A method similar to the shear punching test was devised by Bror Fellenius as early as 1935 (Kalén et al., 2023). Fellenius' punching apparatus resulted a reliable shear strength at the time, and the method was considered as both effective and inexpensive (Lundin, 2000). Figure 1.1 depicts the apparatus used, which comprises a cylindrical container for the soil specimen, with a punch and piston positioned above it (Fellenius, 1938). The punch is connected to a lever with a bucket, which receives water at a constant rate of 0.5 kg/min (Lundin, 2000). As the water in the bucket increases, a sufficiently large force is generated to punch the piston into the clay specimen, resulting in shear failure.

Although the shear punch apparatus was initially regarded as a promising method at the time, there is no further mention of it in the literature (Lundin, 2000, Kalén et al., 2023). One potential explanation for the method's limited impact is that its implementation was more complex than that of other methods used at the time to determine shear strength. Another hypothesis is that the Second World War prevented further development of the method and it was subsequently forgotten. Nevertheless, the precise reason remains unknown.

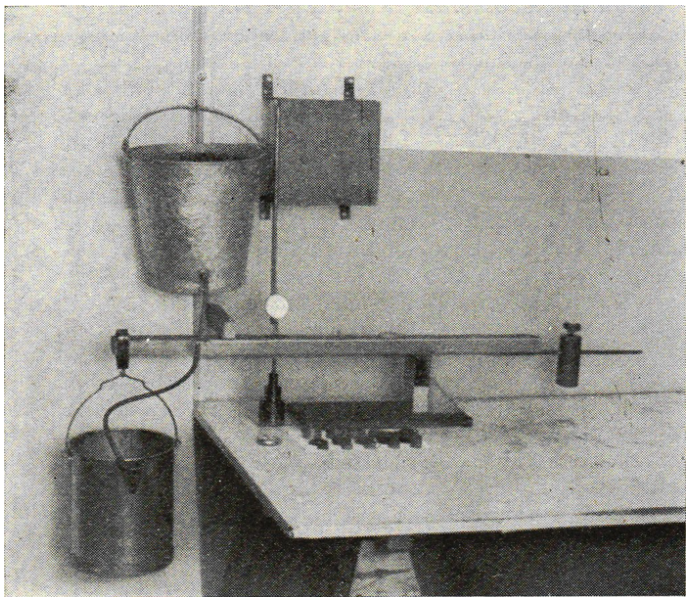

Figure 1.1: Bror Fellenius' shear punching apparatus from 1935 (Fellenius, 1938)

1.2 Problem definition

The fall-cone test, which is a standard procedure for evaluating soil specimens, is a method based on empirical analyses that are challenging to derive mathematically (Kalén et al., 2023). Other methods for determining the undrained shear strength of soil specimens require the input of advanced, calculated data, which is not always available to the engineer. This presented an opportunity to evaluate a new, more straightforward method, which resulted in the shear punching test. As this method is new, its reliability is contingent upon a relatively limited database that has been reviewed and studied during the work of SGI presented in *Indexförsök för bestämning av odränerad skjuvhållfasthet: Skjuvstansning* (2023). Nevertheless, further testing is necessary to enhance the method's credibility. The expansion of the database will also facilitate a deeper comprehension of the circumstances under which the shear punching test is most effective, including the types of soil and conditions in which it performs optimally.

1.2.1 Aim and objective

This study aims to investigate the correlation between the methods fall-cone test, shear punching test and direct shear test (undrained). The thesis focuses specifically on the shear punching test and the potential for it to become a standardized test in geotechnical investigations. This is achieved by *i*) conducting a literature review comparing the methods to each other and *ii*) analyzing results from soil specimens where all relevant methods have been performed. Furthermore, an in-depth stability study is carried out for a section in Gamleby harbor in Västervik, including the results from the shear punching test. Finally, a numerical model of the shear punching test is developed in order to verify the results mathematically.

In line with the objective, the following research questions will be investigated in this study:

1. Can the shear punching test replace the fall-cone test as an index test or complement other existing methods for the evaluation of the undrained shear strength in cohesive soils?
2. In what range is the shear punching test relevant or irrelevant for certain parameters, including density, soil type, water content, liquid limit, organic content, permeability and sensitivity?
3. How does the inclusion of the shear punching test affect the selected shear strength trend and thus the result of the stability analysis in Gamleby Harbor, compared to when the shear strength is based on the fall-cone or DSS test?
4. Is it possible to create a numerical FE model that will produce the same results as those obtained from a shear punch apparatus in a laboratory?

1.2.2 Limitations

This thesis is subject to a few limitations:

- The data included in this thesis is limited to soil specimens from a selected number of locations with equivalent soil composition.
- The material models used in Plaxis 2D are constrained to the Mohr-Coulomb and Soft Soil constitutive models due to a limited time frame and available data.
- The literature review of the material models addresses their limitations and advantages but does not provide a in depth analysis of their construction or operation.
- The stability analysis in Geostudio SLOPE/ W is limited to a single selected cross section in Gamleby harbor.
- Plaxis will be used solely for the purpose of simulating the shear punching test and will not be utilized for stability analysis.

2
Theory

This chapter addresses the properties of cohesive soils, with a focus on gyttja and the impact of organic content on soil properties. Additionally, this text describes the concept of shear strength as a geotechnical parameter and briefly mentions relevant methods for its evaluation. Furthermore, the chapter briefly addresses the issue of localized strain using the Finite Element Method.

2.1 The concept of cohesive soil

All soil specimens which have been tested with the shear punching test were classified as cohesive soils, and the majority have clay as the main content (Kalén et al., 2023). Some of the soil specimens from this case study in Gamleby Harbor, together with some samples provided by LabMind, exhibited a high organic content, which defines them as gyttja.

Soils that exhibit cohesive behaviour, such as clay and gyttja, are defined as soils where the shear strength is determined by both frictional and cohesive forces (sorption, i.e. a physical attraction between particles) between the soil particles. Additionally, these soils often exhibit low permeability (Eriksson, 2016). Except from clay and gyttja, peat and turf is also included in this category.

The cohesive soils can be classified into two subgroups based on their organic content: mineral soils and highly organic soils (Eriksson, 2016). Clay is an example of a mineral soil, while gyttja is an example of a highly organic soil. The designation of soil is dependent on its organic content, as shown in Table 2.1.

Table 2.1: Guideline values for determination of soil type based on organic content.

Soil type	**Organic content**
Clay	<2%
Gyttja-bearing clay	2-6%
Clayey gyttja	6-20%
Gyttja	>20%

Gyttja originates from the decomposition of organic matter, resulting in a soil that is rich in fat and protein (Larsson, 1990). The remains are broken down by three different processes. The first two are decomposing processes with bacteria and living

organisms such as worms, while the third is a fermenting process. These processes gives gyttja its characteristic grey, brown or green color and elastic consistency. However, the organic substance is rarely entirely decomposed, which can result in disturbances of the soil specimen during sampling and laboratory work. It is not uncommon for the specimen to be cut uncleanly.

Organic material has a high capacity for absorbing water and binding sediments which creates a structure with high water content and plasticity (Wang et al., 2022). The water content is significantly correlated with the pre-consolidation pressure (Larsson, 1990). A high water content in gyttja will result in a higher compressibility, lower sensitivity and a lower shear strength since the soil is more unstable with water filling the particle structure. Additionally, a higher water content will result in higher Atterberg limits, i.e. liquid and plastic limit (Wang et al., 2022). For inorganic soils, such as clay, with a higher pre-consolidation pressure, the compressibility and water content will be lower, and the shear strength usually higher.

2.2 Shear strength

Shear strength is a parameter used in a variety of geotechnical applications, including calculating of bearing capacity and conducting stability analyses (Eslami et al., 2020). Shear strength is defined as the resistance to shear stress, with shear failure occurring when the shear stresses exceed the shear strength. It is typically determined by the Mohr-Coulomb failure criterion, described in Equation 2.1.

$$\tau = c + \sigma' \times tan\phi \tag{2.1}$$

where
τ = shear strength,
c = cohesion,
σ' = effective stress,
ϕ = friction angle.

A number of factors influence the MC failure criterion. For instance if the soil is a drained or undrained, whether it is normally- or overconsolidated, and its grain size (fine or coarse). Additionally, time-dependent behaviors, the type of loading, the sensitivity of the soil and its stress paths also influence the criterion (Eslami et al., 2020).

Shear strength can be expressed as either drained or undrained shear strength (Larsson et al., 2007a). Undrained shear strength, often given as c_u, is the most common type of shear strength used in calculations (Larsson et al., 2007a). The main factors influencing the shear strength are soil type, the load case, the pre-consolidation pressure σ'_c and the overconsolidation ratio, OCR. The undrained shear strength varies in different directions and is thus divided into three cases: active, passive and direct shear. Active shear strength is usually the highest, while the passive shear strength is usually the lowest. These are illustrated in Figure 2.1. It is often as-

sumed that the undrained shear strength remains constant over time, with changes only occurring in case of drainage.

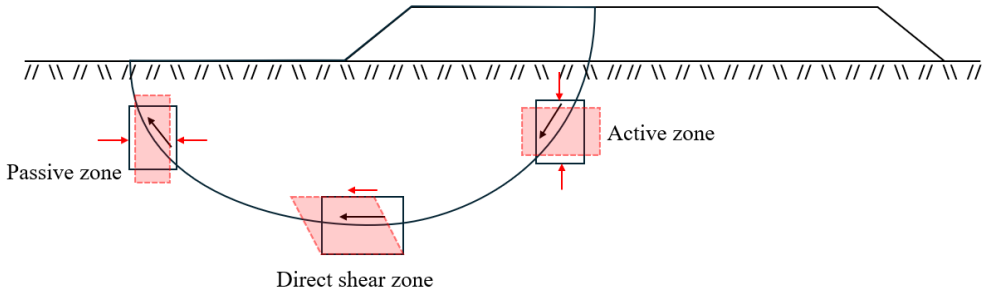

Figure 2.1: The three different shear cases. Black arrows indicates the direction of the shear plane, while red arrows illustrate the change in shape that occurs during movement.

The drained shear strength is most applicable to situations involving friction soils or in overconsolidated cohesive soils (Larsson et al., 2007a). The effective strength parameters c' and ϕ' are used in Equation 2.1 to describe the phenomenon.

The determination of shear strength can be achieved through a number of test methods (Larsson et al., 2007a). The field vane shear test, the fall-cone test and the CPT are test methods for investigating the shear strength. However, results from these tests should be correlated by or compared to the shear strength determined by the direct simple shear test (DSS), which is considered to be a more accurate and applicable test. As the name implies, the direct simple shear test is only applicable to direct shear cases. When the objective is to determine the active or passive shear strength, triaxial tests are more suitable since they can simulate anisotropic behavior, where the shear strength varies in different directions.

The shear strength obtained from the fall-cone test can be used to determine the sensitivity of a clay, which is a necessary parameter for determining whether a clay is classified as quick or not (Swedish Geotechnical Institute [SGI], 2018). The sensitivity is defined as the ratio between the undisturbed and remoulded shear strength, both of which are obtained from the fall-cone test, according to equation 2.2.

$$S_t = \frac{c_u}{c_{u,r}} \tag{2.2}$$

In addition to sensitivity, the value of the remoulded shear strength is also taken into account when classifying the clay as quick (SGI, 2018). In Sweden, the guideline values for quick clay is a $S_t > 50$ and $c_{u,r} < 0.4$ kPa, with greater emphasis on the

sensitivity.

In 1922 when the cone test apparatus had been developed, the sensitivity could be calculated with the strength values H_1 and H_2 representing the remoulded and the partly undisturbed shear strength (Lundin, 2000). The remoulded shear strength was initially introduced because the remoulded specimens were all tested under the same conditions, making the disturbances of the specimen during sampling irrelevant (Statens järnvägars geotekniska kommission 1914-1922, 1922). However, this approach is not used in the same way today. The invention of the piston sampler in 1925 enabled the collection of undisturbed samples, used to determine the undisturbed strength value H_3, allowing for a more accurate determination of the sensitivity (Lundin, 2000).

2.2.1 Empirical relations for undrained shear strength

Empirical relations and correlations are often used for a preliminary estimation of expected soil properties and for assessing the relevance of laboratory test results. One of the most well known empirical relations is Hansbo's relation, presented in Equation 2.3, which is based on the results of fall-cone and field vane tests, which have been corrected for the liquid limit (Larsson et al., 2007b). The correlation is based on normally consolidated clays with a high content of the mineral illite and a sensitivity of approximately 10 (Hansbo, 1957). In normally consolidated and slightly overconsolidated Scandinavian clays, the evaluated undrained shear strength from the fall-cone and field vane test typically follows this relation (Larsson et al., 2007b). However, a considerable degree of scatter is observed in the relation for undrained shear strength obtained from field vane tests. Typical values for Swedish clays are within a range of ± 20 %, with the potential for values to reach up to ± 50 % (Larsson, 1980).

$$c_{u,Hansbo} = \sigma'_c \cdot 0,45 \cdot w_L \tag{2.3}$$

Instead of the proposed relation by Hansbo, SGI has recommended an alternative empirical formula for undrained shear strength (Larsson et al., 2007b). This formula is derived from data obtained from active and passive triaxial tests, as well as DSS tests, and depends on the type of soil, loading, pre-consolidation pressure σ'_c, and OCR (Larsson and Åhnberg, 2003). The empirical formula is presented in Equation 2.4 below.

$$c_{u,SGI} = a \cdot \sigma'_c \cdot OCR^{-(1-b)} \tag{2.4}$$

Both a and b are material constants. a is dependent on the type of soil, load case, and the liquid limit of the soil while b is independent of the load case and is usually found within the interval 0,7-0,9. However, it is typically set to 0,8. a is calculated as follows:

- Active shear: $a \approx 0,33$

- Direct shear: $a \approx 0,125 + 0,205 \cdot w_L/1,17$
- Passive shear: $a \approx 0,055 + 0,275 \cdot w_L/1,17$

In the absence of the liquid limit, a is typically set to 0,22.

In addition to the two previously mentioned empirical relations, other empirical methods are also used. For instance, SHANSEP (Stress History and Normalized Soil Engineering Properties) describes how the undrained shear strength of soil varies in relation to pre-consolidation pressures and OCR, similar to the formula recommended by SGI. Instead, Mesri expressed the undrained shear strength as $c_u = \sigma'_c \cdot 0,22$, which is independent of the plasticity index that Bjerrum included (Larsson, 1980).

Empirical data are generally used to validate the reliability of the obtained results from test methods (Larsson et al., 2007b. The empirical data thus correspond to the normal values against which the obtained data are compared. Depending on the objectives and the engineer, different empirical methods may be used, but SGI nevertheless offers a certain recommendation.

2.3 Material models in Plaxis 2D

Regardless of the material model used in Plaxis 2D, a number of parameters are required for the material models to function properly. The aforementioned parameters are presented in table 2.2 below. The strength reduction factor, R_{inter}, is used in instances where structural elements are incorporated into the model. This factor describes the roughness of the interaction between the soil and the structural element modelled by an *Interface* (Bentley, 2023).

Table 2.2: Parameters that require input for all constitutive material models used in Plaxis 2D.

Standard parameters	
Saturated and unsaturated unit weight	$\gamma_{sat}/\gamma_{unsat}$
Initial void ratio	e_{init}
Initial porosity	n_{init}
Permeability in x and y direction	k_x/k_y
Strength reduction factor	R_{inter}
Lateral earth pressure coefficient at rest	$K0$

2.3.1 Mohr-Coulomb

The Mohr-Coulomb constitutive model (MC model) is a linear elastic perfectly plastic model that is used as an approximation of the behavior of soil, as well as analyzing soil failure (Kartsunen and Amavasai, 2017). The model can be divided into two distinct parts: the linear elastic part and the perfectly plastic part. The linear elastic part is based on Hooke's law regarding isotropic elasticity. The perfectly plastic

part is based on the Mohr-Coulomb failure criteria where pure elastic response is assumed until failure. A useful illustration of the elasto-plastic models can be found in Figure 3 of the report *BEST SOIL: Soft soil modelling and parameter determination* (Kartsunen and Amavasai, 2017).

The MC model is simple to use and only fundamental parameters are necessary to conduct the analysis, resulting in sufficiently good results in the elastic region (Kartsunen and Amavasai, 2017). However, it should be noted that soil is not always behaving linear elastic, particularly when the load is changed. Additionally, the model does not allow for changes in stiffness, as it assumes linear stiffness. Consequently, the model is unsuitable for advanced soil modeling problems.

The parameters necessary for conducting a MC analysis are presented in Table 2.3 below. These parameters are derived using CRS and triaxial tests, or based on the engineer's experience if the available data is limited.

Table 2.3: Necessary parameters for the Mohr-Coulomb constitutive model.

Parameter		**Unit**	**Drainage type**
Young's modulus	E_{ref}	kN/m^2	
Poisson's ratio	ν	-	
Cohesion	c	kN/m^2	Undrained A
Friction angle	φ	^{o}	Undrained A
Tension cut-off and tensile strength	σ_t	kN/m^2	
Dilatancy angle	ψ	^{o}	Undrained A
Reference undrained shear strength	$s_{u,ref}$	kN/m^2	Undrained B

2.3.2 Soft soil

The failure of the Soft Soil constitutive model (SS model) is based on the Mohr-Coulomb failure envelope, as is the MC model. However, the yield surface is based on the Modified Cam Clay model associated with the so-called "flow rule for plastic strains" (Kartsunen and Amavasai, 2017). The yield surface is illustrated in a $p-q'$ diagram and is formed as an ellipsoid. The M-parameter determines the height of the ellipsoid, which in turn determines the ratio between horizontal and vertical stress in the one-dimensional compression. Consequently, M exerts a considerable influence on the coefficient for lateral stress in normal consolidation, K_0^{nc}. The top of the ellipsoid coincides with the M line, which is also known as the critical state line. The critical state is not necessarily where failure occurs, and hence the M line is not always the same as the MC line where failure occurs. The size of the yield surface is contingent upon OCR or POP. If OCR or POP is to be used is determined by the geological history. A comprehensive illustration of this relation can be found in Figure 4 of the report *BEST SOIL: Soft soil modelling and parameter determination* (Kartsunen and Amavasai, 2017).

The SS model is capable of simulating both elastic and plastic soil behaviors. Its stiffness is stress dependent, which means that it is non-linear (Kartsunen and Amava-

sai, 2017). In contrast, there is a logarithmic behavior based on compression and a logarithmic relation between the change in volumetric strain and the change in mean effective stress (p'). Furthermore, the soft soil model incorporates the pre-consolidation pressure.

The SS model is designed for the analysis of soft soil, as the name reveals (Kartsunen and Amavasai, 2017). The hardening soil model can also be used in the analysis of soft soil material. However, the soft soil model is more advantageous when the analysis includes compression but it is limited in its ability to manage compression stress paths but not extension. Furthermore, it does not consider the anisotropy that may occur in the soil. The model also performs poorly on strongly over-consolidated clays, as the stress ratio is located above the MC failure line.

The essential parameters for the SS model are presented in Table 2.4. Some parameters are most simply derived from incremental loading oedometer tests, including unloading and reloading. This type of test is rarely performed in Sweden which causes difficulties for the derivation of parameters.

Table 2.4: Additional parameters that require input for the Soft Soil constitutive model.

Parameter		**Unit**
Modified compression index	$\lambda*$	-
Modified swelling index	$\kappa*$	-
Poisson's ratio for unloading/reloading	ν_{ur}	-
Effective cohesion	c	kN/m^2
Friction angle	φ	^{o}
Dilatancy angle	ψ	^{o}
Tensile strength	σ_t	kN/m^2
Coefficient of lateral stress in normal consolidation	K_0^{nc}	-

2.3.3 Localized strain using FEM

The Finite Element Method (FEM) utilizes approximation functions to represent field variables, such as deformation and stress, within each element (Lopes et al., 2020). However, if these functions are unable to effectively represent local variations, it can lead to inadequate capture of localized strain, often referred to as mesh dependency problem. This issue can arise in materials that exhibit strain softening behavior like the materials used in this thesis. The softening effect caused by soil failure cannot be accurately captured by finite elements, which makes it difficult to solve the boundary value problems that describe the structure's response. Localized strain is displayed as a thin band in the model, with the width of the band dependent on the size of the mesh. However, more advanced constitutive soil models are available that can simulate strain softening, and thus avoid localized strain problems. One such model is the Creep SCLAY-1S model, which is a highly advanced model, that predicts strain softening by accounting for bonding and destructuration (Kartsunen and Amavasai, 2017).

3

Methods to test undrained shear strength

This chapter describes methods for determination of shear strength in soil, both in situ and in the laboratory. Additionally it provides a brief introduction of other punching methods adopted internationally.

3.1 Determination of shear strength in situ

In situ determination of the undrained shear strength of the soil refers to the testing of soil in its current state, without altering the stresses on the soil (Larsson et al., 2007b). This can be done with field vane shear tests and CPT, among other methods.

3.1.1 Field vane shear test

In Sweden, the in situ undrained shear strength in cohesion soils has traditionally been determined using field vane shear tests (Larsson et al., 2007a). The method involves pressing the vane into the soil to the desired depth with minimal disturbance, and then rotating it until failure is obtained (Swedish Institute for Standards [SIS], 2020). The maximum torque, T_{max}, required to induce failure is measured, and together with the geometry of the vane, the peak undrained shear strength can be calculated according to Equation 3.1. The maximum torque obtained is corrected for the internal and external friction of the extension rods. The equation is valid when the ratio of the plate diameter to height is 1:2. Subsequently, the shear strength is corrected for the liquid limit of the soil, W_L.

$$c_{fv} = \frac{6000000 T_{max}}{7\pi D^3} \tag{3.1}$$

The sensitivity of the soil is an important parameter for the detection of quick clay and can be calculated by dividing the undrained shear strength by the remoulded shear strength, which is obtained by vigorously rotating the vane (SIS, 2020). The field vane test is most appropriate for evaluating very loose to solid clay that is relatively homogeneous, as soils with coarser layers or particles are more likely to cause disturbances (Larsson et al., 2007a). If the vane is driven through an overlying firmer layer into a looser layer, there is a risk of material adhering to the blades and thus disturbing the underlying looser soil profile. The presence of coarser grains, embedded layers or plant debris may result in elevated shear strengths and disturbance

due to drainage or the vane getting caught in materials. By pre-drilling through the dry crust and using a protective casting around the vane, the disturbances can be minimized.

3.1.2 Cone Penetration Test

The cone penetration test (CPT) is another in situ method for determining soil parameters in loose and firm soils, frictional soils with occasional gravel grains, as well as fine-grained soils (Larsson, 2015). In contrast to the field vane shear test, which provides a point-based measurement, the CPT measures with a significantly higher reading frequency, resulting in a continuous graph towards depth. The method is therefore useful for assessing the soil sequence and layer boundaries and for providing an overview of the soil parameters. However, it is important to pre-drill through the dry crust in order to obtain the correct results of the underlying loose soil. The method is relatively quick, but due to its sensitivity, extensive preparation is required (Sällfors and Larsson, 2016). The method is among other things, very sensitive to handling, zero readings before and after probing, and temperature stabilization.

During CPT probing, the cone tip pressure, sleeve friction and pore pressure are measured (Larsson, 2015). These parameters can be used to evaluate the soil profile and to determine other useful geotechnical parameters. For instance, the undrained shear strength can be calculated using Equation 3.2a or 3.2b using the net cone tip pressure ($q_t - \sigma_{v0}$) or excess pore pressure (Δu_l). The CPT can also estimate the pre-consolidation pressure, σ'_c. However, the estimation is sensitive to the liquid limit and thus should be regarded as a supporting tool for the assessment of the pre-consolidation variation with depth (Sällfors and Larsson, 2016).

$$c_u = \frac{q_t - \sigma_{v0}}{13,4 + 6,65 w_L} \times \left(\frac{OCR}{1,3}\right)^{-0,2} \tag{3.2a}$$

$$c_u = \frac{\Delta u_l}{16} \tag{3.2b}$$

The undrained shear strength from the CPT is corrected according to the liquid limit, as with fall-cone test and field vane shear test (Sällfors and Larsson, 2016). However, the result is not as dependent on the correction as it is for the other methods. It is important to note that although the CPT provides continuous results for soil properties, weakness zones, variation in shear strength and homogeneity, the results for the geotechnical parameters should be validated against other tests, such as the DSS test. Consequently, the CPT should be used as a preliminary indicator and rather determine where to perform more thorough laboratory tests. Most importantly, it should not be the only method used to determine the characteristics of the soil.

3.2 Determination of shear strength in the lab

There are numerous methodologies for determining undrained shear strength in the laboratory. The choice of test is contingent upon multiple factors, including soil type and the purpose of the test.

3.2.1 Direct simple shear test

The shear strength in the direct shear zone, with a horizontal slip surface can be evaluated from the direct simple shear test, DSS, as previously mentioned in chapter 2.2 (SGF:s laboratoriekommité, 2004). The equipment used in the laboratory test has been developed over a long period of time and was initially introduced by Walter Kjellman in the 1930s. The equipment commonly used in Sweden today is considered to be a simplified version and is called SGI IV, which was developed by SGI in the 1950s. A more advanced, yet more costly, apparatus was subsequently developed at the Norwegian Geotechnical Institute (NGI) and is known as the NGI- or Genor-apparatus. Figure 3.1 depicts the apparatus currently used in SGI's laboratory.

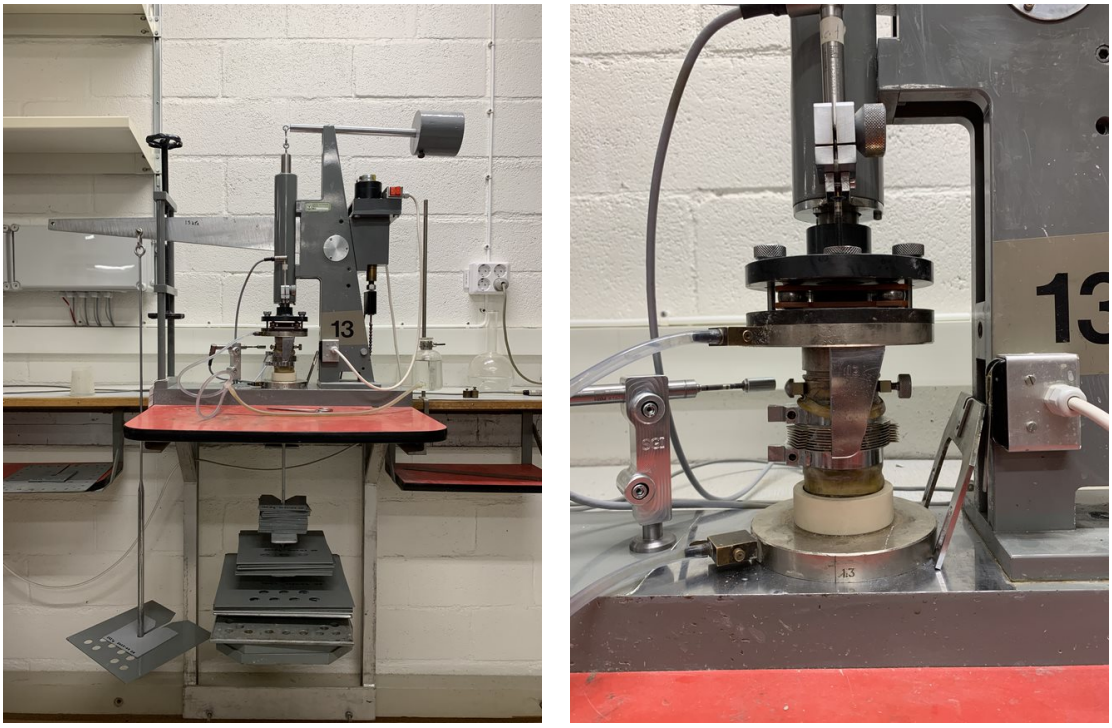

Figure 3.1: A DSS apparatus during the consolidation phase in the SGI laboratory.

The execution of a DSS test varies depending on the device used, but essentially the fundamental method entails four separate steps: installation of the soil specimen, consolidation, unloading, and finally, shearing (SGF:s laboratoriekommité, 2004). The soil specimen should be undisturbed which is achieved by collecting the specimen with a piston sampler. Subsequently, the soil specimen is prepared by cutting

a specimen of 50 mm in diameter and 20 mm in height for undrained tests and with a smaller height for drained tests, usually 10 mm (Swedish Institute for Standards, 1991). Depending on the purpose of the test, the soil specimen is either installed directly on the filter stone or first placed in an oedometer ring.

Subsequently, the soil specimen is consolidated by vertical loading up to the desired consolidation load (SGF:s laboratoriekommité, 2004). If the objective of the test is to not exceed the pre-consolidation pressure, the vertical load does not exceed 0.85% of the pre-consolidation pressure. At this stage, creep should be avoided by not applying the pre-consolidation pressure for too long. The applied load is then reduced to the initial stress for the test, which is maintained for approximately 15 hours (Swedish Institute for Standards, 1991). During the consolidation phase, both the upper and lower parts of the specimen holder are fixed horizontally and the vertical deformations of the soil specimen are recorded.

If the in situ vertical effective stress, σ'_{v0}, where exceeded in the previous step, the soil specimen is unloaded to σ'_{v0} prior to the initiation of shearing (Sällfors and Larsson, 2017).

During the shearing phase, the upper part of the specimen holder is allowed to move horizontally (SGF:s laboratoriekommité, 2004). In a drained test, the height of the soil specimen remains unlocked and the drainage channels remains open, as opposed to an undrained test where the drainage channels are closed and the specimen height is fixed. A shear force corresponding to a deformation rate of 2mm/day is applied in the horizontal direction. During the shear phase, the shear force and horizontal movement are recorded, as well as the vertical deformation in the drained test. Figure 3.2 depicts a simplified model of the DSS apparatus.

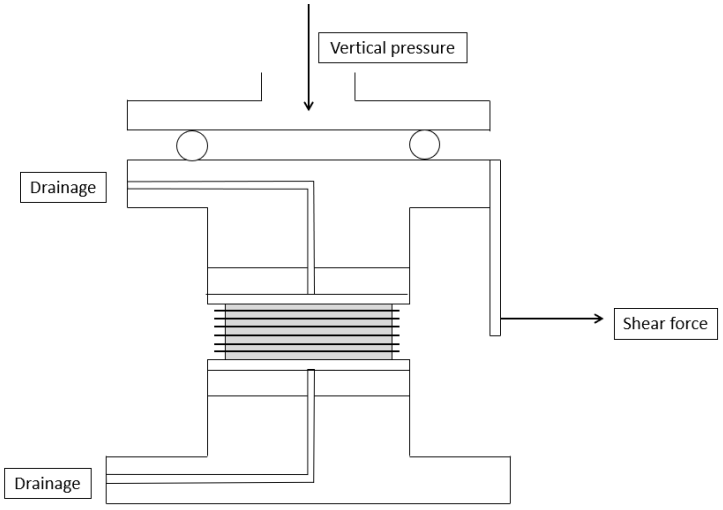

Figure 3.2: Simple sketch of the DSS apparatus.

Before the shearing and evaluation of strength parameters of the soil, the specimen

is consolidated with a predetermined load. This enables the performance of multiple tests with varying consolidation stresses to determine how the soil properties vary under different stress conditions (SGF:s laboratoriekommité, 2004). The DSS test is therefore suitable for investigating the expected properties of the soil during unloading, loading or a specific future load case. As previously stated, the results of the test is most accurate for the direct shear zone, rather than the passive or active shear zone.

From the measurements in the shearing phase, the drained shear strength parameters c' and ϕ' and the undrained shear strength, c_u, can be evaluated from the drained and undrained DSS test respectively (SGF:s laboratoriekommité, 2004). By plotting the shear stress, τ, against the shear strain, γ_s, one can evaluate the undrained shear strength as the maximum shear stress. Alternatively, if failure does not occur within 0.15 radians of shear deformation, the shear strength is evaluated at 0.15 radians. The shear stresses correspond to the ratio of the shear force to the cross-sectional height of the specimen, while the shear deformations, γ_s, are calculated from the horizontal movement that is registered.

Equation 3.3 is used to evaluate the friction angle, ϕ', from the drained DSS (Larsson et al., 2012).

$$\phi' = arctan\frac{\tau}{\sigma'_v} \tag{3.3}$$

Soils composed by clay, silt, or organic matter, as well as layered clay, where an undisturbed specimen can be extracted, are suitable for the DSS test (SGF:s laboratoriekommité, 2004). In the event that cyclic DSS tests are being considered, it may also be appropriate to include fine sand among the suitable soil types.

The cost of performing a drained or undrained direct simple shear test is dependent on the equipment (SGF:s laboratoriekommité, 2004). Tests conducted with the SGI IV apparatus are relatively simple, requiring approximately two days to complete. However, they are considered relatively costly, although not as costly as the triaxial test.

The DSS test provides a shear strength value that does not require correction and can be used directly, which is a significant advantage compared to other tests that necessitate calibration against, for instance, the liquid limit (SGF:s laboratoriekommité, 2004). Furthermore, the shear strength obtained from the field vane test, CPT and fall-cone test can also be verified and calibrated against the shear strength obtained from the DSS.

Nevertheless, there are certain disadvantages associated with testing sand and silt. The friction angle evaluated from the drained DSS tends to differ from the triaxial test which is considered more suitable for these soil types (SGF:s laboratoriekommité, 2004). The drained soil properties are sensitive to alterations in storage density and the small specimen size in the drained test entails difficulties. For instance, the void ratio can be more easily controlled in a triaxial test.

3.2.2 Fall-cone test

The fall-cone test is a test that does not require the use of any complex mechanical devices. The test begins with the placement of a cone in a stand at the smooth surface of a soil specimen (Swedish geotechnical society [SGF], 2018). To perform the test, the cone is dropped freely into the soil specimen, and the depth of the penetrations allows for the determination of the undrained shear strength and liquid limit. The fall-cone apparatus can be seen in Figure 3.3.

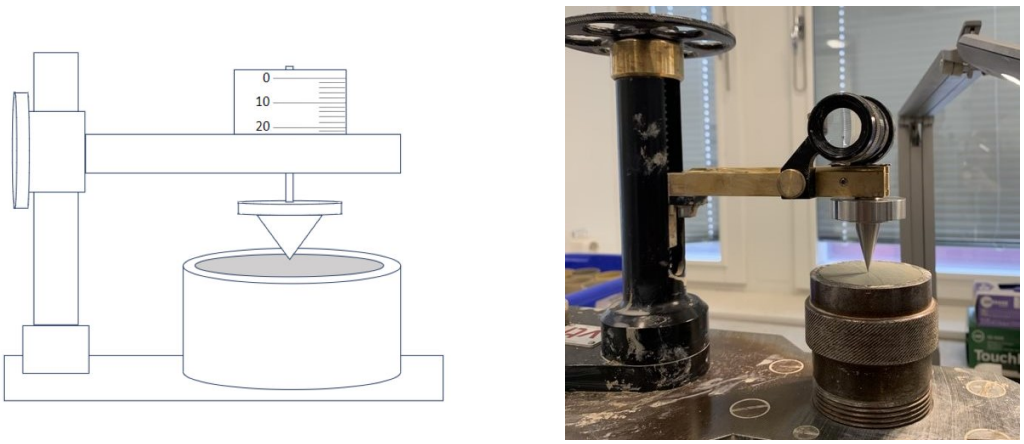

Figure 3.3: Fall-cone test as a simple principal sketch (left) and in the SGI laboratory (right).

The fall-cone test can be done in two ways: on undisturbed and on remolded specimens (SGF, 2018). Undisturbed specimens are preferably conducted on soil in the sample tube. Remoulded specimens can be conducted on soil that already have undergone an undisturbed test but that have been completely mixed.

To assess the outcome of the fall-cone test, a formula developed by Sven Hansbo in 1957 is used (SGF, 2018). The formula is a semi-empirical equation, which is partly derived from Newton's second law and is presented in Equation 3.4 below.

$$\tau = K \times \frac{mg}{i^2} \tag{3.4}$$

where
τ = shear strength (kPa),
K = cone factor (-),
m = weight of cone (g),
g = gravitational acceleration (9,81 m/s^2),
i = cone penetration depth (mm).

The cone factor, K, is calibrated against the field vane shear test for undisturbed specimens and against the laboratory vane shear test for remolded specimens (SGF, 2018). This cone factor enables equivalent results from the fall-cone test, the vane shear test and the DSS test, provided that the specimens are of sufficient quality.

Nevertheless, the results of the fall-cone test should be interpreted with caution, as they tend to have a greater degree of variability than those obtained from other methods.

In addition to the characteristics of the soil itself, the cone also plays a significant role in determining the outcome of the test. The angle, weight, and roughness of the cone's tip are among the most influential properties (Koumoto and Houlsby, 2001). The cone most frequently used in Scandinavia, Japan and Canada for determining the liquid limit has a 60° tip and weighs 60 grams. This cone has been determined to be the most beneficial, exhibiting a greater degree of agreement between theoretical and experimental approaches and being less sensitive to to the roughness of the cone material. In Sweden, a cone with a 30° tip and a weight of 100 or 400 g is used for determining the undisturbed shear strength, as this method not commonly is used for determining other parameters than the liquid limit in the rest of the world. In the UK, New Zealand and France, a cone with a 30° tip and weighing 80 grams is used for determining the liquid limit. Previously, it was assumed that the roughness of the tip had a more significant impact than the cone angle. However, recent investigations have demonstrated that the roughness of the cone does not significantly impact the penetration depth (Houlsby, 1982: Llano and Contreras, 2019). It's important to note that the later investigations have exclusively focused on remoulded soils, rather than also considering undisturbed ones.

The fall-cone test was initially developed with the objective of determining the liquid limit of clay (Houlsby, 1982). However, subsequently it was suggested that determining the liquid limit is essentially equivalent to determining the strength of the clay at that liquid limit. The test is currently primarily used to determine the undrained shear strength of a fine-grained, soft soil. The fall-cone test is most suitable for fine-grained and soft soils, and when a rapid and cost-effective test is desired (Llano and Contreras, 2019). In comparison to other tests that determine the same parameters, the fall-cone test is considered relatively inexpensive.

The shear strength that has been assessed through the fall-cone test is normally adjusted in accordance to the liquid limit. The correction factor is calculated using Equation 3.5b and the corrected shear strength is calculated using Equation 3.5a (Larsson et al., 2007a).

$$\mu = \left(\frac{0,43}{w_L}\right)^{0,45} \geq 0,45 \tag{3.5a}$$

$$c_u = \mu \times \tau \tag{3.5b}$$

The direct shear test is also frequently used for the calibration of the fall-cone test, which is necessary to receive reliable results (Llano and Contreras, 2019). The calibration requires the measurement of s_u (undrained shear strength) from another test, after which the DSS test is frequently used. In the case of low or very low consistency of fine-grained soil, a vane shear test is more preferred as reference test. This indicates that the shear strength evaluated from a fall-cone test is rarely used

as a standalone value, rather, it is typically related to or refined with other more reliable test, such as the DSS test or vane shear test.

In addition to evaluating the liquid limit and shear strength of the soil, the fall-cone test is the only laboratory method whose results can be used to evaluate the sensitivity S_t, as previously mentioned (Sällfors and Larsson, 2017). The sensitivity is calculated as the ratio between the shear strength of the undisturbed and remoulded specimens using Equation 2.2.
The fall-cone test offers several advantages, including its cost-effectiveness, simplicity and rapidity (SGF, 2018). One disadvantage of this method is that it has not been developed in a scientific manner. The fall-cone test was initially developed by geotechnical engineers as a response to the Brinell test, which originated from mechanical engineering. The transition from the use of a bullet to a cone was the result of a process of trial and error by identifying what was most beneficial for soil. However, while the correlation was never proven mathematically, it was observed to function adequately. Because of its difficulty to prove mathematically, it is calibrated against other tests to ensure a reliable and accurate outcome.

3.2.3 Triaxial test

The triaxial test is a method of exposing a cylindrical specimen to pressure in both the vertical and horizontal direction (Westerberg et al., 2012). The horizontal pressure is accomplished by a liquid pressure that is imposed on the specimen in a cell while the vertical pressure is accomplished by a piston applying pressure to the top and bottom of the specimen.

In the context of triaxial testing, it is common to encounter the concept of the three stresses, two strains and a volumetric strain. These are referred to as axial stress and strain, radial stress and strain, pore water pressure and volumetric strain. The stresses are depicted in Figure 3.4, accompanied by a simplified sketch of the triaxial apparatus.

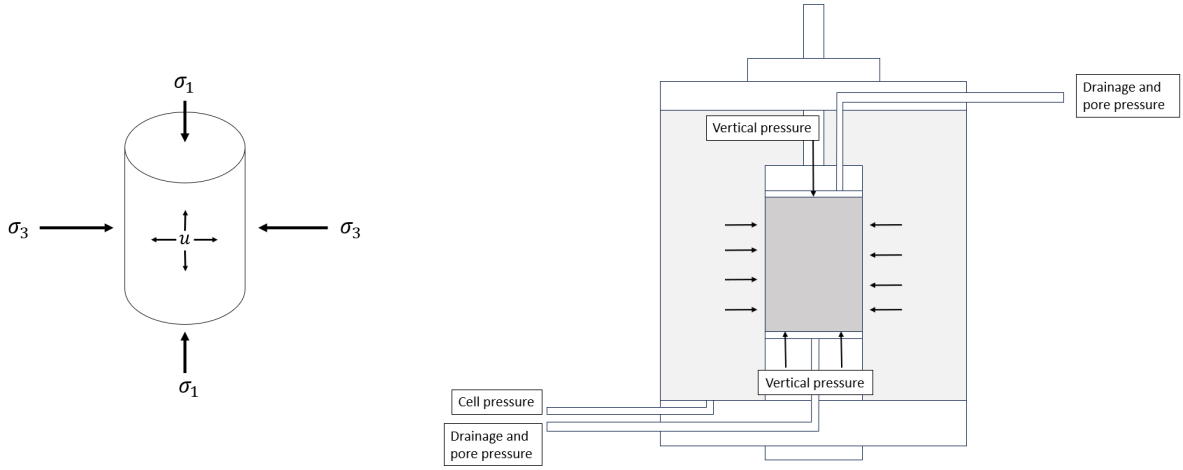

Figure 3.4: Stresses acting on the specimen in a triaxial test (left) and a simple principle sketch of the apparatus (right).

The implementation of the test is divided into two phases, the consolidation phase and the shear phase (Westerberg et al., 2012). The consolidation phase is intended to recreate the stress state in the field. This is achieved by applying the desired axial and radial stresses. Swedish clays are often subjected to at stress level of $0,85\sigma'_c$, after which they are unloaded to in situ stresses in order to prevent the clay structure from breaking before shearing. This phase serves as a preliminary phase for the shearing phase, during which axial and volumetric strains usually measured. During the shearing phase, a constant deformation velocity is added vertically, while a constant cell pressure is maintained radially. This process is continued until failure has occurred or axial strains exceed 15-20%. An undisturbed sample will fail at approximately 1-2% shear strain for an active test and 3-4% for a passive test (Sällfors and Larsson, 2017). Larger strains indicates a poorer quality of the specimen.

The shearing phase can be conducted under either drained or undrained conditions, and as either an active or passive test (Westerberg et al., 2012). If the test is conducted as drained, the pore water can be either enter or exit the specimen during the test. Consequently, the pore water pressure will remain unchanged, whereas the volume will change. In an undrained test, the drainage tubes are sealed, preventing water from leaving the test during the test. This will result in a changed pore water pressure, while the volume remains constant. An active triaxial test is simulating an active shear case, as illustrated in Figure 2.1. This implies that the test will experience a greater load in the vertical direction and be compressed axially during the shearing process. The passive triaxial test simulates the passive shearing case, thus imposing a greater load in the horizontal direction or reducing the vertical pressure while maintaining constant horizontal pressure. This will result in a vertical expansion during the shearing phase.

The parameters presented from a triaxial test vary depending on whether the test is conducted as drained or undrained (Westerberg et al., 2012). The undrained test generates graphs of stress-strain behavior, change of pore pressure with axial strain,

and effective stress paths. The drained test also provides a stress-strain graph and an effective stress path. Instead of change in pore pressure, the volume change or volumetric strain is plotted with the axial strain. Based on the stress-strain plots, the cohesion parameter c/c' and the friction angle ϕ/ϕ' can be determined. The triaxial test is considered the most reliable test for the determining these two parameters (Bishop and Henkel, 1962).

The four stress variables that are determined by the triaxial test and may be used in the stress-strain graphs or effective stress paths are the deviatoric stress, shear stress and mean effective stress which are calculated in two possible ways (Westerberg et al., 2012).

- Deviatoric stress: $q = \sigma'_1 - \sigma'_3$
- Shear stress: $\tau = \frac{\sigma'_1 - \sigma'_3}{2}$
- Mean effective stress: $p' = \frac{\sigma'_1 + 2\sigma'_3}{3}$ or $s' = \frac{\sigma'_1 + \sigma'_3}{2}$

The shear stress can also be presented as the undrained shear strength c_u (Westerberg et al., 2012). The undrained shear strength is determined by evaluating the shear stress at assumed failure in a triaxial test. The elasticity modulus E can be evaluated from the stress-strain graph.

The triaxial test is in many ways connected with the Mohr-Coulomb failure criterion (Sällfors, 2013). The Mohr-Coulomb failure criterion can be illustrated by Mohr circles which are done with σ_1 and σ_3. The failure envelope in the diagram can be plotted using the values of c and ϕ, which are all obtained from the triaxial test. The failure criterion is expressed in Equation 3.6 below. For drained conditions, effective parameters are used instead.

$$\tau = c + \sigma \cdot tan\phi \tag{3.6a}$$

or

$$\tau = c' + \sigma \cdot tan\phi' \tag{3.6b}$$

The Mohr-Coulomb failure criterion is used to illustrate at what vertical and horizontal stresses a soil with certain characteristics is expected to fail and is very useful when for example calculating slope stability (Sällfors, 2013).

The triaxial test is a suitable method for evaluating the properties of a range of soil types, including both cohesive and friction soils (Larsson et al., 2012). However, the friction soil should not be too coarse; a grain size interval of coarse silt to fine sand is considered optimal. Furthermore, the triaxial test is also applicable to use for a range of construction scenarios (Westerberg et al., 2012). For instance, in projects concerning slope stability or the use of sheet pile walls where active and passive shear cases are necessary. The triaxial test is also useful in the case of anisotropic

soil conditions or when the undrained shear strength is anisotropic, as the test can simulate these conditions.

The triaxial test is frequently used for projects despite its high production cost, it is even considered to be the most costly of the tests. The estimated time for the test varies, but it is not considered as a rapid test overall. The triaxial tests popularity despite its high cost indicates that it is a reliable method of testing. No correction of the parameters is necessary (Westerberg et al., 2012). However, it is advisable to conduct at least three tests of good quality if an evaluation of a certain parameter is to be made in order to increase the reliability of the result.

The triaxial test is the most appropriate and widely available test for evaluating the strength and deformation properties of soil (Westerberg et al., 2012). It is possible to recreate stresses and pore pressures that are similar to those observed in the field, which provides a more reliable result than other methods. It is the only method that can determine certain parameters, such as the friction angle, active and passive undrained shear strength, and horizontal pre-consolidation pressure. The accuracy and reliability of the test may result in economic benefits, as geotechnical constructions can be dimensioned with higher reliability with regards to safety against failure and optimized further.

Furthermore, the engineer conducting the test has complete control over parameters such as drainage, stresses, and strains that are applied to the specimen (Bishop and Henkel, 1962). Additionally, it is possible to measure the pore pressure throughout the duration of the test. The test is flexible in that it can simulate a variety of scenarios, including drained or undrained conditions, active or passive cases.

The triaxial test is a costly test that may require a long time to conduct. It also requires advanced and expensive equipment (Westerberg et al., 2012). Another disadvantage is that the rate of testing affects the undrained strength and friction angle, specially for clays (Bishop and Henkel, 1962). Conducting the test at a low rate will result in an undrained strength and friction angle that is up to 5% lower for every 10-fold increase in testing time compared to a normal rate of testing.

3.2.4 CRS-test

The CRS tests are conducted in accordance with the Swedish Standard SS 027126, and the method is suitable for cohesive soils obtained through piston sampling to ensure an undisturbed soil specimen (SIS, 1991). A cylindrical specimen, with a diameter of 50 mm in diameter and a height of 20 mm, is placed in an odometer ring and subjected to a vertical deformation at a constant rate of 0.0025 mm/min. If the test is performed on gyttja-bearing clays, very loose clays, or heavily over-consolidated clays, a lower deformation rate is advised. The vertical force, vertical deformation, and pore pressure at the bottom of the soil specimen are measured. Drainage is allowed at the top of the specimen, while the bottom remains undrained (Larsson, 1986). Although the name of the test suggests a constant rate of strain,

it is in fact performed with a constant rate of deformation. Conducting a CRS test typically requires one to two days and is relatively costly, falling within the same cost range as the DSS test (Sällfors, 2013). A simplified sketch of the CRS apparatus is presented in Figure 3.5.

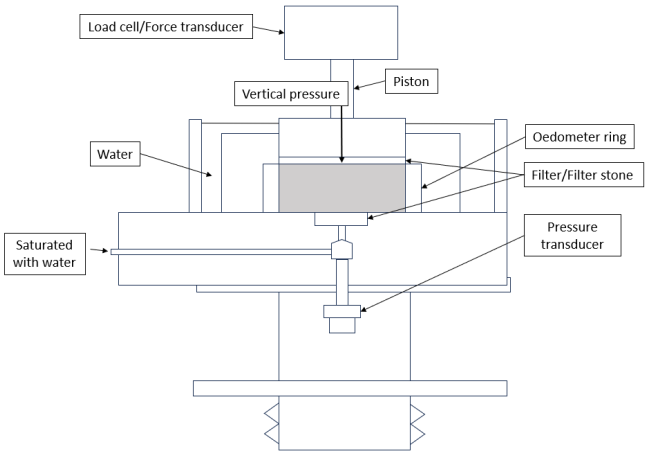

Figure 3.5: Simplified model of the CRS apparatus.

The results from the CRS test can be used to evaluate a number of parameters, including pre-consolidation pressure σ'_c, effective stress where the compression modulus starts to increase σ'_L, compression modules M_0 and M_L, module number M', and permeability, including the permeability coefficient k and coefficient of permeability change β_k (Sällfors and Larsson, 2017). Empirical relations can then be used to estimate the undrained shear strength based on the obtained pre-consolidation pressure. Furthermore, creep parameters may be estimated from CRS tests empirically based on the natural water content or by evaluating the results from the CRS according to the Chalmers method (Olsson, 2010). If the creep parameters are to be evaluated without empirical relations, an incremental loading (IL) oedometer test is required. In the IL oedometer test, the soil specimen is subjected to a series of progressively increasing vertical loads (SIS, 2017). In general, the load is doubled every 24 hours or until the stage of primary consolidation has been completed. The duration of the test may vary depending on whether the creep is to be determined. Additionally, unloading and reloading can be performed to obtain swelling parameters. In contrast to the CRS test, which is based on strain, the IL oedometer test is based on load and deformation.

In addition to evaluating relevant parameters for settlement calculations, the results from the CRS test may be used to determine consolidation stresses for DSS and triaxial tests performed subsequently (Sällfors and Larsson, 2017).

The CRS test generates different stress-strain curves contingent upon the applied strain rate (Claesson, 2003). This, in turn, provides a basis for the evaluation of different pre-consolidation pressures based on the strain rate. It is a general observation that a higher strain rate results in a higher effective stress for a given strain.

The strain rates used for CRS testing are typically higher than those occurring in the field. Consequently, the effects of strain rates are accounted for by evaluating pre-consolidation pressure using the Sällfors method (Olsson, 2010; Claesson, 2003).

The pore pressure measured at the undrained surface of the specimens is affected by inhomogeneities such as root threads (SIS, 1991). Consequently, it is of great importance to conduct a visual inspection of the specimen prior to conducting the test to ensure its quality and thereby reducing potential sources of error.

Furthermore, achieving perfect alignment between the specimen and the piston can be challenging (Sällfors and Larsson, 2017). This may cause initial settlements. The quality of the specimen can be controlled by observing the volume change that occurs when it is re-consolidated, up to the pre-consolidation pressure, in combination with the natural water content, W_N (Larsson et al., 2007b). A consequence of imperfect alignment is that the oedometer modulus evaluated from the overconsolidated region, M_0, is underestimated, leading the soil stiffness being underestimated as well (Olsson, 2010). However, by including unload and reload cycles, which is possible with the IL oedometer test, M_0 can be evaluated more accurately.

The CRS oedometer test is the primary method used in Sweden for determining settlement parameters, including the creep parameters, even though it is done by empiricism (Olsson, 2010). The alternative method is the IL oedometer test, which is more time consuming and costly, but allows for direct evaluation of creep parameters.

3.2.5 Shear punching test

The shear punching test, developed by SGI, consists of a 50 mm wide cylindrical specimen, as the dimensions of a piston sampler, and a height of 15 mm (Kalén et al., 2023). This height was determined through testing of the shear punching test, and the developers deemed it necessary to conserve as much material from the piston samples as possible in order to conduct other methods as well. However, a thickness of 10 mm was found to be insufficient, as it deformed due to its self weight in relation to its thickness. A thickness of 20 mm was deemed to be excessive, but a thickness of 15 mm proved to be an optimal for this method.

A lid with a conical opening, minimum 30 mm in diameter, is placed on top of the sample ring containing the specimen. This is where the soil specimen will be punched through. The conical shape of the opening in the lid reduces the friction between the sheared specimen and the apparatus. A punch is mounted beneath the specimen, with a diameter of 30 mm at the top but reducing to 28 mm with length to avoid friction between the punch and the soil specimen. The punch is pushed through the soil using a load frame. The shear punching apparatus also includes a bottom plate and a fixture designed to maintain the apparatus in position. A principal sketch of the test apparatus is presented in Figure 3.6, while the sequences of the shear punching test are illustrated in Figure 3.7. Furthermore, a photograph of the apparatus in the SGI laboratory is presented in Figure 3.8.

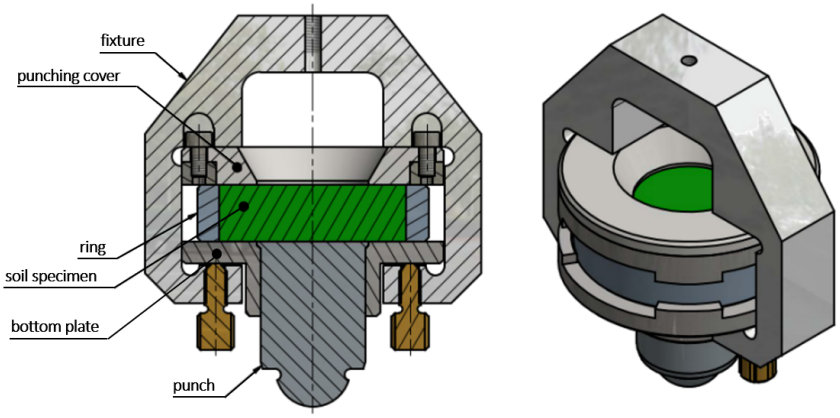

Figure 3.6: Sketch of the shear punching apparatus and its components (Kalén et al., 2023). Adapted with permission.

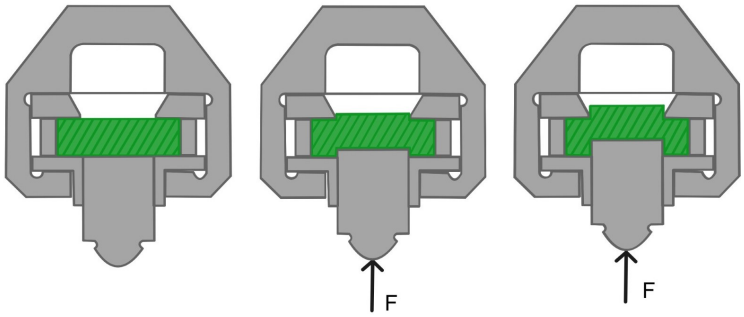

Figure 3.7: Sequences of the shear punching test.

In order to reduce the friction between the surfaces within the apparatus that are subjected to significant frictional forces, the surfaces have been treated to reduce friction. Deformation is measured with a linear transducer. Following series of trials, it was determined that a constant rate of 0,8 mm/min was the most beneficial. As this method was designed to replace or complement the fall-cone test, it was essential that the test would not take an excessive amount of time to perform. Consequently, the rate is considerably higher than that of other tests, for instance, the DSS test.

Figure 3.8: The shear punching apparatus in the SGI laboratory.

The test is initiated by first trimming the soil specimen to remove excess soil (Kalén et al., 2023). The process continues by weighing the ring and the ring with the specimen to determine the density of the soil specimen. Subsequently, the specimen and ring are mounted in the fixture and the load frame is set to the right level, below the end of the punch, before the compression is initiated. The specimen is mounted with the side exhibiting the least visual disturbance oriented downward toward the punch. During the test, the total force and deformation are measured. The test is conducted until the resulting curve provides sufficient information for the purpose. In the majority of cases, the shear strength can be evaluated at 1-4% deformation of clay, however, the test is often run longer until the curve stabilizes.

Based on the measured punching force, the shear stress can be calculated according to Equation 3.7. F is the punching force and A is the lateral area of the sheared part of the specimen. The value 10 is included to convert the answer to kPa, i.e. $1N/cm^2 = 1kPa$ (Kalén et al., 2023).

$$\tau = \frac{F}{A} \times 10 \tag{3.7}$$

The shear stress (kPa) is presented in a graph plotted against the deformation (%), which generates a failure curve, as illustrated in Figure 3.9 (Kalén et al., 2023). The maximum value of shear stress observed in the failure curve, prior to failure represents the undrained shear strength. It is necessary to make corrections due to the self-weight of the punch and the reduced lateral area of the sheared part of the specimen that occurs when it is no longer in contact with the original specimen.

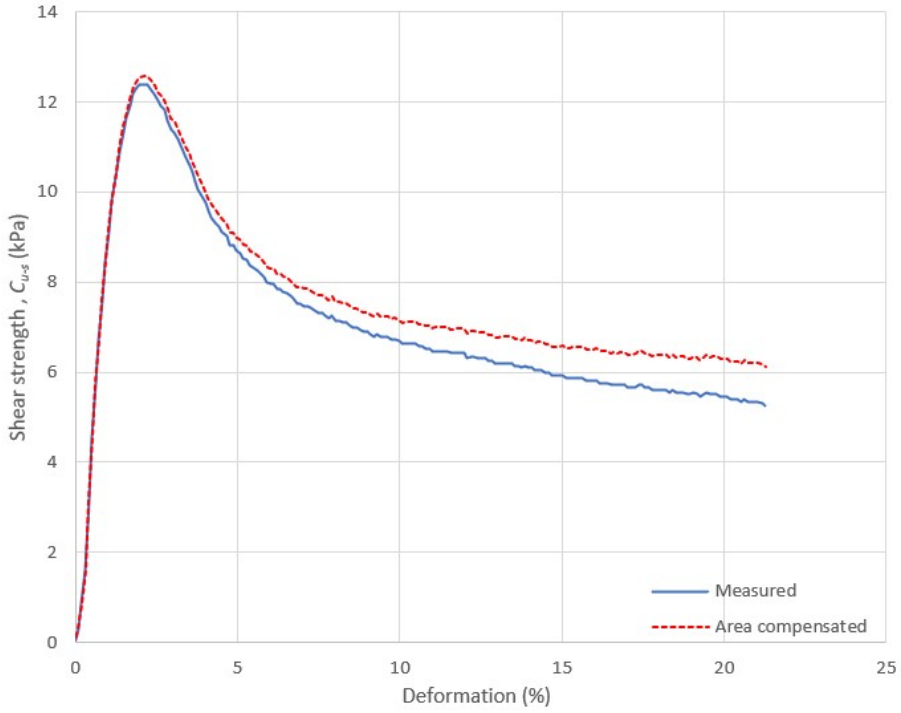

Figure 3.9: Presentation of the failure curve obtained from the shear punching test.

The failure curve can also be used for the determination of additional parameters (Kalén et al., 2023). Nevertheless, this has not yet been established and requires further investigation. The initiating part of the curve, until failure occurs, can possibly be used to evaluate the shear modulus, G. The part of the curve describing the soil behavior right after failure could potentially be correlated to the brittleness of the soil. The area under the failure curve, until the minimum residual strength, represents the energy needed to shear the specimen. This energy may be related to the work required to disturb the soil to its minimum strength, also known as the soils rapidity.

SGI's investigation into the shear punching test has primarily focused on soils with clay as the main fraction (Kalén et al., 2023). Approximately 25% of the specimens were identified as somewhat gyttja-bearing or gyttja-bearing clay, while a comparable portion contained silt, fine sand, shell remains and/or organic matter. The majority of the specimens contained sulphides.

The results of the tests conducted indicate that the shear strength values obtained through the shear punching test tend to be higher than those derived from DSS tests. This may partly be due to the higher rate of deformation observed in the shear punching test (Kalén et al., 2023). This suggests that the results of the shear punching test must be adjusted in order to achieve closer alignment with the shear strength obtained from the DSS test. The correlation factor is derived from regression analysis, in contrast to the shear strength evaluated from the fall-cone test, which is corrected based on the liquid limit.

In the initial investigation of the shear punching test, regression analyses for DSS tests were compared to shear punching and fall-cone tests (Kalén et al., 2023). Furthermore, the fall-cone test results were also compared to those obtained from the shear punching test. This analysis showed the strongest correlation between the DSS test and the shear punching test, with the highest coefficient of determination (R^2 = 0.88). A correlation factor was developed based on the regression line to obtain a 1:1 relationship between the DSS and shear punching results. The equation used to adjust the shear strength from shear punching is shown in Equation 3.8, where C_{u-s} represents the shear strength obtained from the shear punching test. This correlation factor incorporates several factors, including the punching speed and the fact that the shear failure occurs vertically rather than horizontally, as in the DSS test.

$$C_{u-s(corr)} = 0,7531 \times C_{u-s} + 1,6596 \tag{3.8}$$

However, it is observed that there is a greater difference between the methods as the shear strength increases (Kalén et al., 2023). The differences between the DSS, fall-cone and shear punching tests are more significant when the shear strength exceeds 20 kPa, and it is more challenging to discern a correlation. In the subsequent in-depth study with a larger number of high-quality specimens, a new regression analysis was performed, resulting in a higher coefficient of determination ($R^2 = 0{,}95$) and a new equation for the calibration, as shown in Equation 3.9. This equation results in a better compliance at higher shear strengths than Equation 3.8.

$$C_{u-s(corr2)} = 0.6751 \times C_{u-s} + 2,6066 \tag{3.9}$$

A third calibration equation has also been developed, but with requirements of passing through origo and is presented in Equation 3.10.

$$C_{u-s(corr3)} = 0.7301 \times C_{u-s} \tag{3.10}$$

In this thesis, the Equations 3.9 and 3.10 will be referred to as *calibration equation 2* and *calibration equation 3*, respectively, or abbreviated as *corr2* and *corr3*. These equations will be further analyzed in this thesis.

A comparison of results from fall-cone tests corrected with the liquid limit with those from DSS tests revealed a lower coefficient of determination than when comparing DSS with shear punching (Kalén et al., 2023). This suggests that the shear punching test may have the potential to become a standardized method in the future.

The shear punching test offers a number of advantages. Primarily, it is considered a cost-effective approach, with costs comparable to those of the fall-cone test. Additionally, the method is relatively fast, taking approximately 5-10 minutes (Kalén et al., 2023). Furthermore, the results of the regression analysis indicate that it may be more reliable than the fall-cone test. Another advantage of the shear punching test is that it generates a geometrically well-defined shear failure, which can be more

easily derived mathematically in comparison to the fall-cone test.

However, one potential limitation of the method is that the direction of mounting the test is not considered. This includes the orientation of the test in relation to the deposition of the soil. While this may not affect the result, it has not been investigated. Additionally, the fall-cone test is the only laboratory test capable of determining the sensitivity of a soil (SGI, 2018). Consequently, in instances where the sensitivity is necessary, it cannot be assumed that the shear punching test can completely replace the fall-cone test.

3.3 Other punching methods internationally

The testing of shear strength by punching out a sample is already a well-established practice, even though it is typically employed in other, more solid materials. A few of the today existing and practised methods are presented in the following section.

3.3.1 Dynamic shear punch method

The dynamic shear punch method is a method is used for the analysis of brittle and solid materials primarily (Huang et al., 2011). As opposed to the shear punching test, this method is dynamic, and thereby measuring the dynamic shear strength of the material. The dynamic load is applied via a split Hopkins pressure bar system, which applies the force as a pulse to the specimen. The machine is mounted vertically, which eliminates any self weight from the punch on to the specimen. The method has been tested on a variety of materials, including sandstone, composite materials, concrete and marble (Huang et al., 2011; Yao et al., 2017).

3.3.2 Shear punch test

Another similar method is called the shear punch test, which is abbreviated as SPT (Guduru et al., 2005). This method is primarily used in the analysis of metals such as steel, aluminium, zinc and brass but can also be used for the analysis of other materials. Nevertheless, there are some differences between the SPT and the method analyzed in this thesis. For instance, the specimen thickness is considerably smaller, ranging from 255 to 910 micrometers. A series of tests were conducted to investigate the impact of the sample thickness on the results. The results indicate that within a certain range, this is not the case. Another difference is that the specimen is punched from above, which necessitates the inclusion of the self-weight of the punch when calculating the forces required for failure.

3.4 Comparison between methods

Despite the small depth and level differences, natural soil can exhibit significant variations in its properties (Kalén et al., 2023). Even at different depths within a

piston sample, the variation of the evaluated shear strength can vary considerably. For shear punching, DSS and fall-cone tests, only a small amount of soil is used to evaluate the shear strength, which means that the variation in results between the methods can largely be a result of natural variations in the soil.

In the report *Indexförsök för bestämning av odränerad skjuvhållfasthet* (Kalén et al., 2023), duplicate specimens from block samples were analyzed. The results of the report indicated that the variation in the DSS test and shear punching test was reasonably similar, although the variation is not significantly large. When the shear punching was calibrated against the DSS, the variation was slightly smaller. This result will be further analyzed in the report.

The shear strength evaluated from the fall-cone test is typically lower than the shear strength obtained from the DSS test. In contrast, the shear punching test is expected to yield a higher shear strength than the DSS-test (Kalén et al., 2023). However, the shear strength evaluated from the shear punching test is expected to be lower than that obtained from the active triaxial test. The rate and direction of shearing exert a significant influence on the magnitude of the shear strength in cases were the conditions are anisotropic. The strain rate for shear punching is 0.8 mm/min, while that for the direct shear test is 2 mm/day, corresponding to a strain rate of 320 %/h and 0.17 %/h, respectively. As illustrated in Figure 4-46 of the report *Manual on Estimating Soil Properties for Foundation Design* (Kulhawy and Mayne, 1990), an increase in the strain rate by one log cycle is generally associated with an increase in the undrained shear strength by approximately 10 percent. Given the difference in strain rate between shear punching and DSS, it can be anticipated that the shear strength will differ by approximately 30 percent.

4
Methodology

This chapter will describe the methodology used to complete the different modules of this master thesis. An overview is presented in Figure 4.1.

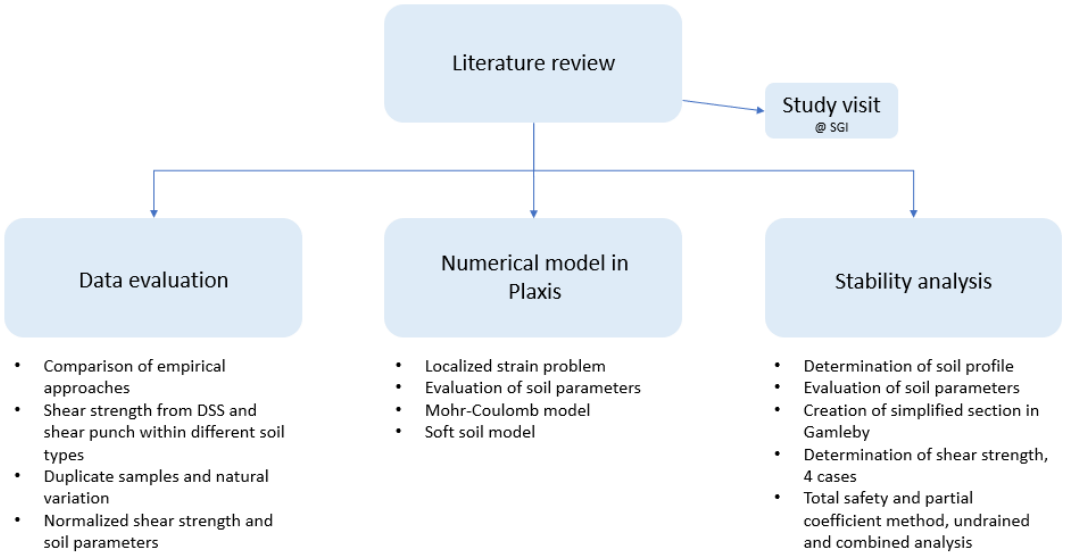

Figure 4.1: An overview of the main modules of the methodology.

4.1 Literature review

A comprehensive literature review was initially conducted in order to gain a deeper insight into the background of the field of study. The review was based on both books and specific online databases and included an historical overview of the shear punching test, an examination of existing tests for evaluation of shear strength, and relevant material models in Plaxis 2D. Furthermore, a study visit to SGI's geotechnical laboratory was made, during which shear punching and fall-cone tests were observed, as well as the equipment used for other tests that determine shear strength.

4.2 Data evaluation

Following the completion of the literature study, the available data from shear punching tests were collected and evaluated. SGI provided a sorted database with results from 143 shear punching tests, which excluded soil samples with unfavorable remarks or disturbances. Three samples from Gamleby that were excluded due to the observation that they did not fill the test ring radially were included in the analysis to provide additional data from Gamleby and soil samples with the main designation of gyttja. In addition, data from 16 soil samples were provided by LabMind. Table 4.1 presents the number of shear punching tests, DSS tests, and fall-cone tests used in the evaluation.

Table 4.1: Number of soil samples analyzed by each test method.

Method	**Number of samples**
Shear punching	162
DSS	154
Fall-cone	136

The given test results were initially evaluated in comparison with two empirical approaches: the Hansbo formula and the SGI recommendation, which is explained in Chapter 2.2.1. The empirical values calculated using Hansbo's formula were plotted against the shear strength (corr3) obtained from the shear punching test. Similarly, the empirical values provided by the SGI recommendation were plotted against the shear strength (corr3) from the shear punching test. When calculating the empirical values based on the SGI recommendation, a was calculated with reference to the direct shear test, and b was set to 0,8.

The shear strength distribution from shear punching, DSS, and fall-cone tests were then compared based on the content of the soil samples. The soil samples were divided into three groups, as presented in Table 4.2.

Table 4.2: Group formation for comparing shear strength distribution based on sample content.

Group	Variations within group	No. of samples
Clay (Cl)	Cl, Cl (su), Cl (su) Cl)su(, Cl sh su, Cl (sh) (su) Cl (sh) su, Cl (si) (su), Cl (fsa)	66
Laminated clay (vCl)	vCl, (v)Cl, vCl (si), vCl si vCl (si) su, vCl su, (v)Cl su (v)Cl pr su, vCl sh su (si)vCl (si) (su), sivCl (si) (sa) (su), vCl (su)	47
Analyzed soil types with evaluated higher organic content, e.g. gyttja	(gy)Cl (su), gyCl (su), gyCl su (gy)Cl su, gyCl (sh) su gyCl (pr) su, gyCl, (gy)Cl pr gyCl fsa su, (gy)siCl pr,gyCl su, clGy su, clGy (su), clGy pr	32
Designation unknown	-	17 *

** Not included in the comparison of the shear strength distribution between the groups.*

The measured shear strength values obtained from the shear punching and fall-cone test were then normalized against the shear strength values measured by the DSS test (C_{u-ds}). This creates a ratio between the shear strengths, as well as a unitless value for comparison. This is done in order to enable the investigation of possible ranges where the shear punching test is more appropriate. The following parameters were then plotted against the normalized shear strength:

- Density, ρ
- Sensitivity, S_t
- Liquid limit, W_L
- Water content, W_N
- Total organic carbon, TOC
- Permeability, k

The graphs that included density, liquid limit and water content were selected based on the amount of data and dispersion, with the objective of further analyzing outliers. A range with an upper and lower limit of 1,3 and 0,7 was applied. The upper and lower limits represent two standard deviations which were chosen as appropriate limits based on reasonable assessments.

4.3 Stability analysis

Subsequently, a stability analysis was conducted using the SLOPE/W Geostudio 2020 software, version 10.2.2.20559. Based on the available borehole data and dock

geometry information, section C was selected as the most appropriate for the analysis. Further details of the selected section can be found in Appendix B. The section was plotted using data from boreholes adjacent to the section. In all analyses, the *grid and radius* tool were used to identify the critical slip surface, were the minimum slip surface depth was set to two meters.

The trend of the undrained shear strength with depth was evaluated for the four different cases presented in Chapter 5.2. Subsequently, the unit weight and friction angle parameters were evaluated based on laboratory data or, alternatively, determined in accordance with the recommendations in TK Geo 13. The friction angles and unit weights for fill, friction material, and till in combination with the friction angle for clay were based on TK Geo 13. In addition, partial coefficients, γ_M, and the conversion factor, η, have been derived for calculations using the partial coefficient method, based on IEG Report 6:2008 Rev 1.

Finally, undrained and combined analyses were conducted for all four cases using the total safety method and the partial coefficient method.

4.4 FE model of the shear punching test

A two-dimensional axisymmetric model of the soil sample and selected components of the shear punch apparatus was constructed in Plaxis 2D, version 22.01.00.452 to simulate the test. In order to minimize friction, interfaces were placed between the soil and steel blocks. Additionally, a prescribed displacement was also placed at the outer edge of the punch to induce a deformation in the soil sample. Further details on the model can be found in Chapter 5.2.

Three soil samples from Gamleby were selected for analysis in Plaxis, 23AW03 at 6 m depth and 23AW04 at 3 and 5 m depth. Based on the results of the laboratory tests, material parameters were developed for the constitutive models Mohr-Coulomb and Soft Soil for each soil sample. For the Soft Soil model, the modified compression and swelling index $\lambda*$ and $\kappa*$, also called the stiffness parameters, were optimized using the Soil Test tool in Plaxis by comparing simulated curves to those obtained in the CRS test. Subsequently, material parameters for steel blocks and steel interfacing were developed.

The analyses conducted with the Mohr-Coulomb constitutive model were divided into three phases: an initial phase, a phase where all interfaces, steel blocks, and boundary conditions were activated, and finally one phase where a prescribed displacement of 3 mm on the punch was activated. The mesh used in the analysis was very coarse, but along edges of the model it was refined.

The analyses conducted with the Soft Soil constitutive model were divided into two phases: an initial phase inducing field stress to the soil sample and a phase 1 were steel blocks, interfaces and the prescribed displacement were applied. A fine mesh

was used for the Soft Soil model. The reason for using a coarser mesh in the Mohr-Coulomb constitutive model was due to problems with localized strain and mesh dependency, which was not a problem to the same extent when using the Soft Soil constitutive model.

The objective of the analysis was to determine the stresses in the punch required for causing failure in the three soil samples. This was extracted by plotting stress and deformation in stress nodes as close to the middle of the punch, i.e. in the lower left corner, as possible. These graphs were then compared with the stress required in the laboratory. Other results were also extracted from Plaxis, for example the total deviatoric strain to observe the generated shear zone, stress-strain plots and excess pore pressure.

5
Technical specifications

This chapter introduces the case study area in Gamleby Harbor and describes the technical specifications of models created in Plaxis 2D and SLOPE/W. It explains the material models used in Plaxis 2D, including the relevant parameters and how they are derived. Additionally, the four different cases in the stability analysis in Gamleby using SLOPE/W are described, as well as the data used in the calculations.

5.1 Case study

The thesis is partially based on an ongoing stability study in Gamleby Harbor, commissioned by Västerviks Municipality and carried out by the geotechnical consulting company Awer at the municipality's request. The harbor is currently closed due to significant stability issues that pose a risk to visitors (Awer Geoteknik, 2023). Along the dock, there are structural elements that have a certain stabilizing effect. However, these are considered to be inadequate and should not be included in a stability analysis because of their poor condition. An example is wooden piles that are likely to have rotted or cracked.

Through SGI, Awer has performed laboratory analyses on soil specimens from the area, which will serve as the primary focus of the stability analyses. The methods used to determine the shear strength of the specimens include CPT, fall-cone test, DSS test, CRS test, shear punching test, and triaxial test. The main soil types in the area have been identified as clay, clayey gyttja and gyttja-bearing clay based on the soil specimens.

Gamleby Harbor is situated approximately 20 km northwest of Västervik. An orientation of the area can be found in Figure 5.1.

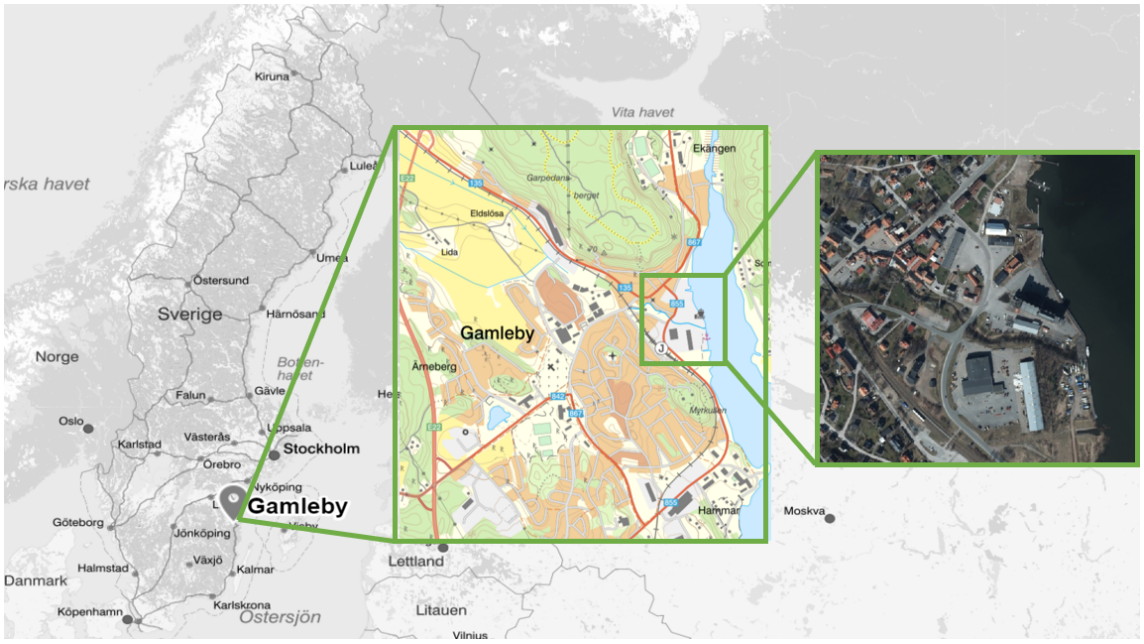

Figure 5.1: Orientation of Gamleby and Gamleby Harbour (©Lantmäteriet).

Figure 5.2 shows SGU's soil type map on the left and soil depth map on the right over Gamleby Harbor. The soil map indicates that the surface layer in the area of interest is primarily composed of glacial clay or fill material with an underlying layer of clay and silt. The estimated soil depth varies between five and twenty meters, which is confirmed by several geotechnical investigations in the area. The depth to the bedrock surface has not been confirmed by soil-rock probing (Awer Geoteknik, 2023). It is assumed that the water table in the majority of the area is at the ground surface.

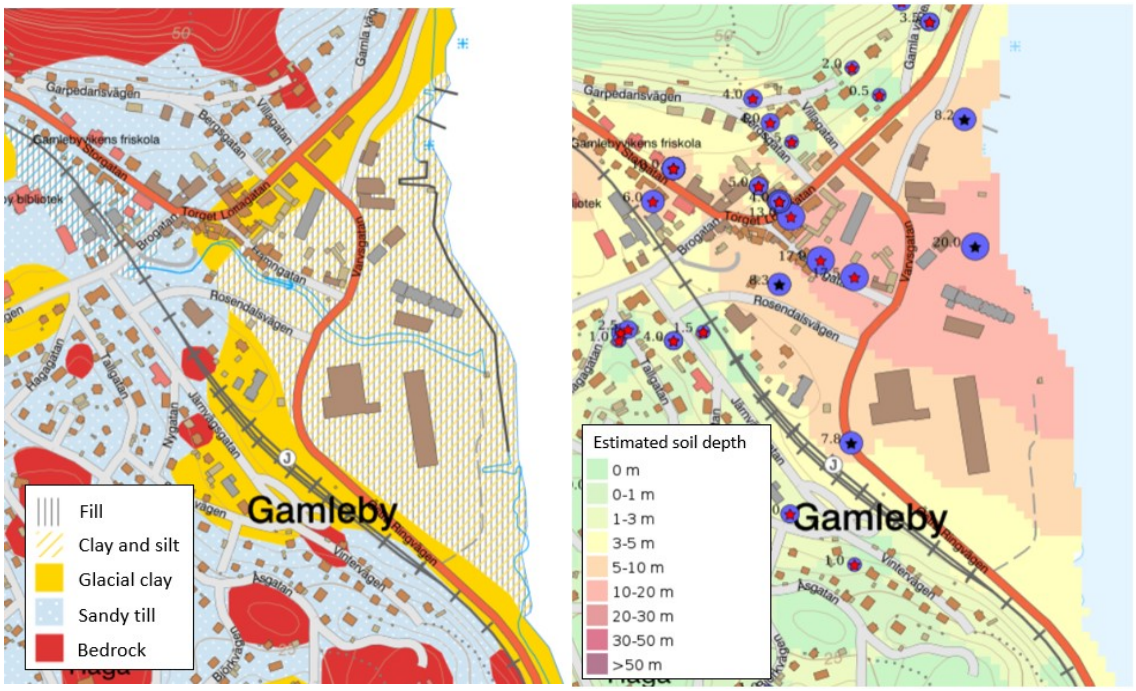

Figure 5.2: Overview of surface characteristics and soil depth in Gamleby harbor (©Geological Survey of Sweden, 2024).

Figure 5.3 shows the density, water content, and liquid limit as a function of depth obtained from boreholes that can be seen in Appendix A. The soil layer sequence consists of both gyttja and clay layers, which results in a relatively broad range of water ratio and liquid limit values. The measured shear strength, obtained from CPT, fall-cone, DSS and shear punching (corr3), is low and increases only slightly with depth, as illustrated in Figure 5.4.

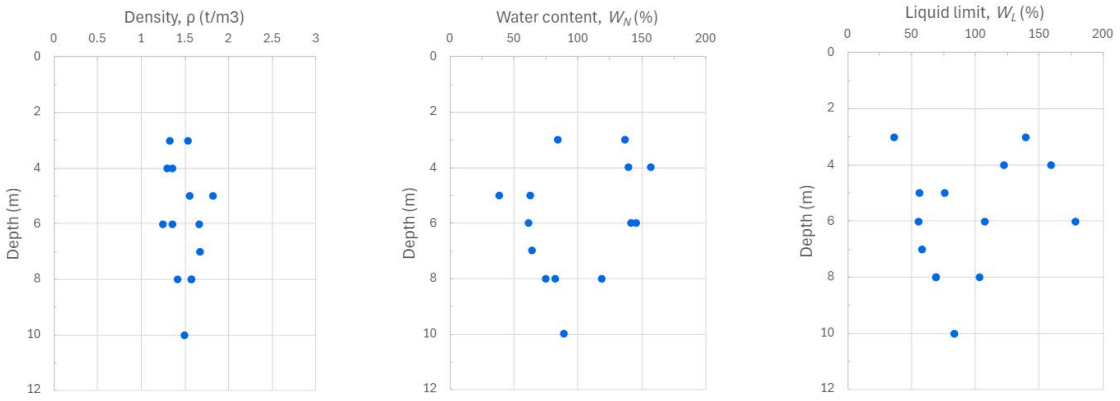

(a) Density **(b)** Water content **(c)** Liquid limit

Figure 5.3: Soil parameters in Gamleby plotted against depth.

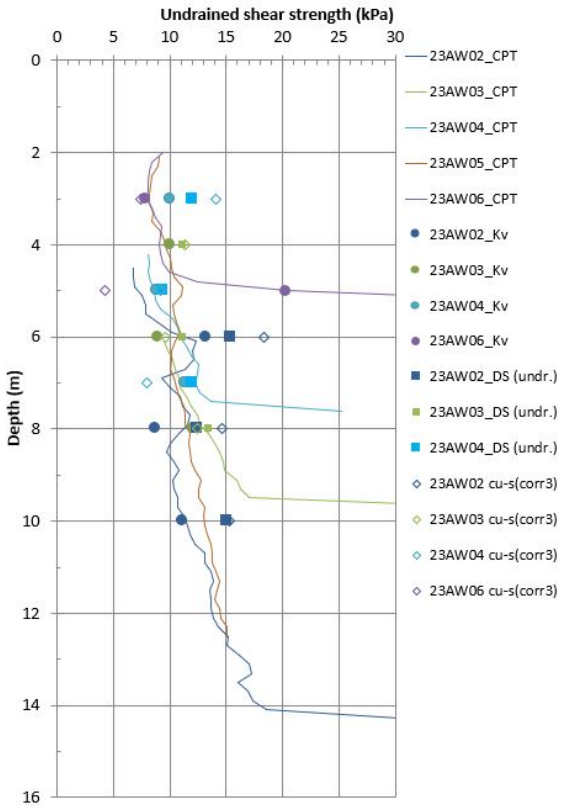

Figure 5.4: Undrained shear strength in Gamleby.

5.2 Stability analysis in Gamleby

The geometry of cross section C is presented in Appendix B while an overview of the location of the section is found in Figure 5.5. The thickness of the soil layers was determined using the given boreholes situated in proximity to the section. The water level is assumed to be at ground level. The section has been simplified for the purpose of analyzing the difference between different shear strengths obtained by different methods, rather than the safety factor for the slope, by ignoring buildings and roads (loads) and slightly adjusting the geometry.

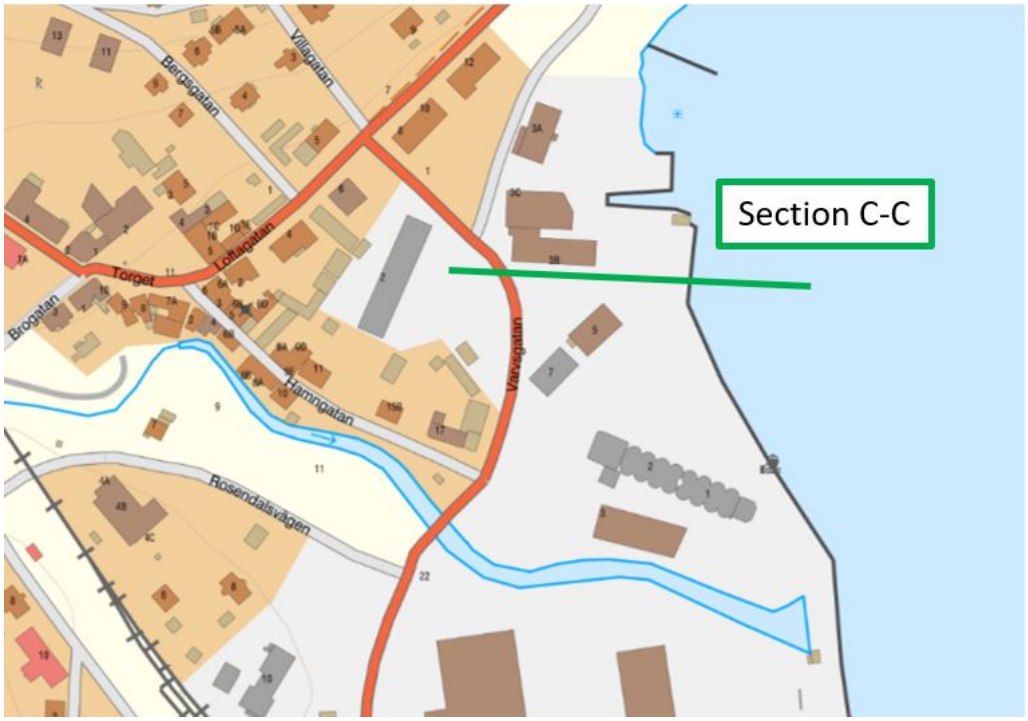

Figure 5.5: An overview of the location of Section C in Gamleby Harbor based on the geotechnical investigation report (© Lantmäteriet).

The soil layering was, as mentioned, determined by boreholes in the region of the section. The following layers were identified:

Fill	Consists of gravel, sand, tile bricks, wood chips and organic material.
Gyttja	A soil with high organic content, water content and liquid limit.
Gyttja/clay	The distinction between gyttja and clay is not clearly defined, given that the layering consists of gyttjig clay and clayey gyttja. Consequently, this material was introduced to represent the transition from gyttja to clay.
Clay	Grey in color that exhibits a naturally layered structure, also characterized with content of sulfide.
Friction material	It is probable that this layer is made of sand as the only known information is that it is a more loosely composed layer above the till. No test have been conducted on the material
Till	No test have been conducted on the material but surrounding shallow till is classified as sandy till (Sveriges Geologiska Undersökning [SGU], n.d.).

The evaluation of the shear strength variation with depth is divided into four different cases. In Case 1, the shear strength is assessed using results from CPT and

fall-cone test which are relatively simple and often obtains lower and less reliable results. In Case 2 and 3, the influence of either the shear punching test or the DSS test on the shear strength trend is evaluated. In Case 4 all test results are included.

- Case 1: CPT + Fall-cone
- Case 2: CPT + Fall-cone + DSS
- Case 3: CPT + Fall-cone + Shear punching
- Case 4: CPT + Fall-cone + DSS + Shear punching

The evaluation of trends excluded the shear strength from borehole 23AW01 due to its results being considered misleading for the remainder of the area. Appendix C presents the selected shear strength trend for each case.

The input data for undrained and combined analysis using the total safety method and undrained and combined analysis with the partial coefficient method are presented in Appendices G and H.

For calculations using the partial coefficient method, IEG Report 6:2008, Rev 1 is applied. The partial coefficient $\gamma_{cu} = 1,5$ is used to convert undrained shear strength and $\gamma_{\phi} = 1,3$ is used to convert the friction angle,ϕ. The conversion factor, η_{cu}, used for the soil layers gyttja, gyttja/clay and clay is presented in Table 5.1. For soil layers fill, friction material and till, the conversion factor, $\eta_{\phi'}$, is set to 1.

Table 5.1: Conversion factor, η_{cu}, for Case 1 & 3 and 2 & 4.

Case 1 & 3	
Conversion factor	Selected value
$\eta_{1,2}$	0,95
η_3	1,05
$\eta_{4,5,6,7}$	0,95
η_8	1
$\eta_{cu} = \eta_{1,2} \cdot \eta_3 \cdot \eta_{4,5,6,7} \cdot \eta_8 = 0,95$	

Case 2 & 4	
Conversion factor	Selected value
$\eta_{1,2}$	0,95
η_3	1,1
$\eta_{4,5,6,7}$	0,95
η_8	1
$\eta_{cu} = \eta_{1,2} \cdot \eta_3 \cdot \eta_{4,5,6,7} \cdot \eta_8 = 0,99$	

5.3 Numerical models of the shear punching apparatus in Plaxis 2D

The shear punching apparatus is modeled as axisymmetric models in Plaxis 2D, as illustrated in Figure 5.6. A three-dimensional visualization of the model is presented in Figure 5.7. The model comprises a blue block representing the soil specimen and two pink blocks representing the punch on the left and fixed base plate on the right. The punch and fixed base plate included in the model to easily be able to obtain an evenly distributed stress required to fail the soil specimen. Figure 5.6 also indicates the location of the point used for stress-strain plots, which is situated in the middle of the shear zone.

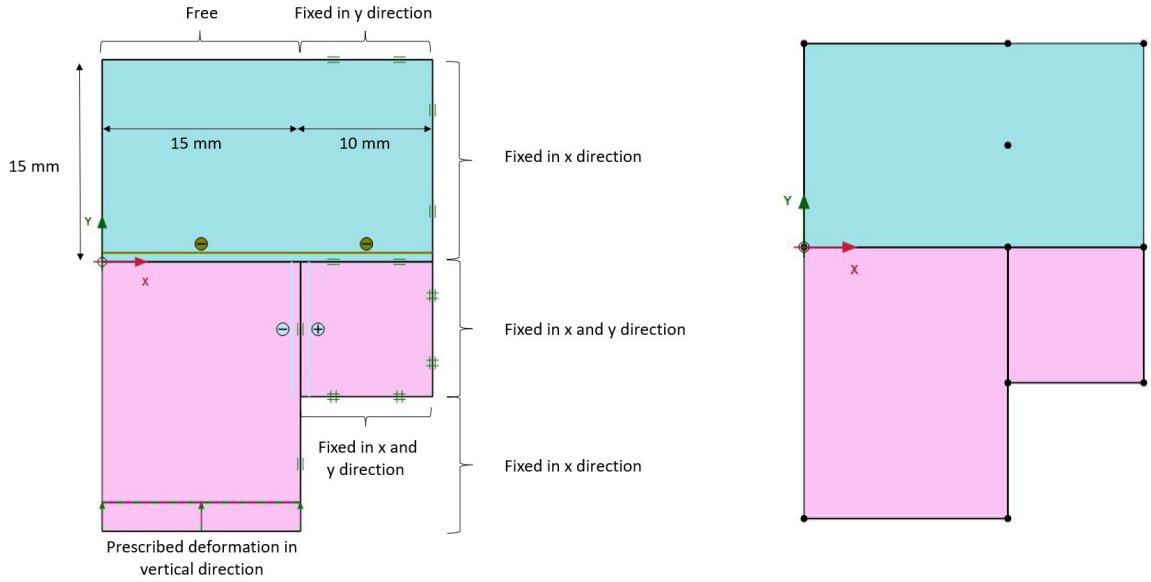

Figure 5.6: Axisymmetric model of the shear punching apparatus in Plaxis 2D (left) and point used for stress-strain plots (right).

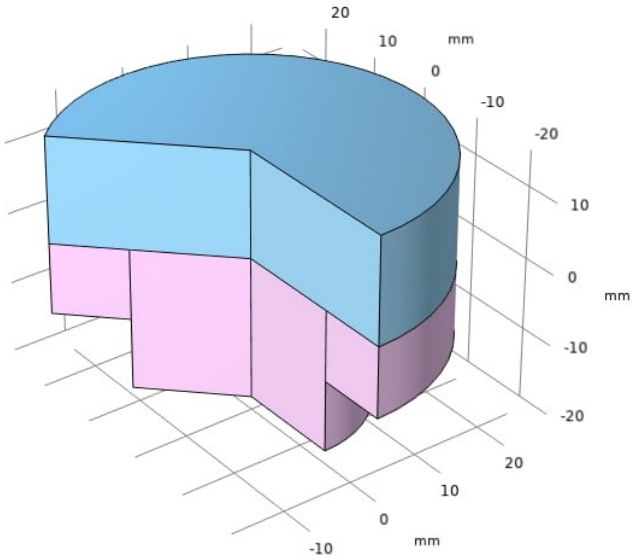

Figure 5.7: The axisymmetric model of the shear punching apparatus as a 3D model with a cross sectional view.

The interface between the two pink steel blocks has been designed with the objective of minimizing friction. The interface adjacent to the soil has been designed to create a realistic interaction between it and the surrounding materials. The material parameters used in the MC model and SS model can be found in Tables F.1 and F.2 in Appendix F.

Young's modulus, E_{ref}, is calculated using Equation 5.1, where G is the shear modulus evaluated as G_{50} from the DSS tests.

$$E = 2 \cdot G(1 + \nu) \tag{5.1}$$

The analysis of the MC model conducted in Plaxis 2D is divided into three different phases, with the initial phase and phases 1-2. The initial phase is designated as K0-procedure calculation type with staged construction. The purpose of this phase is to initiate the materials, soil and steel blocks, into the calculation. The subsequent phases 1-2 are all plastic calculations, also with staged construction. Settings such as updated mesh, ignored suction and ignored undrained behavior are also employed. Phase 1 initiates the incorporation of additional elements, such as interfaces between the materials. Phase 2 incorporates a prescribed displacement of 3 mm applied to the punch. The phases are depicted in Figure 5.8.

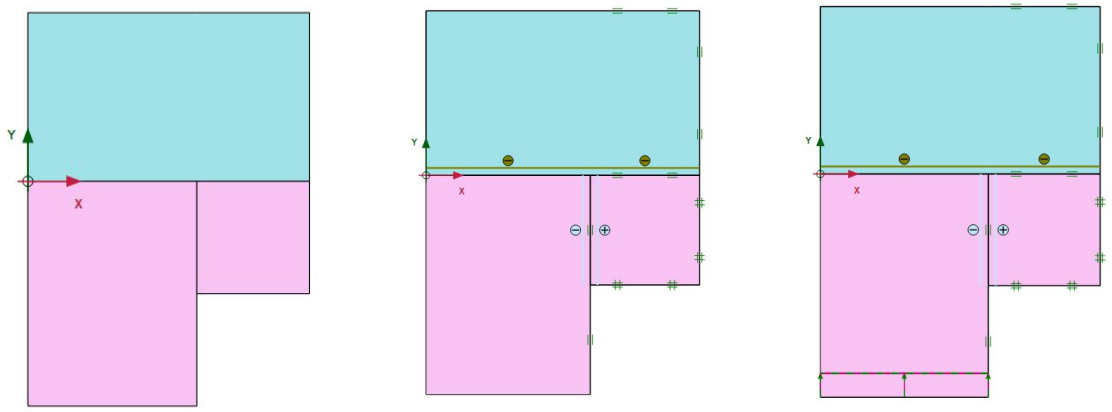

(a) Initial phase **(b)** Phase 1 **(c)** Phase 2

Figure 5.8: Phases for the shear punching test in the Plaxis 2D analysis using the Mohr-Coulomb constitutive model.

In the SS model, the additional elements, such as interfaces between the materials and the deformation are introduced together in phase 1, resulting in a total of two phases instead of three, as can be seen in Figure 5.9. This is done to avoid consolidation before the start of the test. The initial phase is designated as the calculation type field stress, rather than the K0 procedure. The value of the field stresses are presented in Table 5.2. The vertical field stress in Plaxis, σ_1 is equal to σ_v, which is given from the DSS laboratory test. The horizontal field stresses σ_2 and σ_3 are equal to $\sigma_h (= 0,5 \cdot \sigma_v)$. Phase 1 is designated as a consolidation phase with staged construction, with a duration of 0,0034 days, which is the approximate time of the test conducted in a the laboratory.

Table 5.2: Input data for field stresses

Soil sample	σ_v (kPa)	σ_h (kPa)
23AW03 6m	42	21
23AW04 3m	23	11,5
23AW04 5m	31	15,5

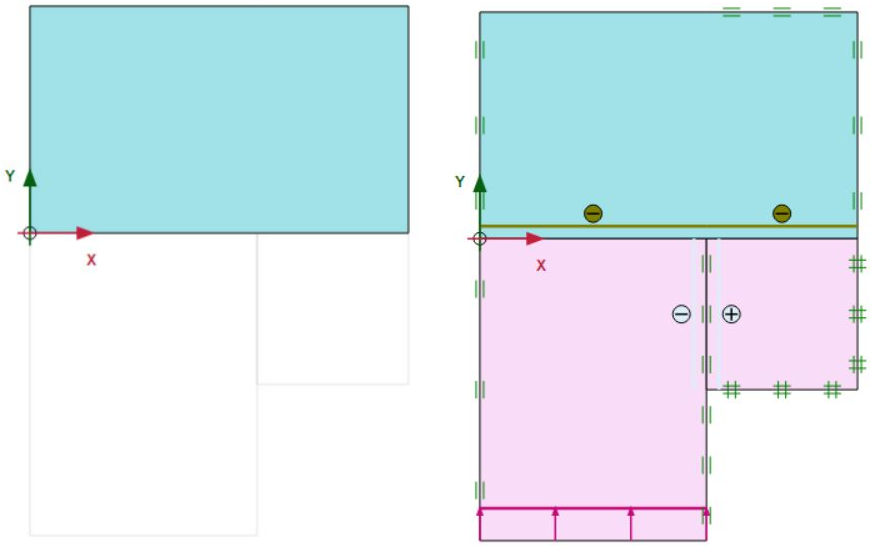

(a) Initial phase **(b)** Phase 1

Figure 5.9: Phases for the shear punching test in the Plaxis 2D analysis using the Soft Soil constitutive model.

The vertical stresses in the punch extracted from the Plaxis models for the three soil samples are compared with the calculated stress from the shear punching performed in the laboratory. The stress in the punch, derived from the laboratory test, is calculated by first determining the reduced area of the shear surface, A_r, using Equation 5.2, where A_s is the total shear surface area (1414 mm^2) and ε_s is the vertical deformation in mm. The force applied to the punch, corrected for the self-weight of the punch, is calculated using Equation 5.3. Subsequently, Equation 5.4 is used to calculate the stress at the center of the punch, where A_p is the surface area of the punch (1,07 cm^2).

$$A_r = A_s - (3 \cdot \pi \cdot \frac{\varepsilon_s}{10}) \qquad [cm^2] \tag{5.2}$$

$$F = \frac{A_r \cdot \tau}{10} - 1,8 \qquad [N] \tag{5.3}$$

$$\sigma_p = \frac{F}{A_p} \cdot 10 \qquad [kPa] \tag{5.4}$$

6
Results

This chapter will present the results of the analyses and investigations conducted on the data evaluated, stability analysis and FE models.

6.1 Evaluation of data

The evaluation of the data entails a comparison of the shear strength obtained from the shear punching test with empiricism. Additionally, the shear strength obtained from the shear punching test is also compared with the shear strength obtained from DSS tests on soil samples with varying contents. Moreover, the distribution of shear strength between the two methods is also included by comparison of duplicate samples. Finally, the evaluation includes an analysis of the normalized shear strengths variation with different soil parameters.

6.1.1 Empirical validation

In Figure 6.1 the two analyzed empirical approaches that were analyzed are presented. As illustrated by the graphs, SGI's recommendation for evaluating empirical shear strength (Equation 2.4) is better aligned with the measured values in comparison to Hansbo's formula (Equation 2.3). The values obtained with Hansbo's formula are frequently higher than those measured with the shear punching test.

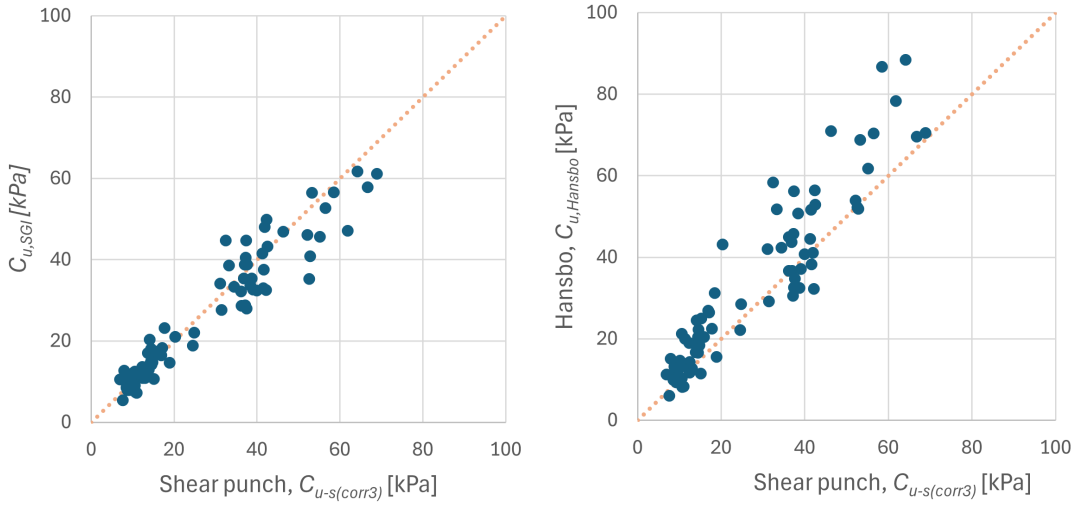

Figure 6.1: Comparison between Hansbos's formula (left) and SGI's recommendation (right) for empirical validation.

6.1.2 Comparison of undrained shear strength from shear punching tests versus direct simple shear tests

Comparisons for the undrained shear strength were conducted in subgroups based on the soil content. The samples were divided into three categories: those containing gyttja, those containing laminated clay, and the remainder, which primarily had clay content. The shear strength obtained from the shear punching test, calibrated with either equation 2 or 3, were compared to the undrained shear strength obtained from the DSS test. Additionally, a few dotted lines are included in the graphs. The yellow line represents a 1:1 relationship between the shear strengths, the dark blue line is the trend line for the data set, and the grey lines show the upper and lower 95% confidence interval.

A comparison of the clay samples, as shown in Figure 6.2, indicates a satisfactory alignment between the trend line and the 1:1 line for both equations 2 and 3. Nevertheless, there is a certain degree of variability in the result, with a few samples falling outside the 95% confidence interval. This is however to be expected given the natural variability among the data.

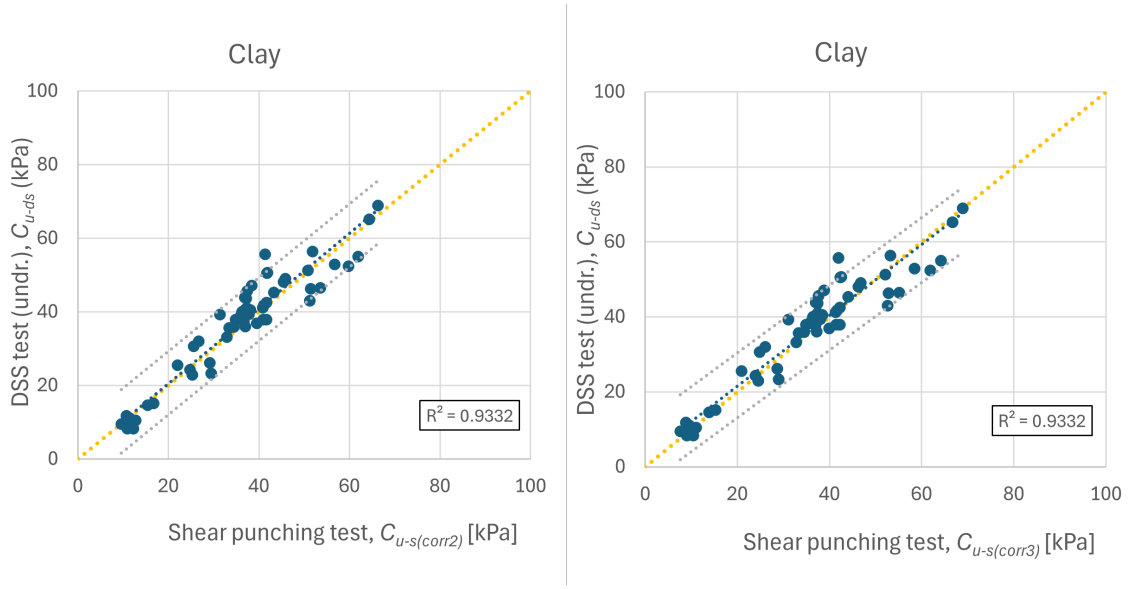

Figure 6.2: Comparison of undrained shear strength for direct shear test and shear punching test, for soils with clay as main content. Comparisons are done for corrections made with both calibration equation 2 (left) and 3 (right).

A comparison of the undrained shear strength for samples containing laminated clay are presented in Figure 6.3. The graphs show a greater degree of variability, which can be explained by the categorization of the clay itself. Laminated clay may contain thin layers of silt or sand, which in turn may result in a greater degree of variability in the shear strength values, since silt and sand have different properties in comparison to clay. When analyzing the trend lines in Figure 6.3, it becomes clear that both exhibit a bit of discrepancy. However, the majority of all samples fall within the confidence interval.

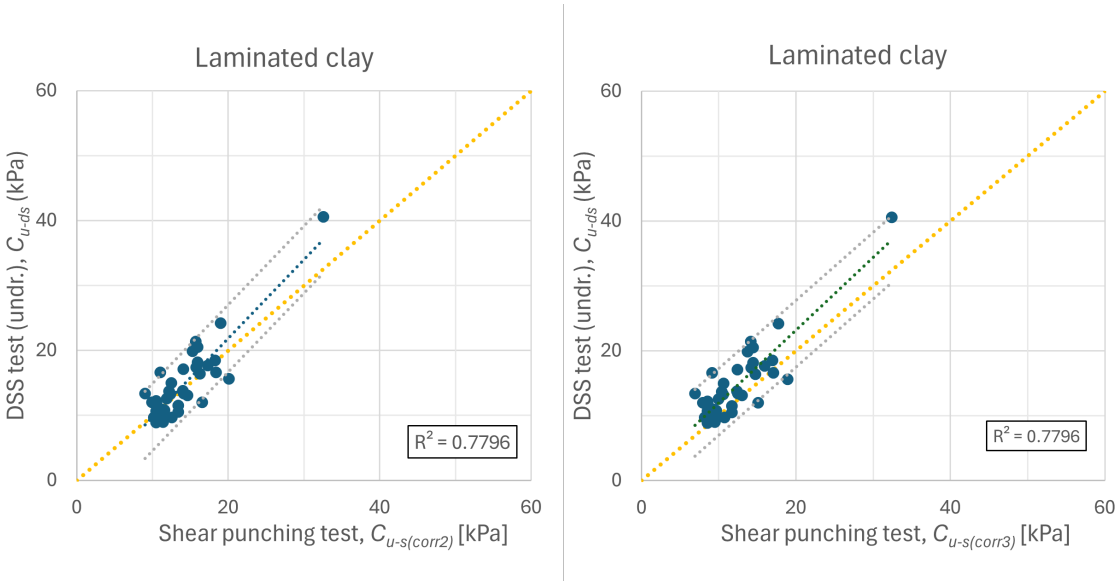

Figure 6.3: Comparison of undrained shear strength for direct shear test and shear punching test, for soils containing laminated clay. Comparisons are done for corrections made with both calibration equation 2 (left) and 3 (right).

The comparison of soil samples containing gyttja, shown in Figure 6.4, shows a satisfactory alignment between the trend line and the 1:1 line, at least for lower shear strengths. There is minimal dispersion in either graphs as well.

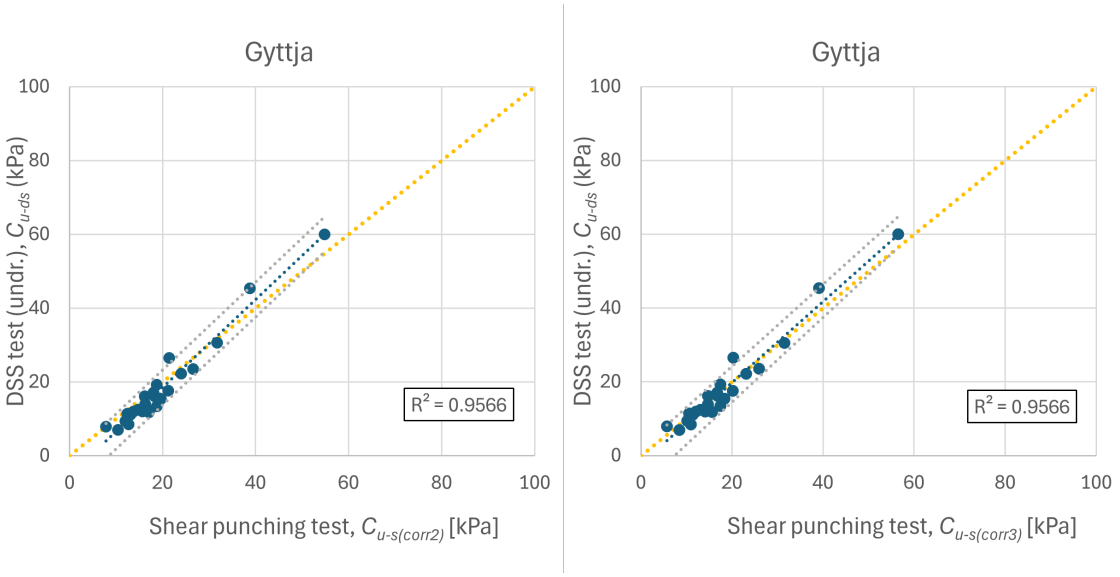

Figure 6.4: Comparison of undrained shear strength for direct shear test and shear punching test, for soils containing gyttja. Comparisons are done for corrections made with both calibration equation 2 (left) and 3 (right).

In all comparisons between calibration equations 2 and 3 in Figures 6.2, 6.3 and 6.4, they appear to be identical, which is not the case. The shear strength values differ by a few kPa, but this is not visible because of the scale. Similarly, the R values are

the same, although there are small variations in the trend lines.

It is important to note that the calibration equations for the shear punching test were developed with regard to the DSS test. Consequently, the values are expected to align with the 1:1 relation line, which is the fundamental purpose of the calibration equation. However, a few samples that were not included in the development of the equation have subsequently been included, and these values appear to be consistent with the calibrations.

6.1.3 Analysis of duplicate samples

To validate the development of the shear punching test against the DSS test, duplicate tests have been carried out on block samples from Skå-Edeby (Kalén et al., 2023). In Figure 6.5, the distribution of the shear strength, for both the shear punching and DSS test, is presented against depth. As the figure illustrates, the difference between the two duplicate tests reaches a maximum of 1,5 kPa for the shear punching test and 2,5 kPa for the DSS test. Nevertheless, neither 1,5 nor 2,5 is kPa is significant, and further tests at greater depths are required to reach a conclusion.

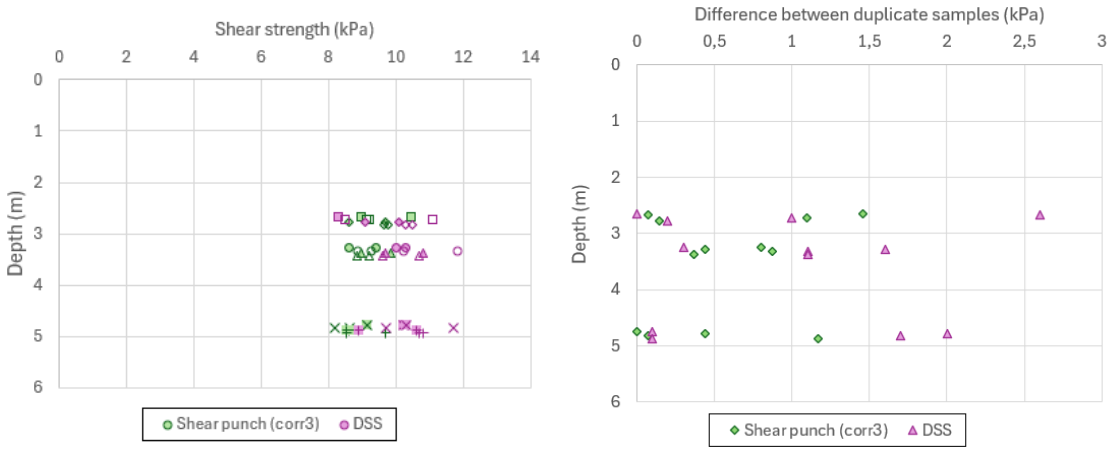

Figure 6.5: Distribution of shear strength (left) and difference in shear strength (right) obtained from DSS tests and shear punching tests of duplicate samples.

6.1.4 Normalized shear strength

Figure 6.6 illustrates the relationship between the normalized shear strength and density, ρ. The yellow lines represent a limit of $\pm 30\%$ compared to the 1:1 ratio, which is approximately two standard deviations. The colored points that fall outside of the limits are considered as outliers and are represented by the same color for each graph, allowing for comparison of variations between ratios or parameters. Outliers in graphs including $C_{u,s(corr2)}$ are colored in the graphs including $C_{u,s(corr3)}$ and vice versa, even if the outlier is now within the $\pm 30\%$ limits. As seen in Figure 6.6a, the majority of the outliers are located above the upper limit, indicating that

the calibration equation 2 typically obtains a higher shear strength for the shear punching test than for the DSS test. The trend line also indicates a tendency for lower shear strengths from the shear punching test at higher densities. Figure 6.6c shows the opposite, with the majority the outliers situated below the lower limit. This indicates that the shear strength obtained from the fall-cone test is typically lower than that obtained from the DSS test. Nevertheless, Figure 6.6b demonstrates the lowest number of outliers, despite a dispersion within the specified limits. Neither of the data sets in Figure 6.6b or 6.6c shows any notable tendencies with their trend lines.

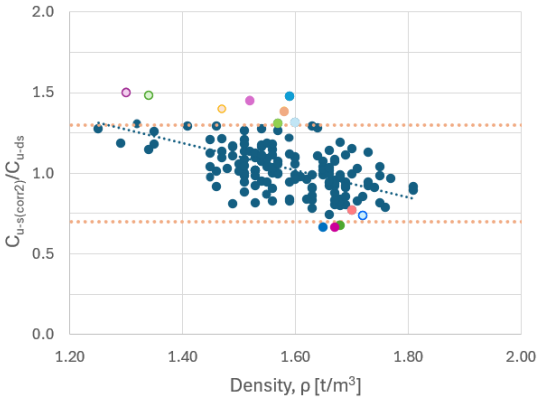

(a) $C_{u,s(corr2)}/C_{u,ds}$ vs. density

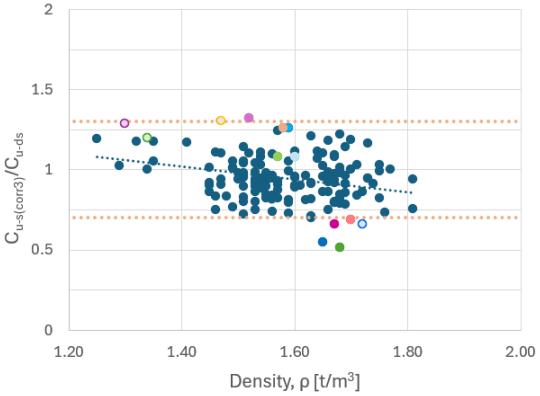

(b) $C_{u,s(corr3)}/C_{u,ds}$ vs. density

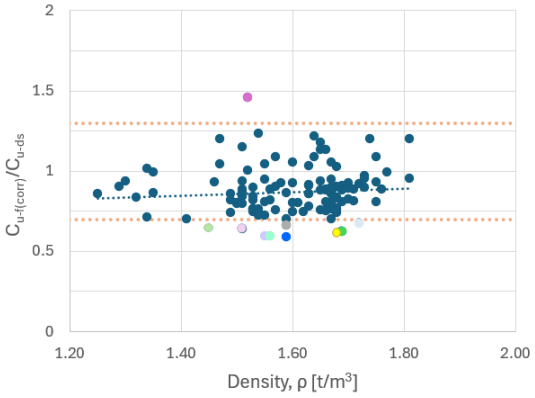

(c) $C_{u,f(corr)}/C_{u,ds}$ vs. density

Figure 6.6: Normalized shear strength plotted with density.

As with the density, the normalized shear strength is plotted against the liquid limit W_L. The plots in Figure 6.7 show the same pattern with higher shear strengths and more outliers from the shear punching test calibrated with equation 2, lower shear strength from the fall-cone test and the least spread with calibration 3. However, the trend lines in the plots in Figures 6.7a and 6.7b show that the shear strength is generally higher at higher liquid limits from the shear punching test than from the DSS test. However, there are fewer values at higher liquid limits which can be misleading for the trend lines. No significant trend is shown in Figure 6.7c for the fall-cone test.

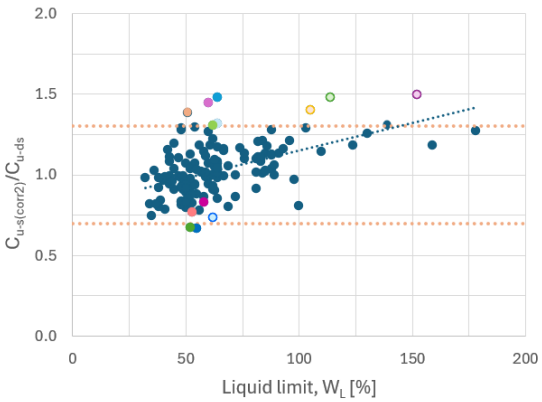

(a) $C_{u,s(corr2)}/C_{u,ds}$ vs. liquid limit

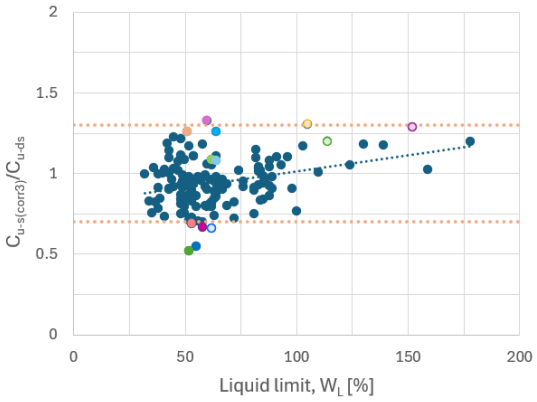

(b) $C_{u,s(corr3)}/C_{u,ds}$ vs. liquid limit

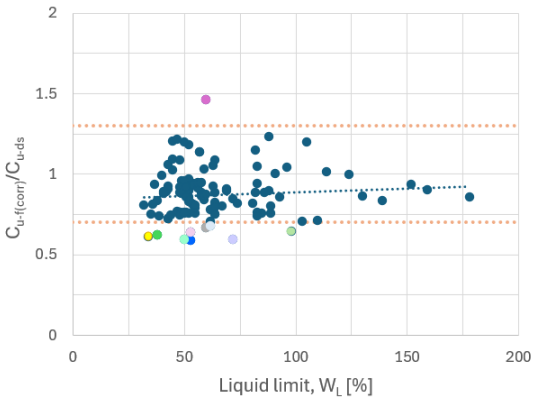

(c) $C_{u,f(corr)}/C_{u,ds}$ vs. liquid limit

Figure 6.7: Normalized shear strength plotted with liquid limit

The normalized shear strength is also plotted against the water content, W_N, in the same way as for the density and liquid limit. The same pattern as observed for Figure 6.6 and 6.7 is also evident in the graphs in Figure 6.8. The graphs show that calibration 2 results in a higher ratio and more outliers compared to calibration 3 and the fall-cone test. The trend lines in Figure 6.8a and 6.8b indicates that the shear strength evaluated from the shear punching test is generally higher than that evaluated from the DSS test at higher water content. However, the number of values with high water content is relatively low, which may result in misleading trend lines. In Figure 6.8c with the fall-cone test, there is no clear tendency.

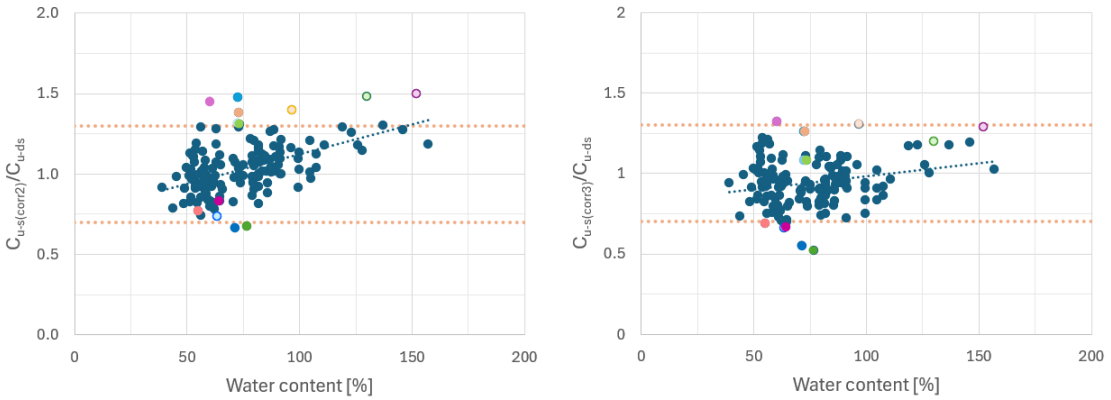

(a) $C_{u,s(corr2)}/C_{u,ds}$ vs. water content **(b)** $C_{u,s(corr3)}/C_{u,ds}$ vs. water content

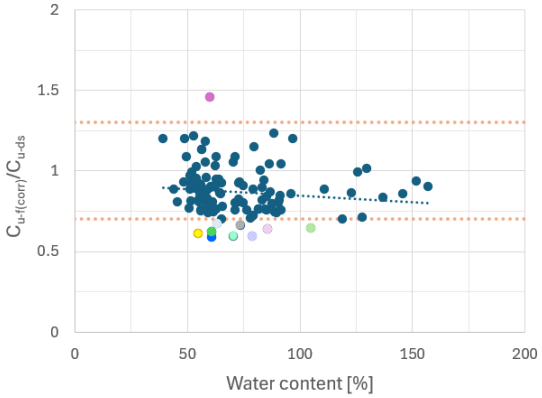

(c) $C_{u,f(corr)}/C_{u,ds}$ vs. water content

Figure 6.8: Normalized shear strength plotted with water content.

Additional graphs displaying the normalized shear strength can be found in Appendix D where parameters such as sensitivity, TOC and permeability have been evaluated. Plots in Figure D.1 all show considerable degree of variability in the data, making it challenging to perform further analysis. The plots in Figure D.2 and D.3, respectively, only includes data from Gamleby, which is insufficient data for drawing any conclusions.

In Appendix E the outliers in the normalized data plots are being classified based on the content of the samples. The outliers in the plots are the same for all parameters and ratios, and the colors remain consistent across all plots, despite the fact that the plots used to classify the outliers are only the ones with density. For the shear punching test, gyttja generally is representative of the outliers with a ratio of 1,3 or above, while laminated clay is representative among the outliers with a ratio of 0,7 or below. It can also be observed that the number of outliers are greater with corr2 than for corr3. For the fall-cone test it is more complex to interpret due to the fact that all soil types are represented among the outliers with a ratio of 0.7 or below.

Further analysis of the observed patterns in the sample content in the plots, within the upper and lower limit, reveals that samples containing silt are distributed uni-

formly within the range 0,7 to 1,3, with a few outliers, both upper and lower. The observed pattern for corr2, corr3 and fall-cone ratio is consistent. With regard to gyttja, the distribution varies between corr2, corr3 and fall-cone. For corr2, the values are typically situated towards the upper limit with a number of upper outliers. The pattern is more similar for corr3 and the fall-cone test, with an even distribution within the interval, with only a few outliers, either only above the upper limit or both. In the case of laminated soil, the values are distributed within the specified interval for all cases, although they are generally situated below 1. This indicates that the DSS test obtains a higher value than the compared method. Laminated clay also contributes with a few outliers.

6.2 Stability analysis in Gamleby

Table 6.1 presents the calculated safety factors for each case, and analysis method. The safety factors are generally the lowest for case 1, although, this is also where the lowest results are expected due to the conservative interpretation of the fall-cone and CPT test results. The outcomes of case 2 and case 4 are identical, as both datasets include results from DSS tests, which is considered to be one of the more reliable test methods. Consequently, the interpretation of the results is not as conservative. The safety factor for case 3 is slightly lower than for cases 2 and 4, as a more conservative interpretation is necessary due to the exclusion of results from DSS tests and the fact that the included tests are less reliable in comparison. Detailed images from all the stability analyses can be found in Appendices G and H.

Table 6.1: The Factor of Safety for the four different cases of the stability analysis.

Case / Analysis	Case 1	Case 2	Case 3	Case 4
Total, undrained	0.848	0.937	0.903	0.937
Total, combined	0.828	0.909	0.876	0.909
Partial, undrained	0.549	0.638	0.578	0.638
Partial, combined	0.544	0.624	0.575	0.624

Table 6.1 shows that all safety factors are below 1, which for the total safety analysis indicates that the slope has already failed with set geometry of soil regions and material parameters. As previously mentioned in Chapter 5.2, there are ground reinforcement used to stabilize the soil, such as sheet pile walls, piles, and anchors. These are however old and damaged and are thus not regarded in the analysis.

6.3 FE model of the shear punching test

The FE model of the shear punching test has been constructed in two separate constitutive models in PLAXIS 2D, the Mohr-Coulomb and the Soft Soil. The results from each model are presented in the following section.

6.3.1 Mohr Coulomb

Figure 6.9 presents three distinct shear zones, extracted from each of the three soil samples, collected from Phase 2 in Plaxis. The shear zones and the subsequent behavior of the soil following failure, exhibit slight differences between samples due to the varying properties of the soil. Due to the simplification of the model in combination with the very coarse mesh, the observed soil movements may diverge from those observed in the actual test. For example, the horizontal displacement of the soil following failure may occur, despite the cone that is present to prevent deformation to some extent, which is not included in this model.

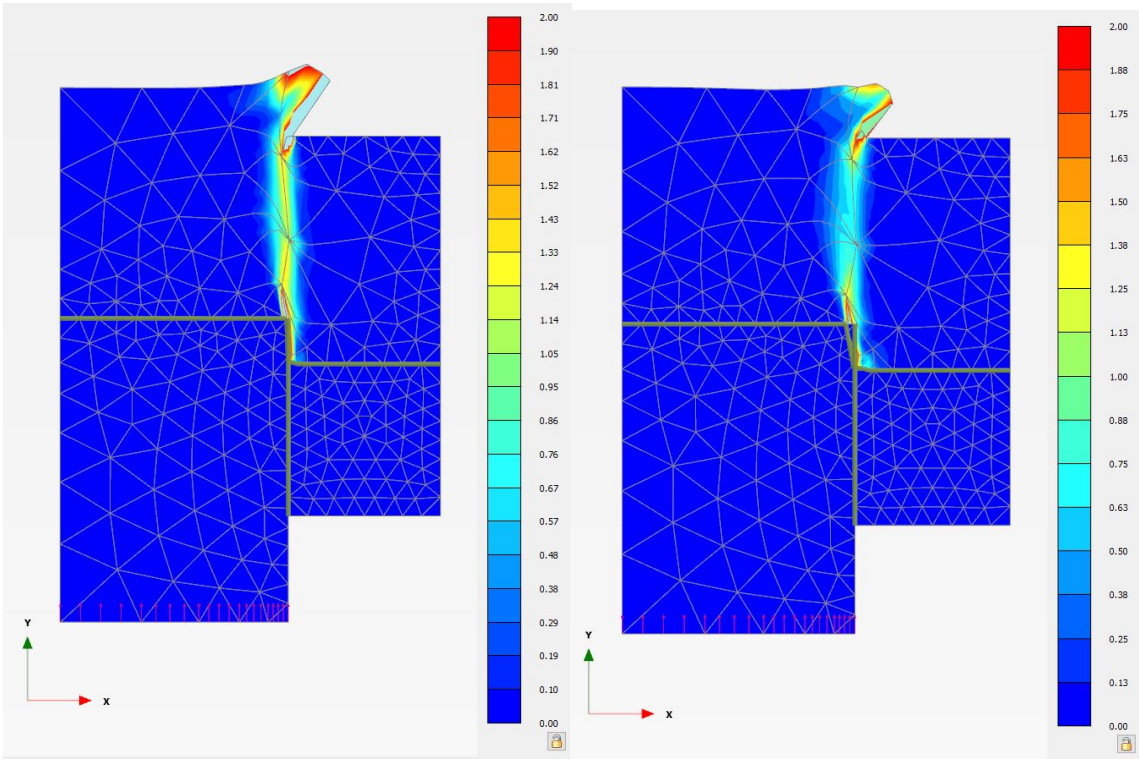

(a) 23AW03 6m

(b) 23AW03 3m

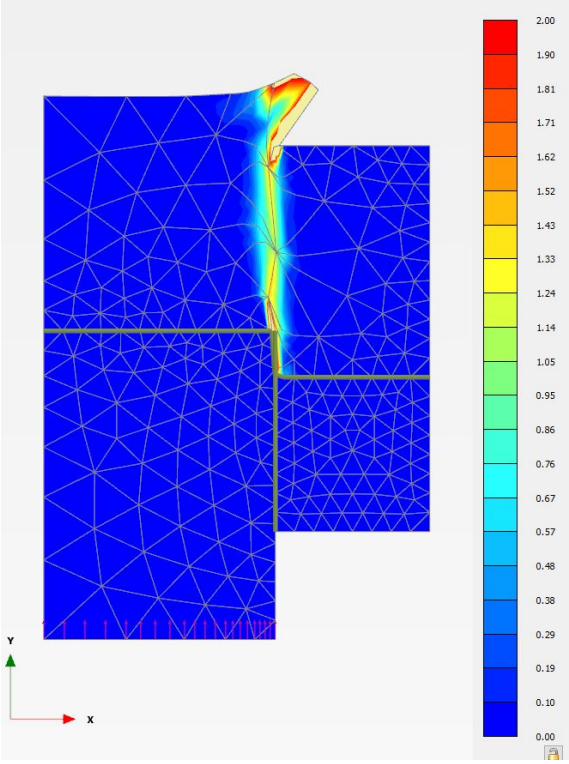

(c) 23AW03 5m

Figure 6.9: Shear zones from the modelled shear punching apparatus after 3 mm deformation, for all three samples.

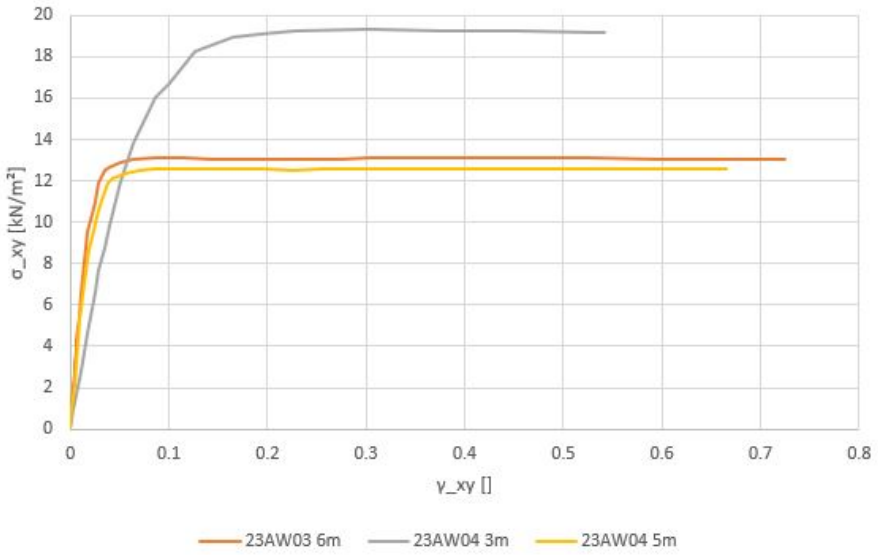

Figure 6.10: Stress-strain plots for a single point located at the center of the shear zone.

Figure 6.10 presents the stress-strain plots for each soil sample. Each plot reaches the predefined shear strength $s_{u,ref}$, with all samples reaching the undrained shear strength at relatively low strain. It can be observed that the curve for 23AW04 (3m) differs from the other two samples. A higher shear strain is obtained before failure occurs. This is likely due to the composition of the sample, which is primarily gyttja, in contrast to the other two samples, which are primarily composed of clay.

The accumulation of stress in the soil and steel blocks is presented in Figure I.1 in Appendix I. In the absence of the stress accumulation, the blocks would be in stress equilibrium with a stress value of 0 kN/m^2. The main stress accumulation is located close to the corner of the punch and the surface between the two steel blocks. This persists even when the fixed steel block adjacent to the punch is excluded from the model. Stress accumulation can occur in corners an in this case is not related to friction in the model.

6.3.2 Soft soil

Figure 6.11 presents the shear zones extracted from each of the three soil samples, collected from phase 1 in Plaxis 2D. A shear zone is observed through the entire specimen for all three cases.

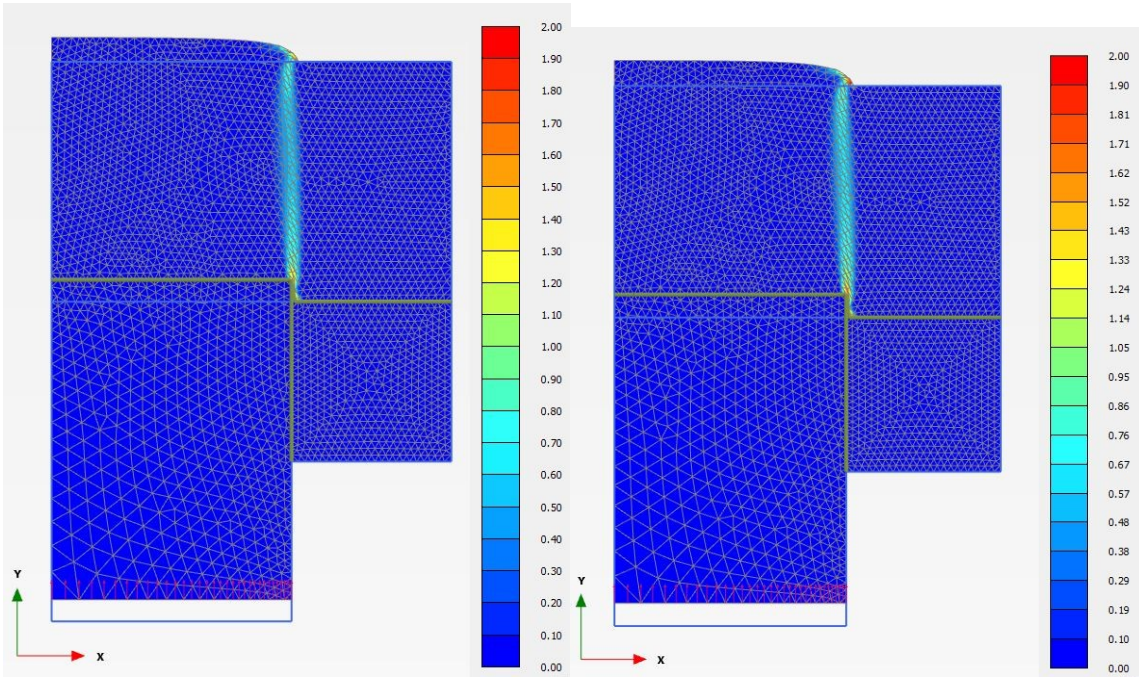

(a) 23AW03 6m

(b) 23AW03 3m

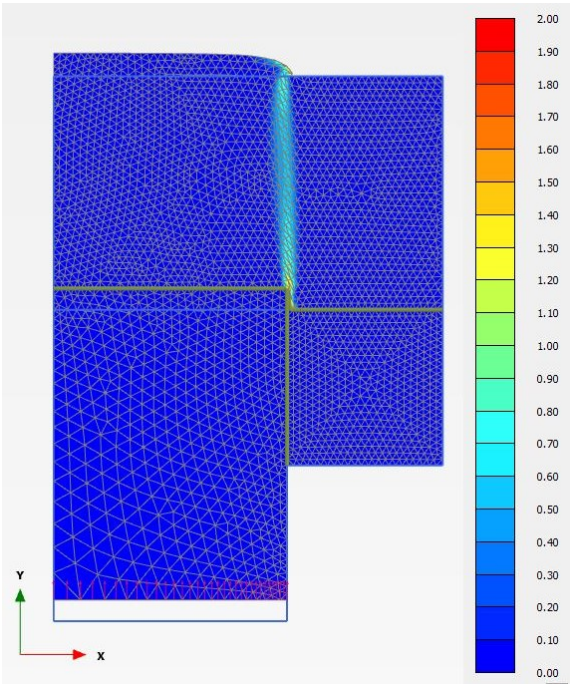

(c) 23AW03 5m

Figure 6.11: Shear zones from the modelled shear punching apparatus after failure, for all three samples.

Figure 6.12 presents the $p' - q$-plots for all three soil samples. Depending on the initial conditions in the soil, the yield surface intersects the MC failure line at different stresses.

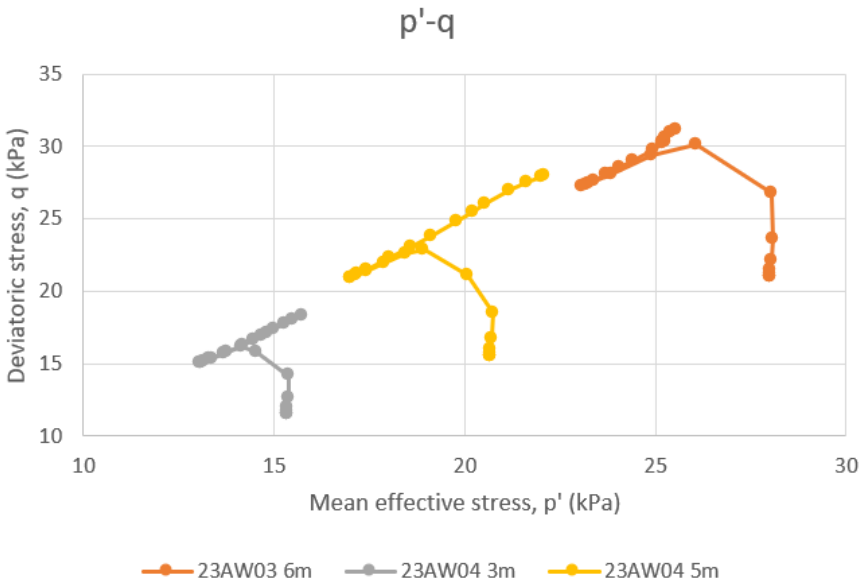

Figure 6.12: p'-q plot for all three soil samples in the Soft Soil analysis.

The model builds up an excess pore pressure at the fixed upper corner and along the interface between the soil and the punch. Additionally, there is also build up of a negative pore pressure, also called suction, in the soil at the corner of the punch and along the opening where the specimen is punched through, which can be seen in Figure J.1 in Appendix J. In the same appendix, shear strength and strain diagrams for each soil sample are presented in Figure J.2. The three graphs plotted are extracted by a single point in the shear zone in the Plaxis model, by the Plaxis DSS Lab Test tool and by a DSS test conducted in the laboratory.

6.3.3 Comparison between obtained and simulated stress in the punch

The calculated stress with and without correction for the self-weight of the punch, together with the simulated vertical stresses from Plaxis are plotted with the vertical deformation in Figure 6.13 for the three soil samples.

The simulated vertical stress obtained from the MC model in Figure 6.13a and 6.13c are found to to be in relatively good agreement with the initial part of the curves for calculated stress. However, the simulated vertical stress obtained from the MC model in Figure 6.13b does not align well with the calculated stress. The simulated vertical stress obtained from the SS model also aligns to some extent. However, this cannot be stated for sample 23AW04, 3m. Reasons for the behavior of the Plaxis models, or the shear punching apparatus, are discussed in Chapter 7.

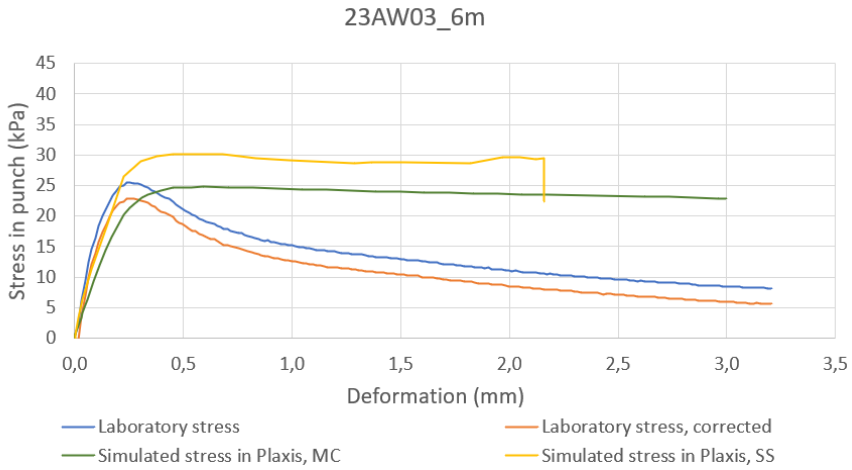

(a) 23AW03 6m, classified as Cl (fsa)

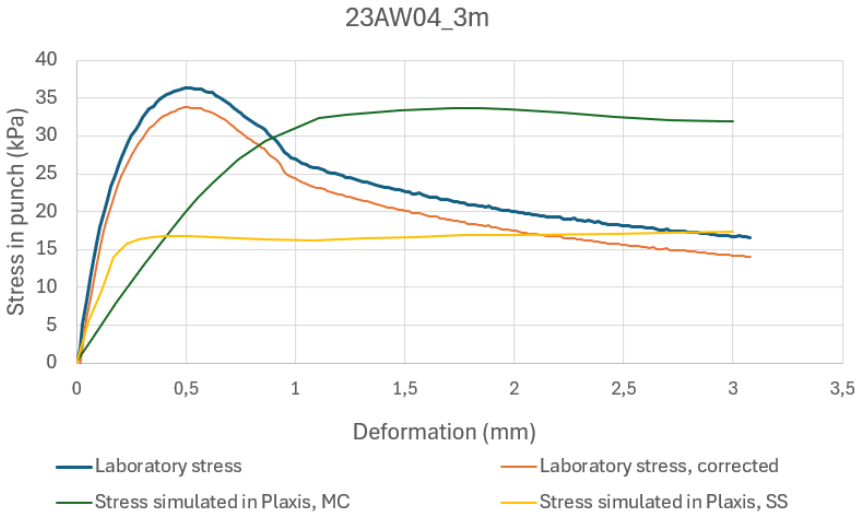

(b) 23AW04 3m, classified as clGy pr

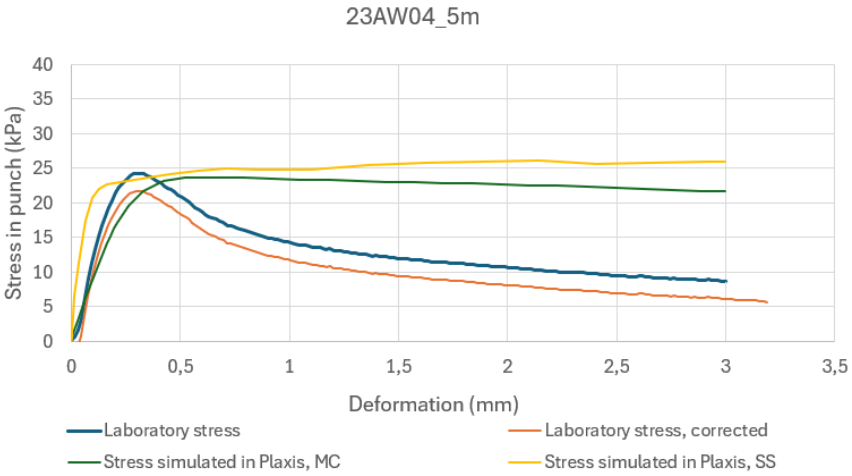

(c) 23AW04 5m, classified as Cl su

Figure 6.13: Obtained stress from the laboratory shear punching test and simulated stress in Plaxis in (a) for 23AW03 at 6 m depth, in (b) for 23AW04 at 3 m depth and in (c) for 23AW04 at 5 m depth.

7
Discussion

This chapter will discuss findings in the study, including notable discoveries, challenges and possibilities for future work. This will be divided into three sections: the execution of the test, the evaluation of test results, and the use of the test in practice.

7.1 The execution of the test

The extracted soil samples that contain mainly gyttja are in several cases classified as disturbed when setting up the specimen, as the material does not fill the test ring radially. Consequently, the results are of a lower quality and are less reliable for geotechnical design purposes. The low quality of the results is a consequence of the necessity for the test ring to be filled before the shearing process, which can give misleading results. The radial filling of the specimens is likely impeded by organic fibers or interference from the piston sampling, which is pulled against the sample sleeve due to friction. This issue is generally more pronounced in organic soils than in non-organic ones. It is possible that the test results could have been improved if a 45 mm sample had been extracted from the 50 mm obtained from the field, in order to exclude the disturbed outer layer.

When executing the test, the direction of the mounting of the test is not considered, i.e. the orientation of the test in relation to the deposition of the soil. The test is simply mounted with the neatest surface towards the punch. This may potentially lead to the generation of misleading results, as the soil may have deposited to a specific shear strength, depending on its structure or due to the loading conditions of the soil. Conducting the shear punching test in the opposite direction can give either favorable or unfavorable results, which may not accurately reflect the shear strength in situ.

When comparing shear punching with other methods, particularly the DSS test, it has been observed that parameters such as shear rate and direction have an impact on the outcome. Shear punching is performed at a faster rate than the DSS test and in a vertical shear, which results in an increased shear strength. However, a vertical shear does not provide as accurate a representation of a general sliding surface as a horizontal shear does. This prompts the question of why shear punching is not simply conducted as a faster DSS, given that the horizontal shear surface is more natural and representative. However, the assembling of a DSS test is a

complex process, and testing requires a consolidation phase before shearing can be performed. Therefore, the shear punching would follow the same principle as a shear box if the shear punching were to be performed with a horizontal shear without the consolidation phase.

7.2 Evaluation of the results of the test

The uncalibrated shear strength obtained from the shear punching test is found to be greater than the shear strength obtained from the DSS and fall-cone tests. When calibration equation 3 is applied, the ratio between the shear strength obtained from the DSS-test and shear punching test is typically lower compared to when calibration equation 2 is applied. However, for the shear punching test to be able to complement the DSS-test or replace the fall-cone test, C_{u-s} should be as similar as possible to the value of C_{u-ds} after calibration, but preferably not exceed it. An alternative approach to the development of calibration equation 3 could be to assess whether the results can be corrected solely in relation to the shear rate, rather than calibration against results from the DSS test. Calibration equation 3 is comparable to the anticipated discrepancy related to the rate effect, which was calculated to be approximately 30% in Chapter 3.4. The rate effect calculated in this thesis is a theoretical estimate based on the rate effects of other test methods. For this to be relevant, further investigations into the shear rate effect is necessary, specifically for she shear punching apparatus. By determining the effects of the shear rate, the effect of other factors such as the shear direction can also be evaluated.

However, the results obtained from the shear punch test corrected with correlation equation 3 appear to align with relevant empiricism. The results are more closely aligned with the empirical approach recommended by SGI (Equation 2.4) than with Hansbo's relation (Equation 2.3). This may be partly due to the fact that Hansbo's relation takes fewer parameters into account. A number of the soil samples were highly over-consolidated and are therefore not expected to follow Hansbo's relation to the same extent. The empirical formula recommended by SGI considers the impact of the OCR and is therefore more suitable for overconsolidated clays.

Usually when correcting the undrained shear strength for other methods such as CPT or the fall-cone test it is typically done by the liquid limit. For shear punching, an equation is used to calibrate it to be similar to the results from the DSS, which contributes to less spreading of the calibrated values. These are two completely different ways of correcting or calibrating the undrained shear strength, making it difficult to compare the spreading of the results. Shear punching provides more accurate results than the fall-cone test in relation to the DSS. Since this is a new and different way of handling the undrained shear strength, more research and investigation is needed to make sure this approach is valid for all types of soft soils. The majority of the data used in the thesis has also been used to develop the calibration equations. Therefore, the relationship between DSS results and shear stress is expected to follow a 1:1 ratio. Exceptions include samples designated as gyttja and some samples described as gyttja bearing. The variation within each method

results in a natural deviation that is unavoidable.

When comparing the duplicate samples it can be seen that there is not much of a difference in shear strength for neither the shear punching test or the DSS test. The maximum difference of just over 2,5 kPa is not significant and can easily be explained by natural variation or disturbance during sample extraction from the ground or the block. Usually when using block samples, one sample is taken from the center of the block to serve as reference, as this sample is unlikely to be disturbed during extraction. The block samples on which this analysis is based on were instead divided into four parts, which means that there is no reference sample. However, the depth of where the duplicate samples have been taken is approximately 2,5-5 m, which is insufficient to draw any further conclusions.

When plotting the normalized shear strength from the shear punching and DSS test against water content and liquid limit, there were tendencies to increasing trends. It is, however, important to note that the available data had a considerably smaller proportion of soil samples with high values of W_L and W_N. Consequently, few sample results had a major impact on the resulting trend line. Nevertheless, in several cases, the evaluated shear strength from shear punching tests on soil samples containing gyttja, which have high W_N and W_L, tended to be greater than those obtained from the DSS tests. To determine whether the increasing trend is due to the amount of data or not, is is necessary to evaluate a greater number of samples with high W_L and W_N. Although trends may be observed when plotting the normalized data against various parameters, the available data is relatively evenly distributed. Therefore, it is difficult to identify specific ranges where shear punching is more or less appropriate.

After analyzing the outlier classification results, we can see that gyttja is more prevalent among the higher outliers, while laminated clay is more common among the lower outliers. It's important to consider the disturbance during testing as a potential contributing factor for the predominance of gyttja among the higher outliers. It's worth noting that the punching mechanism, rather than the piston sampler, should be held responsible for this outcome. The piston sampler is used for both shear punching and DSS, and therefore should equalize even when normalizing the result. The lower outliers containing laminated clay can be unpredictable due to significant differences in only a few centimeters within the sample. Moreover, the direction of the shear can affect the results, with the layering of sand and silt having a greater impact on shear punching than on DSS.

Given that a significant proportion of the upper outliers are classified as gyttja, it would be beneficial to develop a separate calibration equation for organic soils. The current equation was developed using primarily clay samples and since gyttja have several properties that differentiates it from clay, it behaves differently. Therefore, it might be appropriate to specify the equations according to the type of soil.

Based on the data available today, it appears that shear punching is the most favor-

able method for soil within the density range of 1.45-1.7 t/m^3. This range contains the greatest number of samples, and the calibration equations are therefore most adapted for samples within this range. Although a few samples located outside this range have also been calibrated with this equation and relatively close to the 1:1 ratio, further data collection is necessary to confirm the effectiveness among samples outside of this range.

7.3 The use of the test in practice

In the industry, there is a significant interest in the use of this method as new methods are not frequently developed. However, it remains to be seen whether the method will be successful. In order for the shear punching test to be considered an effective option to other methods in the market, it is essential that it becomes more profitable than the fall-cone test, which shear punching was initially intended to replace. Currently, it is not possible to obtain the sensitivity from the shear punching test. However, it can be easily obtained from the fall-cone test. A potential approach for calculating sensitivity is to calculate the ratio between undrained shear strength, measured by the shear punch, and remoulded shear strength, measured by the fall-cone test. However, it is important to consider whether this approach is appropriate. It should also be noted that the fall-cone test still is required for this approach to accurately determine sensitivity, although the shear punching test could replace the fall-cone test to some extent. It is possible that the shear punching test also to some extent could complement the DSS test. This should at present only be used for estimation purposes or at the initial stages of analysis.

One limitation of the fall-cone test is that there is no way to control the quality of the soil sample without empirical values of shear strengths or comparison with other field tests, as the result is only a single value. Results from laboratory tests as triaxial, DSS and CRS can be used to assess sample quality. All three of these laboratory tests are advanced and expensive. As the fall-cone test is an index test, it is typically conducted at an earlier stage, and the advanced methods are not always performed to the same extent. The sensitivity is significantly affected by the undisturbed shear strength. A minor discrepancy can result in considerable variation in sensitivity, which in turn can influence whether or not a clay is classified as quick and the potential retrogression of a landslide. This raises the question of whether it is reasonable to base this on a test method where sample quality cannot be assessed and the shear strength is often underestimated.

The results from the shear punching test is presented in a format that documents the deformation to failure. For other test methods, the sample quality is assessed based on the amount of deformation before failure occurs. If this could be evaluated from the curve of the shear punching test, it would potentially be possible to assess the reliability of the sensitivity assessment of the clay without performing advanced and expensive tests.

In conducting the stability analysis, the results are based on different approaches

for determining the shear strength of the soil, which are specified as case 1-4. The results obtained from SLOPE/W, which was used for the stability analysis, are not unexpected but rather anticipated. This is due to the fact that the shear strength for the different cases has been deliberately evaluated with lower or higher values, depending on the reliability of the included tests. It is to be expected that the shear strengths determined in cases that included laboratory data from the DSS test would be higher than those not including such data, due to the reliability of the test. The shear strength for case 3 including laboratory data from the CPT, fall-cone test, and shear punching test were determined to be a lower shear strength in contrast to case 2 and 4, which includes the DSS test, resulting in lower safety factors. This is due to the fact that the shear punching test has not been assessed as reliable as the DSS test, and should not be done in the future either. Consequently, the outcomes are expected.

The development of the FE models of the shear punching test presented a number of challenges. One of the difficulties encountered was the mesh dependency along the shear zone using the Mohr-Coulomb constitutive model, caused by the model's inability to effectively capture the localized strain. Consequently, a coarser mesh than initially intended was used in the simulations. This made it impossible to conduct a mesh sensitivity analysis on the model, as only the very coarse mesh could be used without the model collapsing. The use of a coarser mesh in the simulation results in less accurate outcomes. However, due to the absence of a mesh sensitivity analysis, the extent of the impact cannot be determined. The limitations of the model are primarily related to the constitutive model and its limited ability to accurately reflect the behavior of the soft soil.

As previously presented in Appendix I, there is evidence of stress build-up in the steel blocks. In attempt to avoid this, a frictionless interface between the blocks have been simulated. Moreover, the fixed steel block has been excluded without any impact on the results. Consequently, the accumulation of stress at this point is likely due to the fact that it is a corner where stress concentrates. This indicates that the stress accumulation is difficult to avoid in the model and that it cannot be excluded that it affects the final results.

The graphs in Figure 6.13 indicates that the simulated MC model never fails, which it is not expected to do. The Mohr-Coulomb constitutive model is a linear elastic model, and as such, it is incapable of failure. Due to this, it also has problems handling soil softening and stays at a somewhat constant stress after failure, even though the stress should reduce. In order to ascertain the relevance of the model, it is necessary to compare the simulated graph to the calculated graph at the point of failure, to verify that they are at similar stress levels, which they are to some extent.

However, as illustrated in Figure 6.13, the stress development in the punch appears to be completely different for the gyttja sample (23AW04 3m). This is probably due to the fact that the Mohr-Coulomb constitutive model was not designed to accurately represent strain in a realistic manner, as explained in Chapter 5. The

initial part of the curve may be related to the shear modulus of the soil. The shear modulus from the shear punching test is not necessarily the same as the one evaluated from the DSS test, which is the one used for the simulations. This may result in differences in the shape of the plots. The determined E-modulus of the gyttja sample is significantly lower than those of the clay samples, which is likely the cause of its behavior. This in turn indicates that Plaxis, or the Mohr-Coulomb constitutive model, is not optimal for gyttja. Alternatively, gyttja may require a different approach when modelling.

With the MC model, the three specific laboratory tests have been recreated with input data from shear punching tests carried out in the laboratory. However, this does not validate the shear punching test, but it does demonstrate that it is possible to somewhat recreate the test with the Mohr-Coulomb constitutive model. As previously stated, the behavior of the gyttja sample differs in the model compared to the laboratory. Similar to the MC model, the SS model is unable to handle the soil softening that occurs subsequent to failure, as can be seen in Figure 6.13. Constitutive models such as Soft Soil Creep and SCLAY-1S are more effective in capturing this behavior. It is difficult to compare the graphs and come to a conclusion on if the test is successfully simulated. It is clear that there are large differences between the results from simulation and the laboratory test, however there is no definitive answer what the answer is supposed to look like. The soil parameters in the SS model simulation are derived from CRS-tests, which does not necessarily mean that the simulated results will look like the resulting graphs from the laboratory shear punching test.

In the $p' - q$ diagram in Figure 6.12, the stress paths are observed at a point in the shear zone for the three soil specimens in the SS model. The model has a reasonable behavior until failure occurs, after which mesh problems arise while the model is unable handle soil softening. As can be seen in Figures J.2b and 6.13b, the model seems to interpret the indata in the SS model causing the shear strength of the soil and stresses in the punch to be lower than expected for the gyttja sample. There can also be a difference in how the CRS, DSS and shear punching tests applies to gyttja.

8

Conclusion and further work

This chapter will conclude the most important findings of this master thesis and offer recommendations for future work.

8.1 Conclusion

In conclusion, the shear punching test cannot be considered a complete replacement for the fall-cone test as an index test, as it is unable to determine the sensitivity of the soil. However, it can be used as a complement to other tests for the purpose of evaluating the undrained shear strength in cohesive soils. Given the considerable spread of the results observed in the normalized shear strength, it is not possible to identify a specific range for certain parameters when the shear punching test is relevant or not. It can however be stated that the shear punching method is relatively accurate within the range that has already been tested, where a certain outcome can be expected. To further examine this objective, it is necessary to analyze additional data within ranges where there is currently limited representation. However, it is important to remember that the shear punching test is still in its developmental stage.

The inclusion of results from the shear punching test affects the selected shear strength for the purposes of stability analysis to some extent. In general, the shear strength tends to be derived higher based on the shear punching test than that derived from the fall-cone test. However, the situation becomes more complex regarding the DSS test. Given that this test is regarded as one of the most reliable tests for determining shear strength, it can be concluded that the shear strength derived from the shear punching test should not exceed the one derived from the DSS test at present. It has been proven that is is possible to recreate a shear punching test in Plaxis 2D using the Mohr-Coulomb constitutive model that produces results that are comparable to those obtained from the shear punching apparatus in the laboratory. The model created is however simple, using the linear-elastic Mohr-Coulomb constitutive model. The Soft Soil constitutive model is not using in data from the shear punching apparatus and thus simulates a shear punching test based on parameters from the CRS and DSS test. This means that the Soft Soil model does not recreate a shear punching test performed in the laboratory but simulating one, with varying results.

8.2 Further work

There are several interesting aspects of the shear punching method that have not been evaluated in this thesis but could be the subject of further investigations. During the data analysis, the idea was raised to develop the existing calibration equation. One approach is to assess its applicability on other soil types, and if necessary, new calibration equations could be developed for other soil types than clay, or based on ranges within certain parameters.

The impact of the shear rate on the shear strength was only evaluated theoretically in this thesis. Further investigations could be conducted by comparing the impact of varying rates of the shear punching test with the CRS and triaxial test. This could be studied by simulating the tests in Plaxis 2D with a time-dependent, constitutive material model as Soft Soil Creep, in order to determine the trends of shear rate. Alternatively, the test could be conducted at varying rates within the laboratory setting. For instance, it would be of interest to ascertain if the relationship between shear rate and shear strength is linear.

In order to make the shear punching test more industrially applicable and to some extent replace the fall-cone test, it is necessary to evaluate additional parameters from the test. This includes investigations of whether it is possible to evaluate the sample quality based on the results from the shear punching test as well as whether the undisturbed shear strength from the shear punching test potentially could be used in the calculation of the sensitivity of the soil.

As previously stated, it is also of interest to develop the numerical model in Plaxis with more advanced constitutive models that can more accurately capture the behavior of the soft soil. For instance, the Soft Soil creep, SCLAY-1S, or the Hardening Soil models may be considered.

Bibliography

Awer Geoteknik. (2023). *1125-MUR-01 Geoteknik - Fördjupad stabilitetsutredning Gamleby hamn*.

Bentley. (2023). *PLAXIS 2D 2024.1:2 - Reference Manual*. https://communities.bentley.com/cfs-file/__key/communityserver-wikis-components-files/00-00-00-05-58/PLAXIS_5F00_2D_5F00_2024.1_5F00_2D_5F00_2_5F00_Reference-Manual.pdf

Bishop, A. W., & Henkel, D. J. (1962). *The measurement of soil properties in the triaxial test*. Edward Arnold Publishers LTD.

Claesson, P. (2003). *Long term settlements in soft clays*. Chalmers Reproservice.

Eriksson, L. G. (2016). *Jordarternas indelning och benämning* (tech. rep. No. 1:2016). Swedish geotechnical society, SGF.

Eslami, A., Moshfeghi, S., MolaAbasi, H., & Eslami, M. M. (2020). 2 - background to foundation engineering. In A. Eslami, S. Moshfeghi, H. MolaAbasi, & M. M. Eslami (Eds.), *Piezocone and Cone Penetration Test (CPTu and CPT) Applications in Foundation Engineering* (pp. 25–53). Butterworth-Heinemann. https://doi.org/https://doi.org/10.1016/B978-0-08-102766-0.00002-X

Fellenius, B. (1938). Apparat för undersökning av lerors skärhållfasthet. *Teknisk Tidskrift, Väg- och vattenbyggnadskonst*, (p. 9–10).

Guduru, R., Darling, K., Kishore, R., Scattergood, R., Koch, C., & Murty, K. (2005). Evaluation of mechanical properties using shear–punch testing. *Materials Science and Engineering: A*, *395*(1), 307–314. https://doi.org/https://doi.org/10.1016/j.msea.2004.12.048

Hansbo, S. (1957). *A new approach to determination of the shear strength of clay by the fall-cone test*. Royal Swedish Geotechnical Institute.

Houlsby, G. T. (1982). Theoretical analysis of the fall cone test. *Géotechnique*, *32*(2), (p. 111–118).

Huang, S., Feng, X. T., & Xia, K. (2011). A dynamic punch method to quantify the dynamic shear strength of brittle solids. *Review of Scientific Instruments*, *82*(5), 053901. https://doi.org/10.1063/1.3585983

Kalén, R., Holmén, M., Burman, F., Vesterberg, B., & Andersson, M. (2023). *Indexförsök för bestämning av odränerad skjuvhållfasthet, Skjuvstansing* (2nd ed.). Swedish Geotechnical Institute, SGI. https://swedgeo.diva-portal.org/smash/get/diva2:1629908/FULLTEXT03.pdf

Kartsunen, M., & Amavasai, A. (2017). *BEST SOIL: Soft soil modelling and parameter determination*. Chalmers University of Technology. https://research.chalmers.se/publication/522789/file/522789_Fulltext.pdf

Koumoto, T., & Houlsby, G. T. (2001). Theory and practice of the fall cone test. *Géotechnique*, *51*(8), (p. 701–712).

Kulhawy, F., & Mayne, P. (1990). Manual on estimating soil properties for foundation design.

Larsson, R. (1980). Undrained shear strength in stability calculation of embankments and foundations on soft clays. *Canadian Geotechnical Journal*, *17*(4), 591–602. https://doi.org/10.1139/t80-066

Larsson, R. (1986). *Consolidation of soft soils* (Report 29). Swedish geotechnical institute, SGI.

Larsson, R. (1990). *Behaviour of organic clay and gyttja. Results from investigations in Swedish gyttja-bearing soils supplemented with results from a similar Finnish investigation and experience from sulphide-rich soils (svartmocka).* (No. 38). Swedish Geotechnical Institute. https://urn.kb.se/resolve?urn=urn:nbn:se:swedgeo:diva-204

Larsson, R. (2015). *Cpt-sondering. utrustning - utförande - utvärdering.* (Information 15). Swedish geotechnical institute, SGI. https://sgi.se/globalassets/publikationer/info/pdf/sgi-i15.pdf

Larsson, R., & Åhnberg, H. (2003). *Long-term effects of excavations at crests of slopes* (tech. rep. No. 61). Swedish geotechnical institute, SGI.

Larsson, R., Åhnberg, H., & Holmén, M. (2012). *Bestämning av dränerad skjuvhållfasthet med olika laboratorieförsök* (Varia 630). Swedish geotechnical institute, SGI. https://www.diva-portal.org/smash/get/diva2:1300524/FULLTEXT01.pdf

Larsson, R., Sällfors, G., Bengtsson, P.-E., Alén, C., Bergdahl, U., & Eriksson, L. (2007a). *Skjuvhållfasthet - utvärdering i kohesionsjord* (2nd ed.). Swedish Geotechnical Institute, SGI. https://www.sgi.se/globalassets/publikationer/info/pdf/sgi-i3.pdf

Larsson, R., Sällfors, G., Bengtsson, P.-E., Alén, C., Bergdahl, U., & Eriksson, L. (2007b). *Skjuvhållfasthet-utvärdering i kohesionsjord* (Information 3). Swedish geotechnical institute, SGI. https://www.sgi.se/globalassets/publikationer/info/pdf/sgi-i3.pdf

Llano, M., & Contreras, L.-F. (2019). The effect of surface roughness and shear rate during fall-cone calibration. *Géotechnique*, *70*, 1–39. https://doi.org/10.1680/jgeot.18.p.222

Lopes, B., Arruda, M., Almeida-Fernandes, L., Castro, L., Silvestre, N., & Correia, J. (2020). Assessment of mesh dependency in the numerical simulation of compact tension tests for orthotropic materials. *Composites Part C: Open Access*, *1*, 100006. https://doi.org/https://doi.org/10.1016/j.jcomc.2020.100006

Lundin, S.-E. (2000). *Geotekniken i Sverige 1920–1945* (1:2000). Swedish geotechnical society, SGF.

Olsson, M. (2010). *Calculating long-term settlement in soft clays - with special focus on the gothenburg region.* Chalmers Reproservice.

Sällfors, G. (2013). *Geoteknik : Jordmateriallära: Jordmekanik* (5. ed.). Cremona förlag.

Sällfors, G., & Larsson, R. (2016, December 20). *Bestämningar av odränerad skjuvhållfasthet med specialiserade metoder i praktiska tillämpningar - Delrapport 3, Sammanställning av "Case Records"*. Swedish Transport Administration. https://fudinfo.trafikverket.se/fudinfoexternwebb/pages/PublikationVisa.aspx?PublikationId=3127

Sällfors, G., & Larsson, R. (2017). *Metodik för bestämning av skjuvhållfasthet i lera - en vägledning* (1:2017). Swedish geotechnical society, SGF. www.sgf.net

SGF:s laboratoriekommité. (2004). *Direkta skjuvförsök - en vägledning* (SGF Notat 2:2004). Swedish geotechnical society, SGF. www.sgf.net

Statens järnvägars geotekniska kommission 1914-1922. (1922). *Slutbetänkande avgivet till kungl. järnvägsstyrelsen den 31 maj 1922* (Geotekniska meddelanden nr 2). Statens Järnvägar.

Sveriges Geologiska Undersökning. (n.d.). SGU:s Kartvisare, Jordarter 1:25 000 - 1:100 000. Retrieved April 17, 2024, from https://apps.sgu.se/kartvisare/kartvisare-jordarter-25-100.html?zoom=575099.2370898356,6414303.047569606,593019.2729299073,6422129.063221637

Swedish Geotechnical Institute. (2018). *Metodik för kartläggning av kvicklera, Vägledning* (Publikation 46). Linköping.

Swedish geotechnical society. (2018). *Fallkonförsöket* (SGF Notat 2:2018). www.sgf.net

Swedish Institute for Standards. (1991). *Geotechnical tests - compression properties - oedometer tests, crs test - cohesive soils* (SS 02 71 26). SIS. https://www.sis.se/produkter/anlaggningsarbete/markarbete-utgravning-grundlaggning-arbete-under-jord/ss27126/

Swedish Institute for Standards. (1991). *Geotechnical tests - shear strength - direct simpe shear test, cu- and cd-tests - cohesive soils* (SS 02 71 27). SIS. https://www.sis.se/en/produkter/civil-engineering/earthworks-excavations-foundation-construction-underground-works/ss27127/

Swedish Institute for Standards. (2017). *Geotechnical investigation and testing – Laboratory testing of soil – Part 5: Incremental loading oedometer test (ISO 17892-5:2017)*. https://www.sis.se/api/document/get/8025732

Swedish Institute for Standards. (2020). *Geotechnical investigation and testing – Field testing – Part 9: Field vane test (FVT and FVT-F) (ISO 22476 9:2020)*. https://www.sis.se/produkter/anlaggningsarbete/markarbete-utgravning-grundlaggning-arbete-under-jord/ss-en-iso-22476-92020/

Wang, G., Bian, X., Wang, Y.-J., Cui, Y.-J., & Zeng, L.-L. (2022). Effect of organic matter content on atterberg limits and undrained shear strength of river sediment. *Marine Georesources & Geotechnology*, *40*(9), 1060–1072. https://doi.org/10.1080/1064119X.2021.1961955

Westerberg, B., Hov, S., & Holmén, M. (2012). *Triaxialförsök - en vägledning* (SGF Rapport 2:2012). Swedish geotechnical society, SGF. www.sgf.net

Yao, W., Xu, Y., Yu, C., & Xia, K. (2017). A dynamic punch-through shear method for determining dynamic mode ii fracture toughness of rocks. *Engineering Fracture Mechanics*, *176*, 161–177. https://doi.org/https://doi.org/10.1016/j.engfracmech.2017.03.012

A

Boreholes in Gamleby Harbor

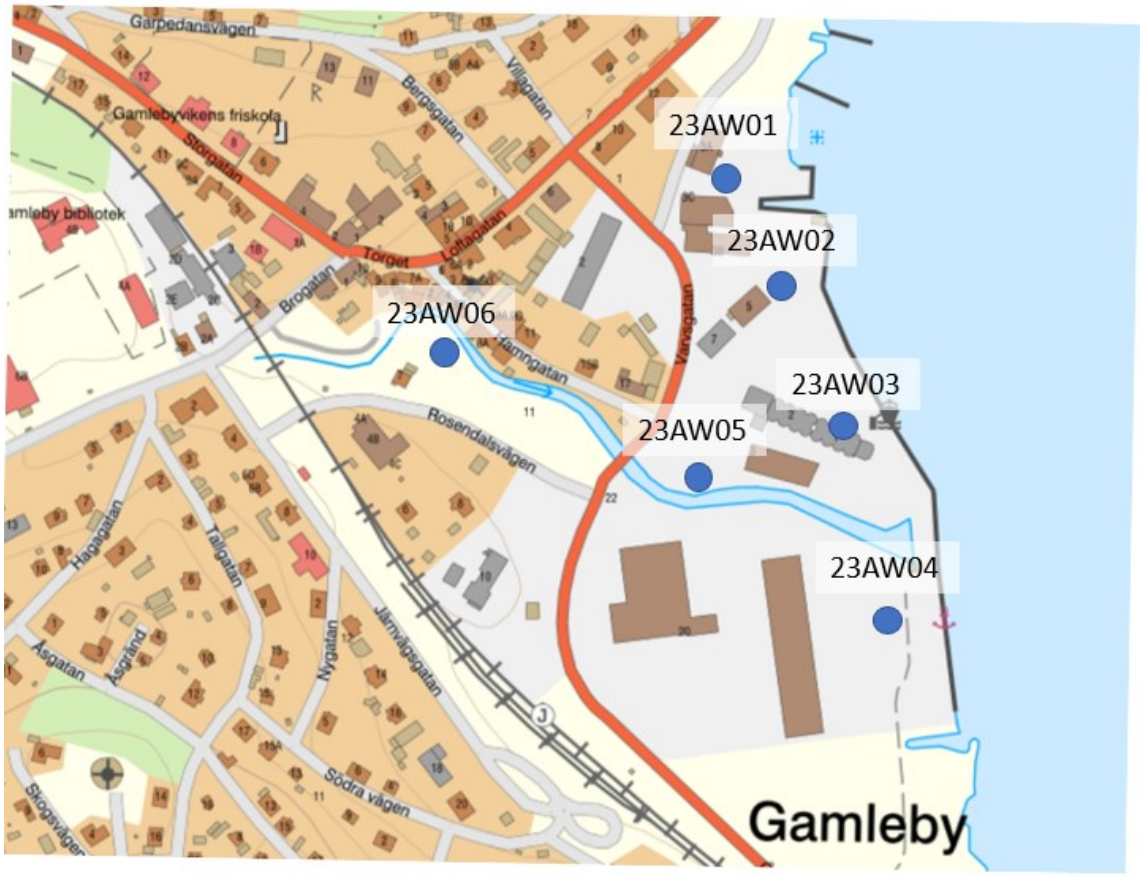

Figure A.1: Overview of boreholes 23AW01-23AW06 in Gamleby Harbor (©Lantmäteriet).

B

Geometry for stability analysis

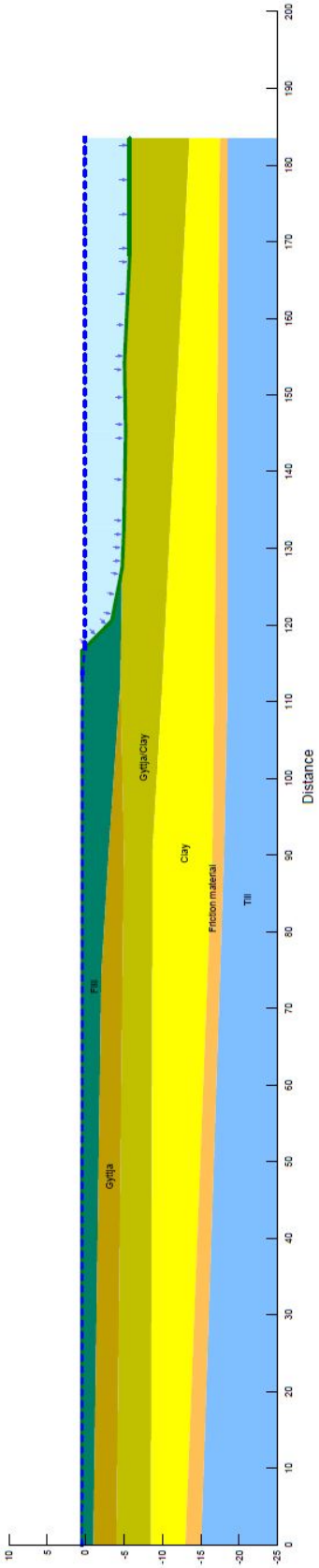

Figure B.1: Cross section C in Gamleby used for stability analysis.

C

Chosen shear strength s_u for stability analysis

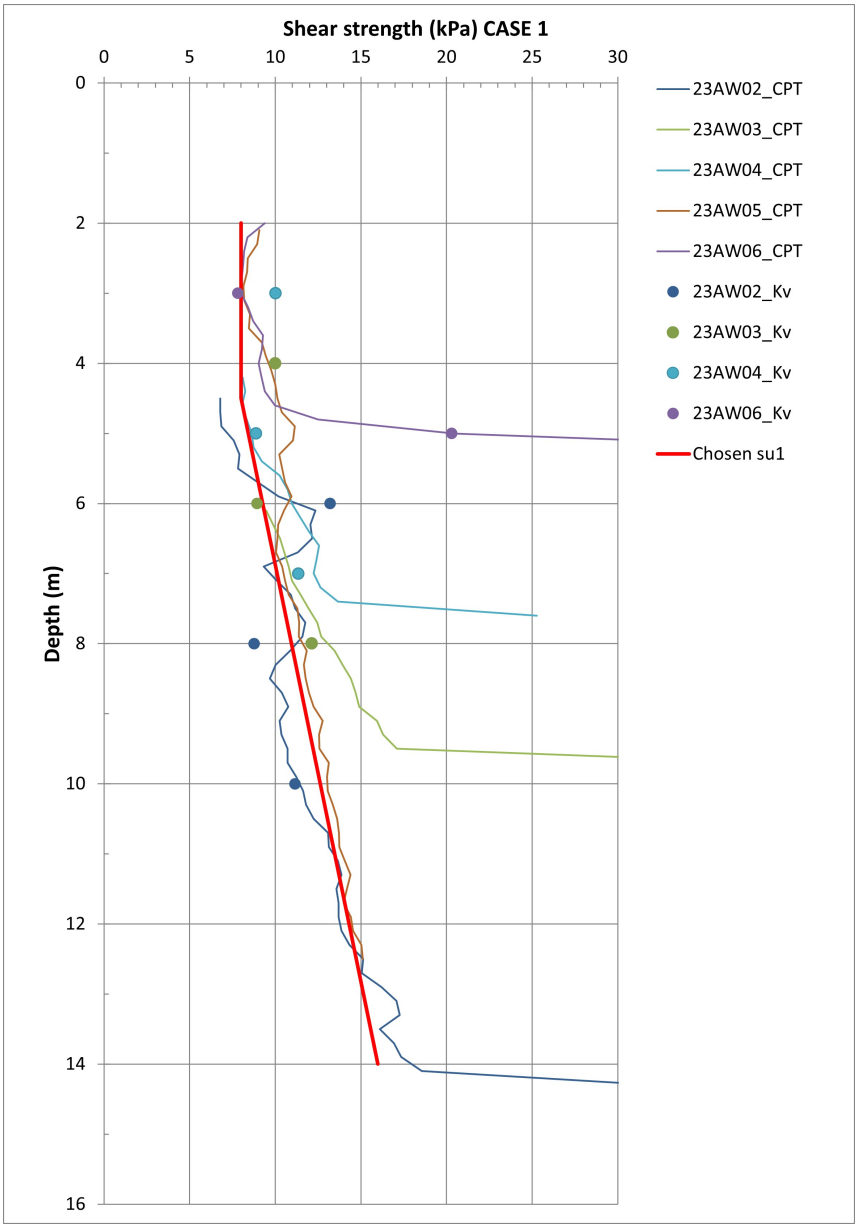

Figure C.1: Chosen shear strength s_u for stability analysis, case 1.

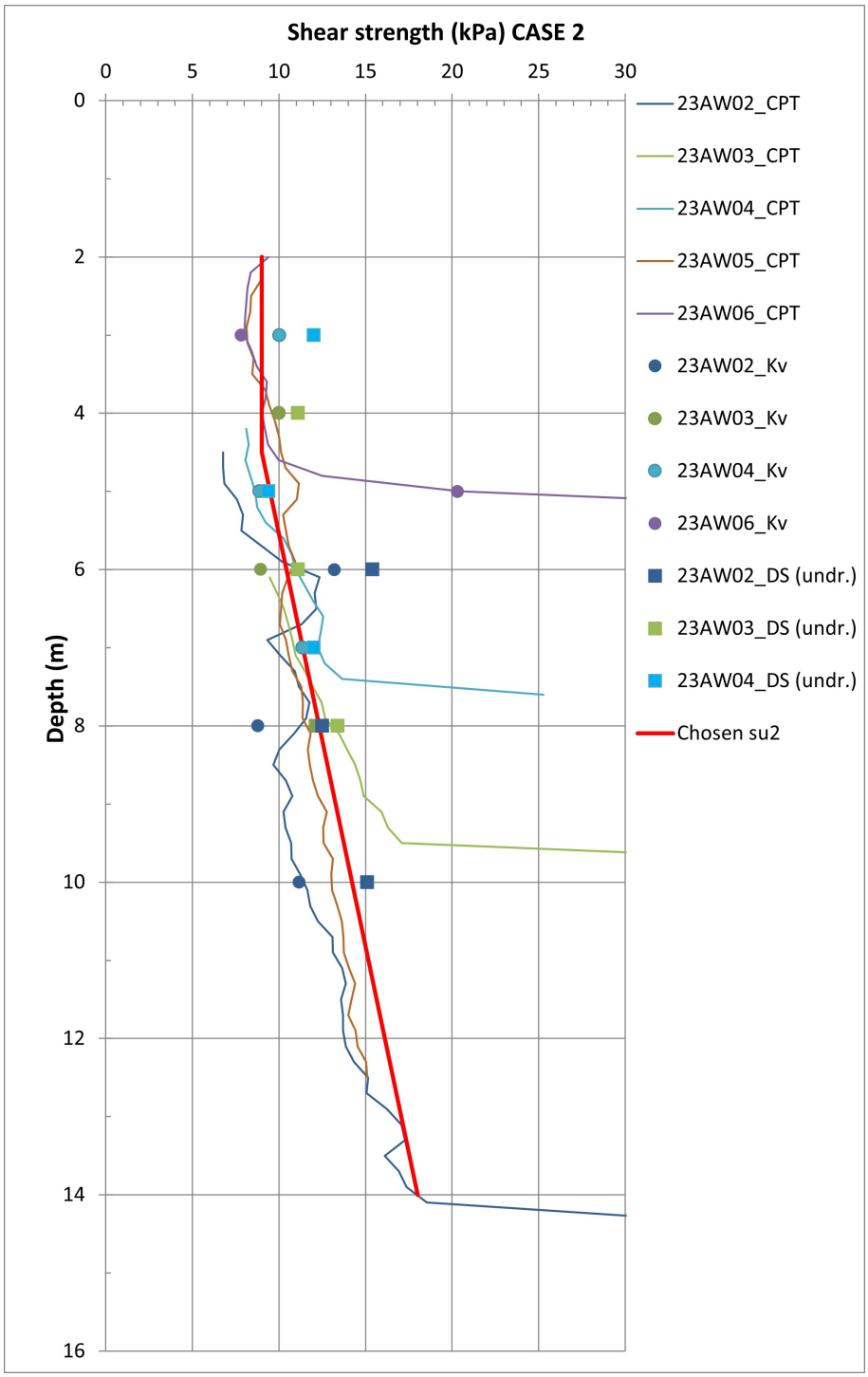

Figure C.2: Chosen shear strength s_u for stability analysis, case 2.

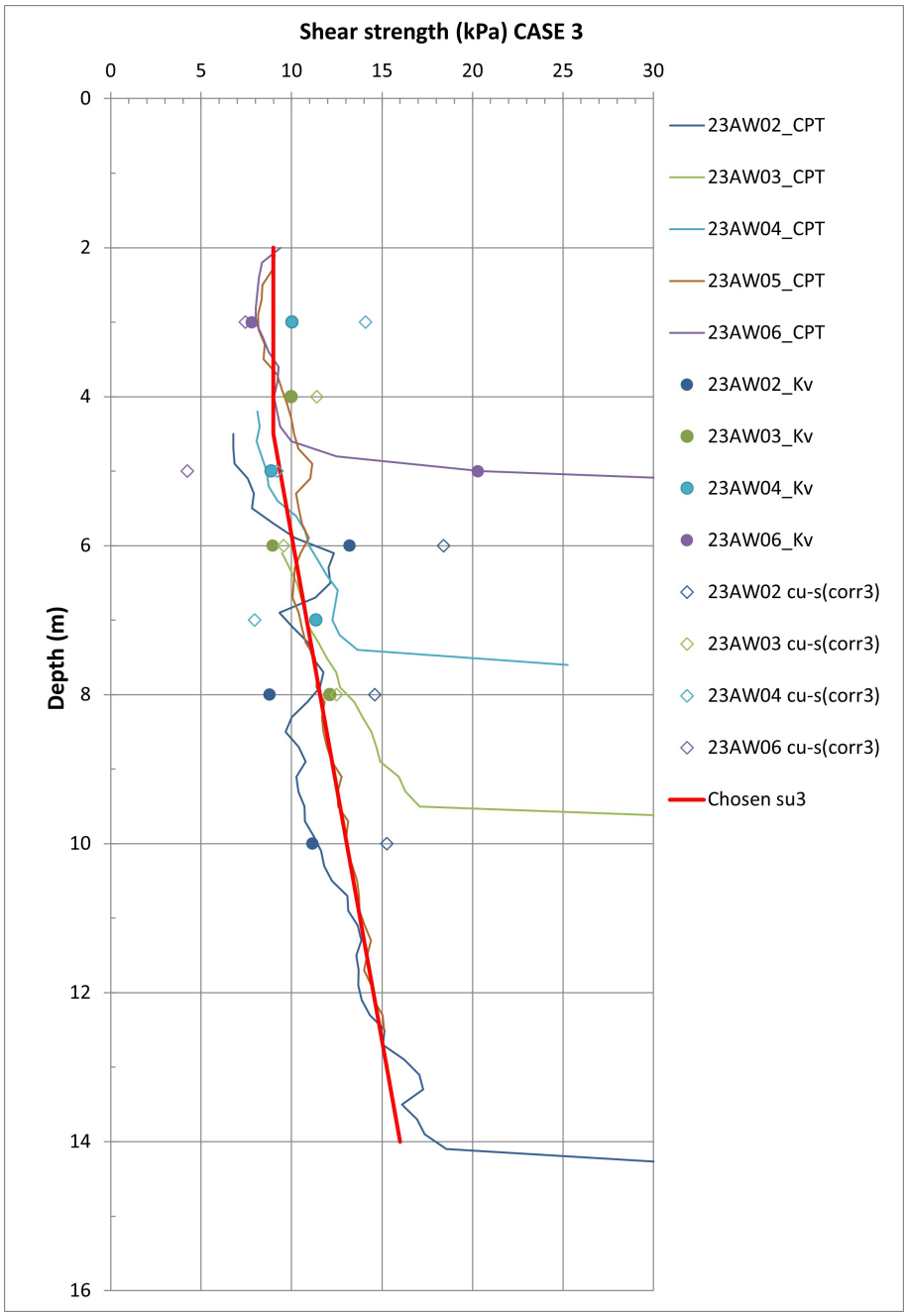

Figure C.3: Chosen shear strength s_u for stability analysis, case 3.

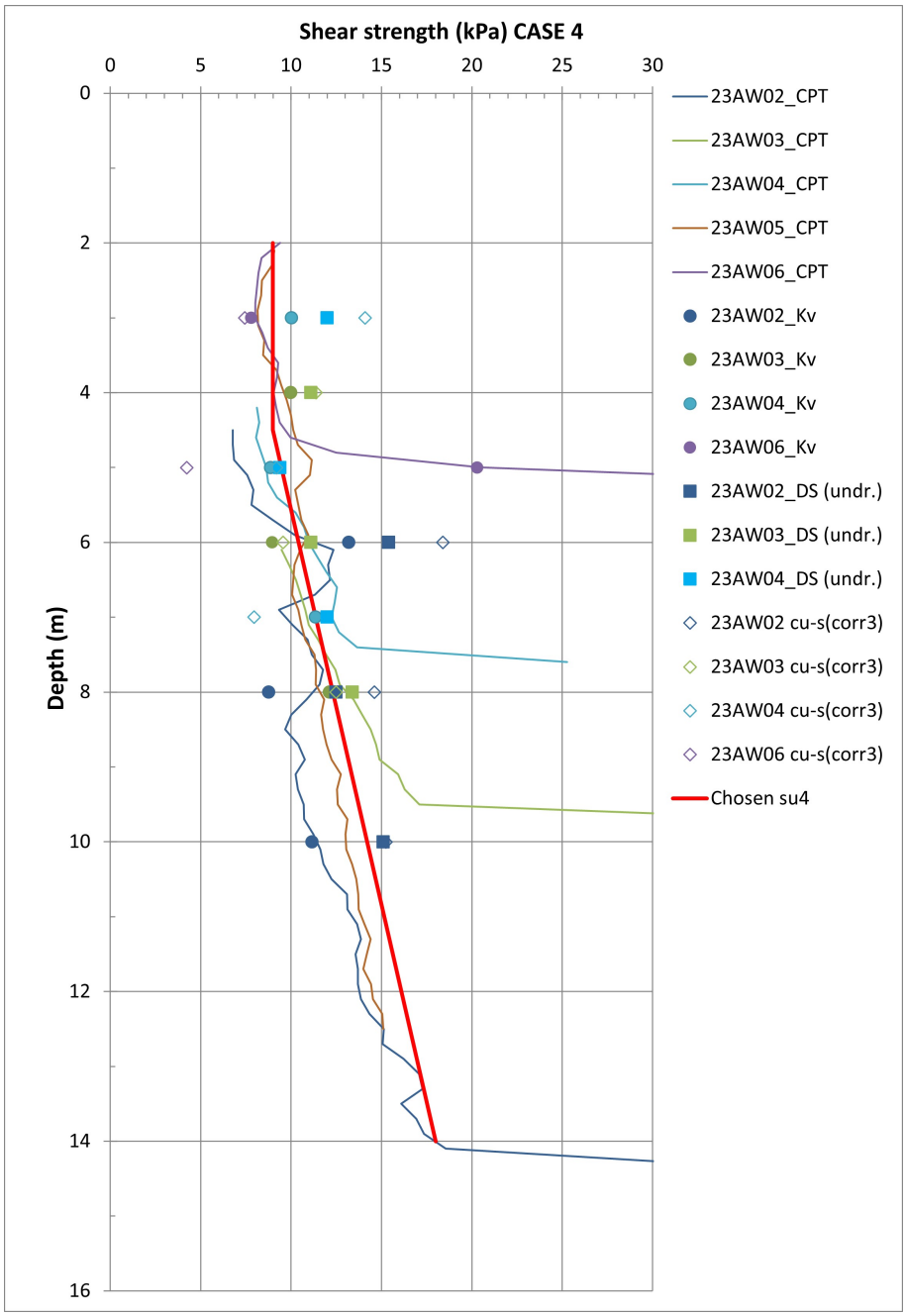

Figure C.4: Chosen shear strength s_u for stability analysis, case 4.

D

Normalized shear strength

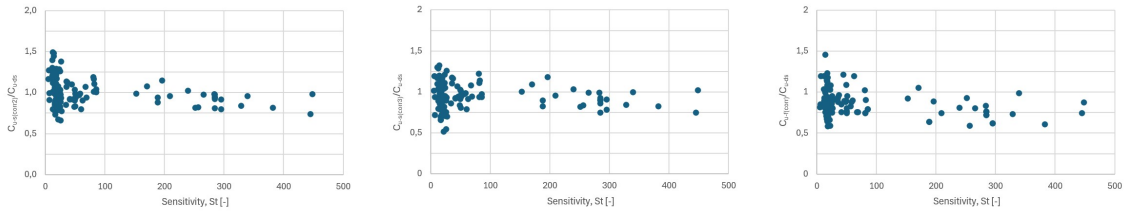

(a) $c_{u-s(corr2)}/c_{u-ds}$ vs S_t **(b)** $c_{u-s(corr3)}/c_{u-ds}$ vs S_t **(c)** $c_{u,s(corr3)}/c_{u,f(corr)}$ vs S_t

Figure D.1: Normalized shear strength plotted against sensitivity.

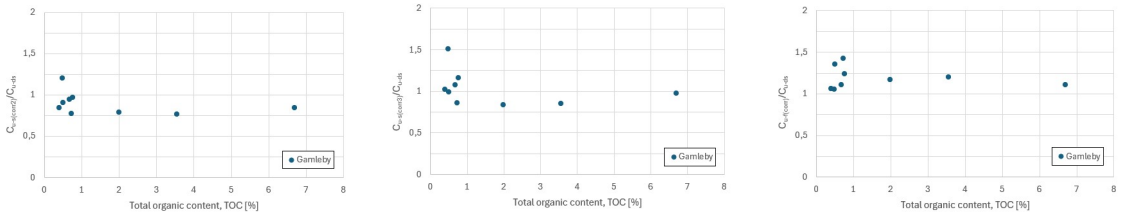

(a) $c_{u-s(corr2)}/c_{u-ds}$ vs TOC **(b)** $c_{u-s(corr3)}/c_{u-ds}$ vs TOC **(c)** $c_{u,s(corr3)}/c_{u,f(corr)}$ vs TOC

Figure D.2: Normalized shear strength plotted against TOC.

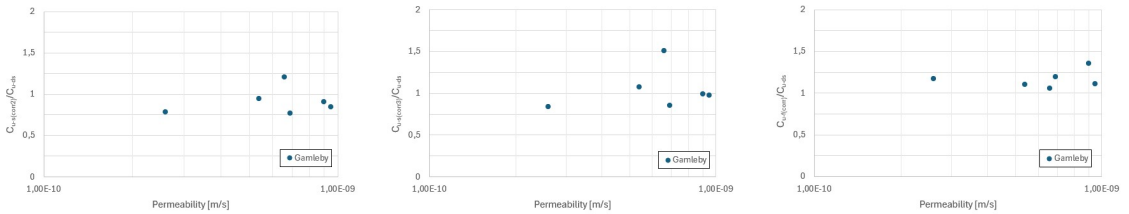

(a) $c_{u-s(corr2)}/c_{u-ds}$ vs k **(b)** $c_{u-s(corr3)}/c_{u-ds}$ vs k **(c)** $c_{u,s(corr3)}/c_{u,f(corr)}$ vs k

Figure D.3: Normalized shear strength plotted against permeability.

E

Classification of outliers

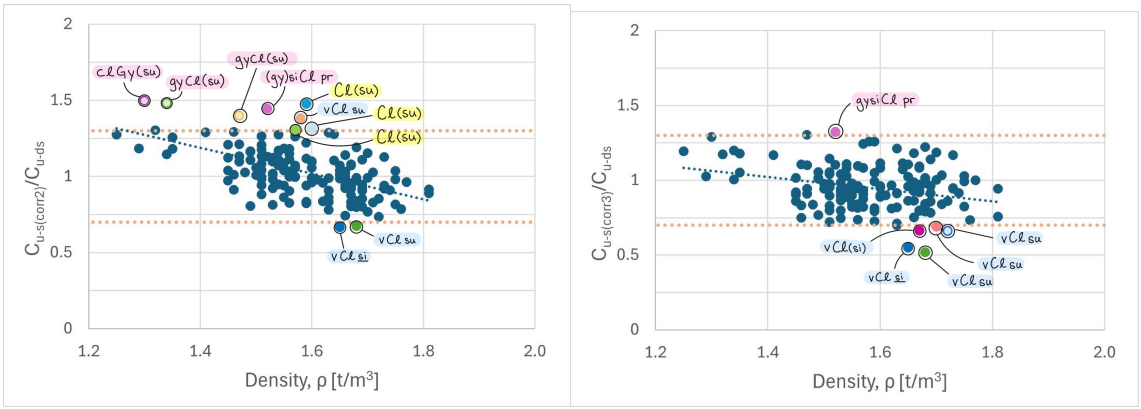

(a) $C_{u-s(corr2)}/C_{u-ds}$

(b) $C_{u-s(corr3)}/C_{u-ds}$

(c) $C_{u-f(corr)}/C_{u-ds}$

Figure E.1: Classification of values of normalized shear strength that deviate by more than ± 30% from the 1:1 ratio for the cases (a), (b) and (c). That the normalized shear strength is plotted against density is of no consequence, rather, it is the relation to the 1:1 ratio that is of importance.

F

Model parameters for the Plaxis model.

Table F.1: Model parameters for the soil materials in the Plaxis 2D model.

Sample	Parameter	Value	Unit
MC Soil			
23AW03 6m	E_{ref}	1903	kN/m^2
	$\gamma_{sat/unsat}$	16,6	kN/m^3
	e_{int}	0,038	
	ν	0,2	
	$S_{u,ref}$	13,1	kN/m^3
	k_x, k_y	$5,79E^{-5}$	m/day
	R_{inter}	0,6	
23AW04 3m	E_{ref}	758	kN/m^2
	$\gamma_{sat/unsat}$	13,2	kN/m^3
	e_{int}	0,037	
	ν	0,2	
	$S_{u,ref}$	19,3	kN/m^3
	k_x, k_y	$5,96E^{-5}$	m/day
	R_{inter}	0,6	
23AW04 5m	E_{ref}	1610	kN/m^2
	$\gamma_{sat/unsat}$	15,5	kN/m^3
	e_{int}	0,022	
	ν	0,2	
	$S_{u,ref}$	12,6	kN/m^3
	k_x, k_y	$5,36E^{-5}$	m/day
	R_{inter}	0,6	

Sample	Parameter	Value	Unit
Soft soil			
23AW03 6m	λ^*	0,17	
	κ^*	0,025	
	ν_{ur}	0,2	
	c'_{ref}	1,31	kN/m^2
	φ	30	^{o}
	ψ	0	
	OCR	1,2	
	k_x, k_y	$5,79E^{-5}$	m/day
	$K_{0,x}, K_{0_z}$	0,6	
	R_{inter}		
23AW04 3m	λ^*	0,15	
	κ^*	0,025	
	ν_{ur}	0,2	
	c'_{ref}	1,93	kN/m^2
	φ	25	^{o}
	OCR	1,2	
	k_x, k_y	$5,96E^{-5}$	m/day
	$K_{0,x}, K_{0_z}$	0,6	
	R_{inter}		
23AW04 5m	λ^*	0,11	
	κ^*	0,014	
	ν_{ur}	0,2	
	c'_{ref}	1,26	kN/m^2
	φ	30	^{o}
	OCR	1,2	
	k_x, k_y	$5,36E^{-5}$	m/day
	$K_{0,x}, K_{0_z}$	0,6	
	R_{inter}	0,6	

Table F.2: Model parameters for steel materials in the Plaxis 2D model.

Material	Parameter	Value	Unit
Linear elastic, non porous			
Steel block	E_{ref}	$2 \cdot 10^9$	kN/m^2
	γ_{unsat}	0	kN/m^3
	ν	0,2	
	$Rinter$	0,1	
MC, non porous			
Steel interface	γ_{sat}	0	
	E_{ref}	1,0	kN/m^2
	ν	0,2	
	c_{ref}	1,0	kN/m^2
	φ	0,1	^{o}
	R_{inter}	0,01	

G

Stability analysis using the total safety method

Color	Name	Model	Unit Weight (kN/m³)	Cohesion (kPa)	Cohesion' (kPa)	Phi' (°)	Constant Unit Wt. Above Water Table (kN/m³)	C-Top of Layer (kPa)	C-Rate of Change ((kN/m²)/m)	C-Maximum (kPa)
	Clay	S=f(depth)	15.2					11.6	0.84	17.7
	FillI	Mohr-Coulomb	23		0	35	20			
	Friction material	Mohr-Coulomb	20		0	35	18			
	Gyttja	Undrained (Phi=0)	13	8						
	Gyttja/Clay	S=f(depth)	14.5					8	0.84	11.6
	Till	Mohr-Coulomb	22		0	42	20			

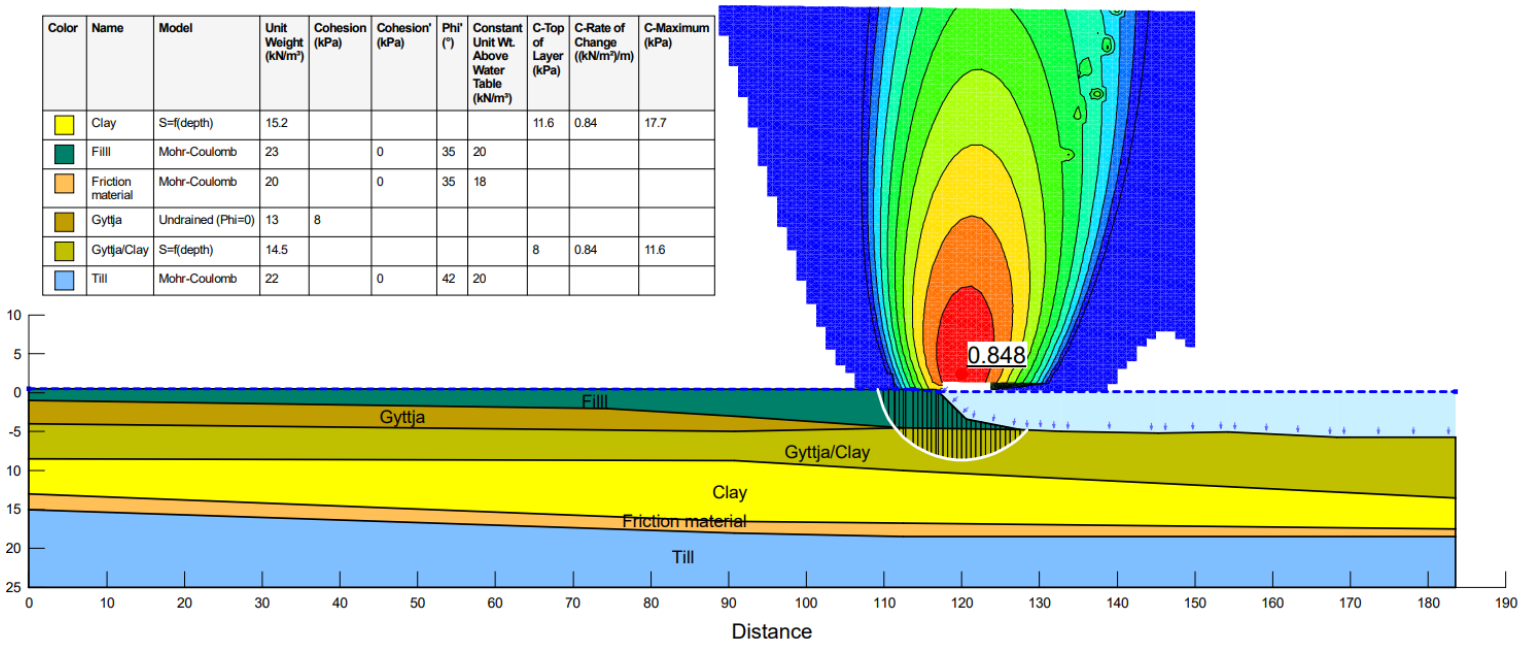

Figure G.1: Undrained analysis in Slope\W with the total safety method, case 1.

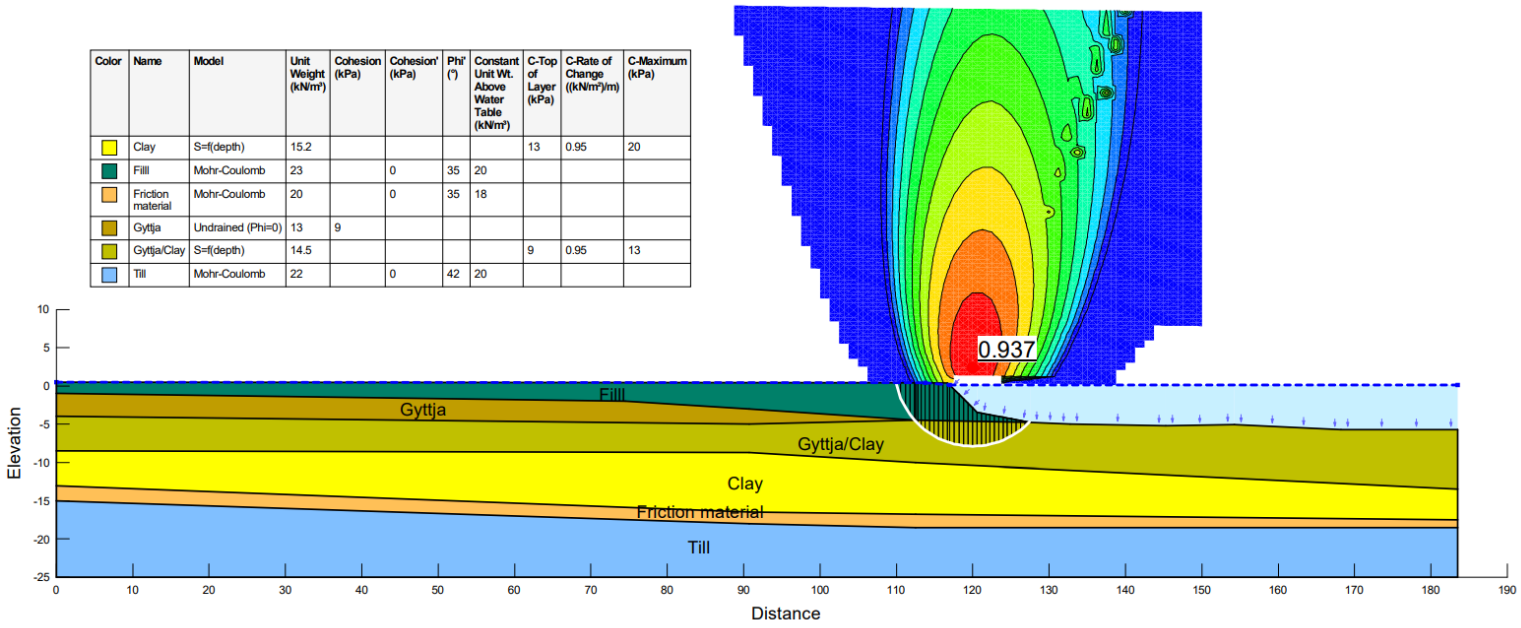

Figure G.2: Undrained analysis in Slope\W with the total safety method, case 2.

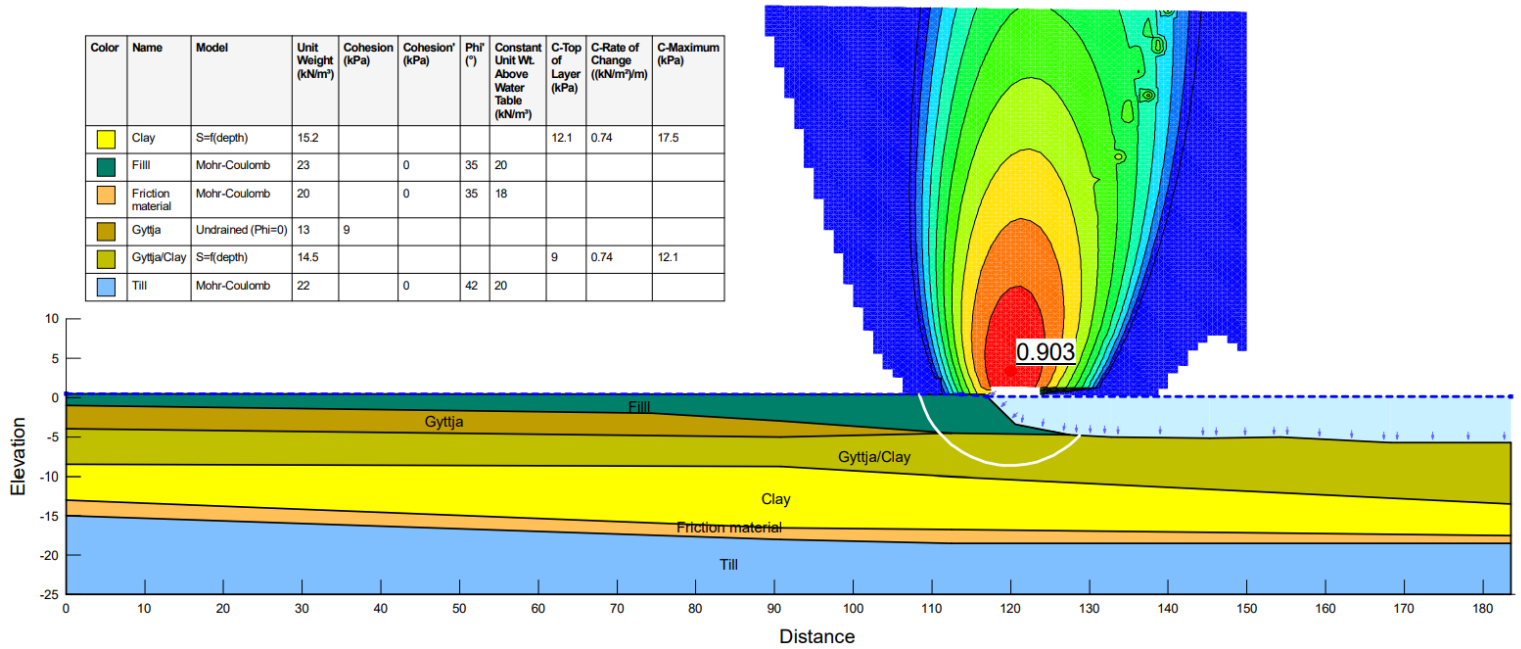

Figure G.3: Undrained analysis in Slope\W with the total safety method, case 3.

Color	Name	Model	Unit Weight (kN/m³)	Cohesion (kPa)	Cohesion' (kPa)	Phi' (°)	Constant Unit Wt. Above Water Table (kN/m³)	C-Top of Layer (kPa)	C-Rate of Change ((kN/m²)/m)	C-Maximum (kPa)
	Clay	S=f(depth)	15.2					13	0.95	19.9
	Fill	Mohr-Coulomb	23		0	35	20			
	Friction material	Mohr-Coulomb	20		0	35	18			
	Gyttja	Undrained (Phi=0)	13	9						
	Gyttja/Clay	S=f(depth)	14.5					9	0.95	13
	Till	Mohr-Coulomb	22		0	42	20			

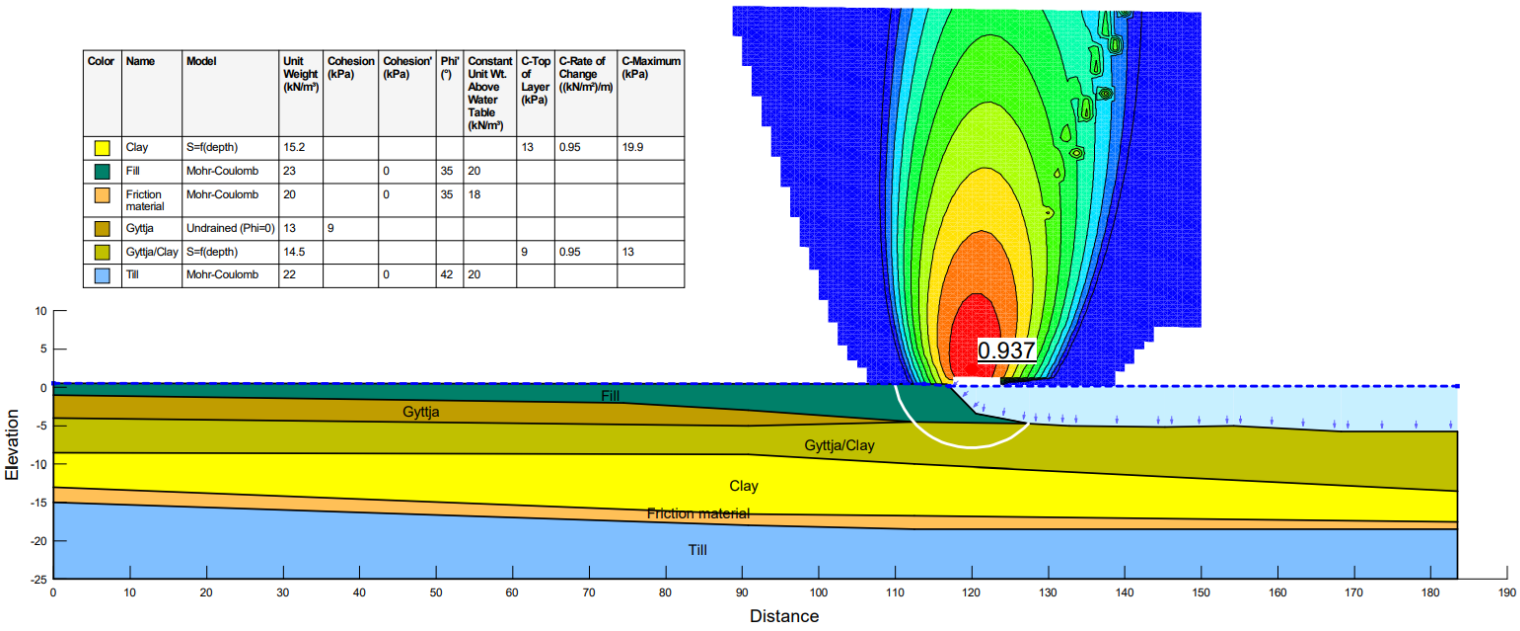

Figure G.4: Undrained analysis in Slope\W with the total safety method, case 4.

Color	Name	Model	Unit Weight (kN/m³)	Cohesion' (kPa)	Phi' (°)	Constant Unit Wt. Above Water Table (kN/m³)	C-Top of Layer (kPa)	C-Rate of Change ((kN/m²)/m)	Cu-Top of Layer (kPa)	Cu-Rate of Change ((kN/m²)/m)	C/Cu Ratio
	Clay comb.	Combined, S=f(depth)	15.2		30		1.16	0.084	11.6	0.84	0.1
	Filll	Mohr-Coulomb	23	0	35	20					
	Friction material	Mohr-Coulomb	20	0	35	18					
	Gyttja comb.	Combined, S=f(depth)	13		25		0.8	0	8	0	0.1
	Gyttja/clay comb.	Combined, S=f(depth)	14.5		25		0.8	0.084	8	0.84	0.1
	Till	Mohr-Coulomb	22	0	42	20					

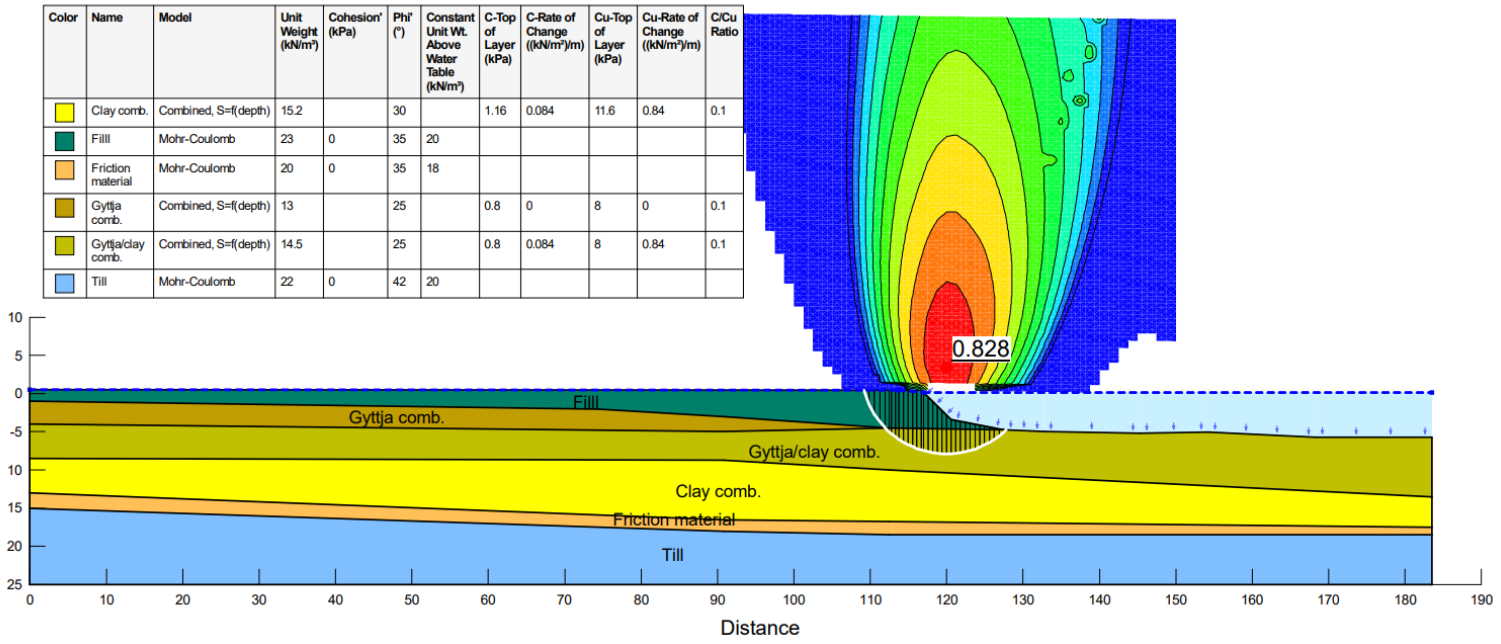

Figure G.5: Combined analysis in Slope\W with the total safety method, case 1.

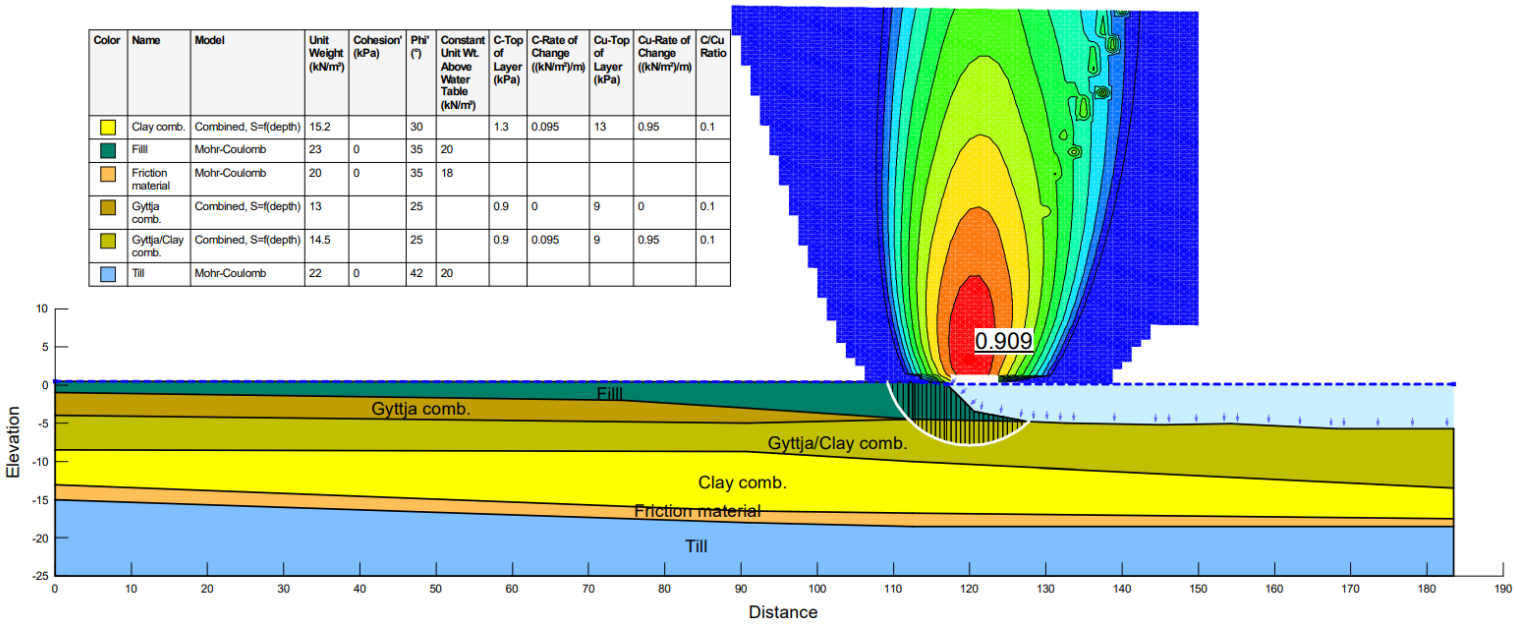

Figure G.6: Combined analysis in Slope\W with the total safety method, case 2.

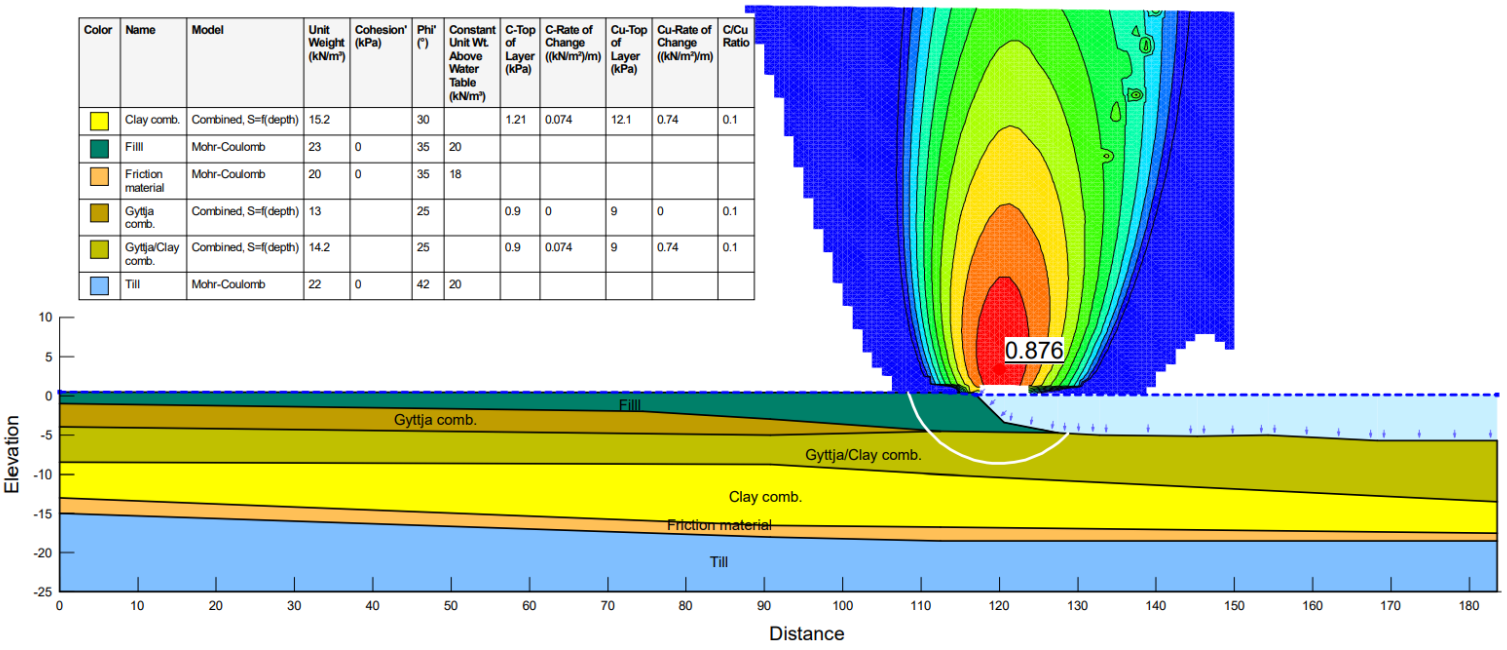

Figure G.7: Combined analysis in Slope\W with the total safety method, case 3.

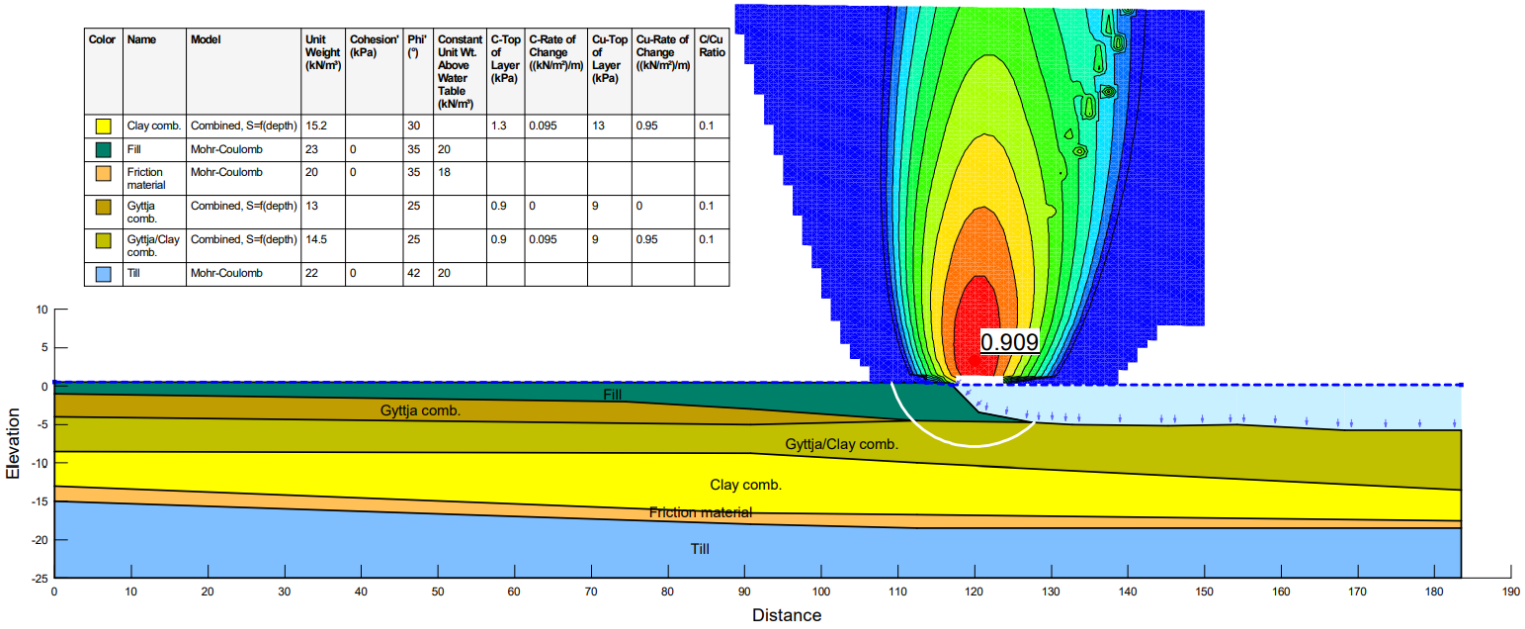

Figure G.8: Combined analysis in Slope\W with the total safety method, case 4.

H

Stability analysis using the partial safety factor method

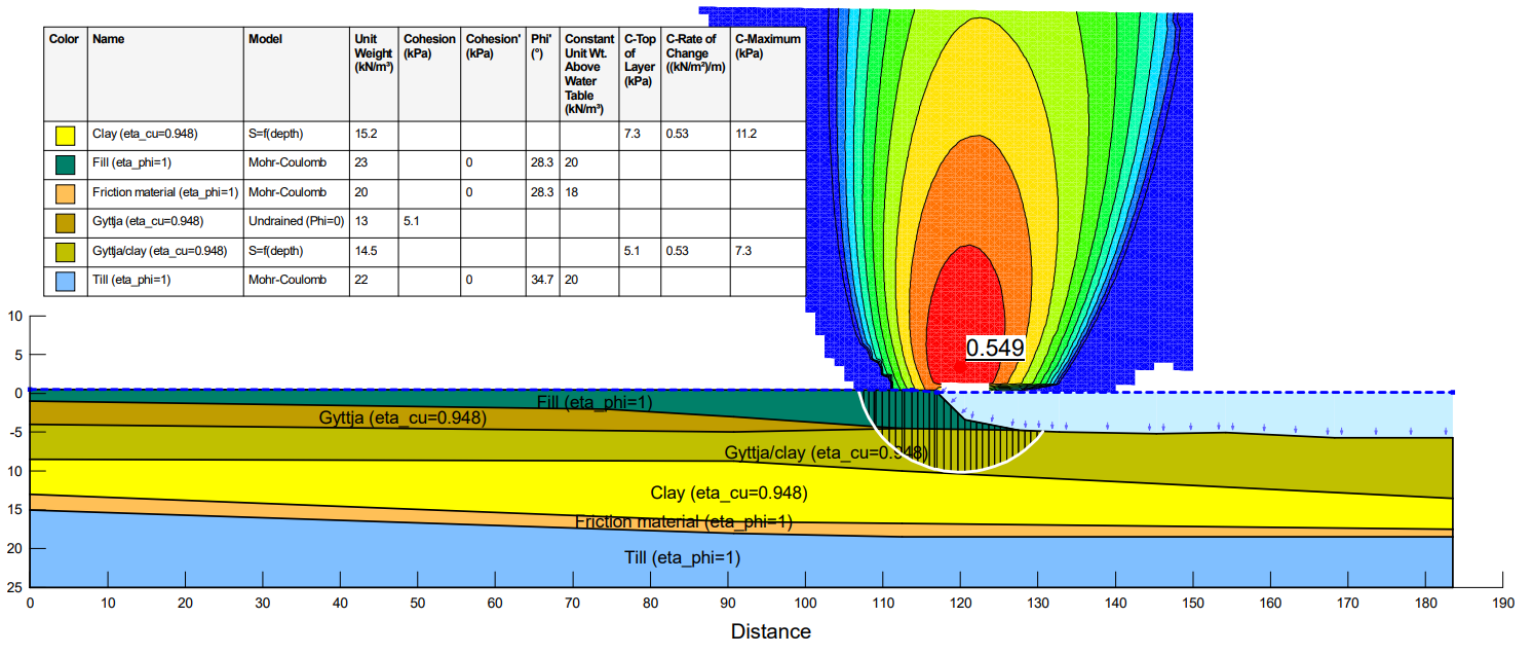

Figure H.1: Undrained analysis in Slope\W with the partial safety factor method, case 1.

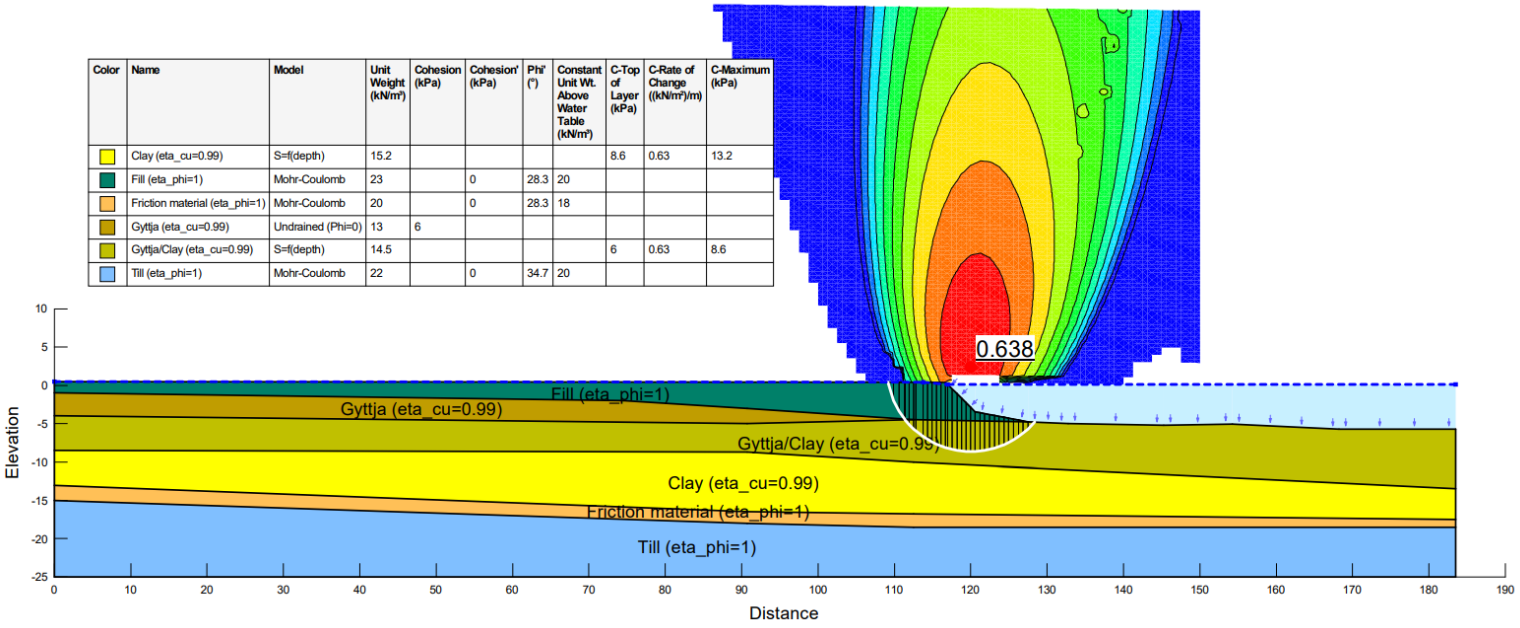

Figure H.2: Undrained analysis in Slope\W with the partial safety factor method, case 2.

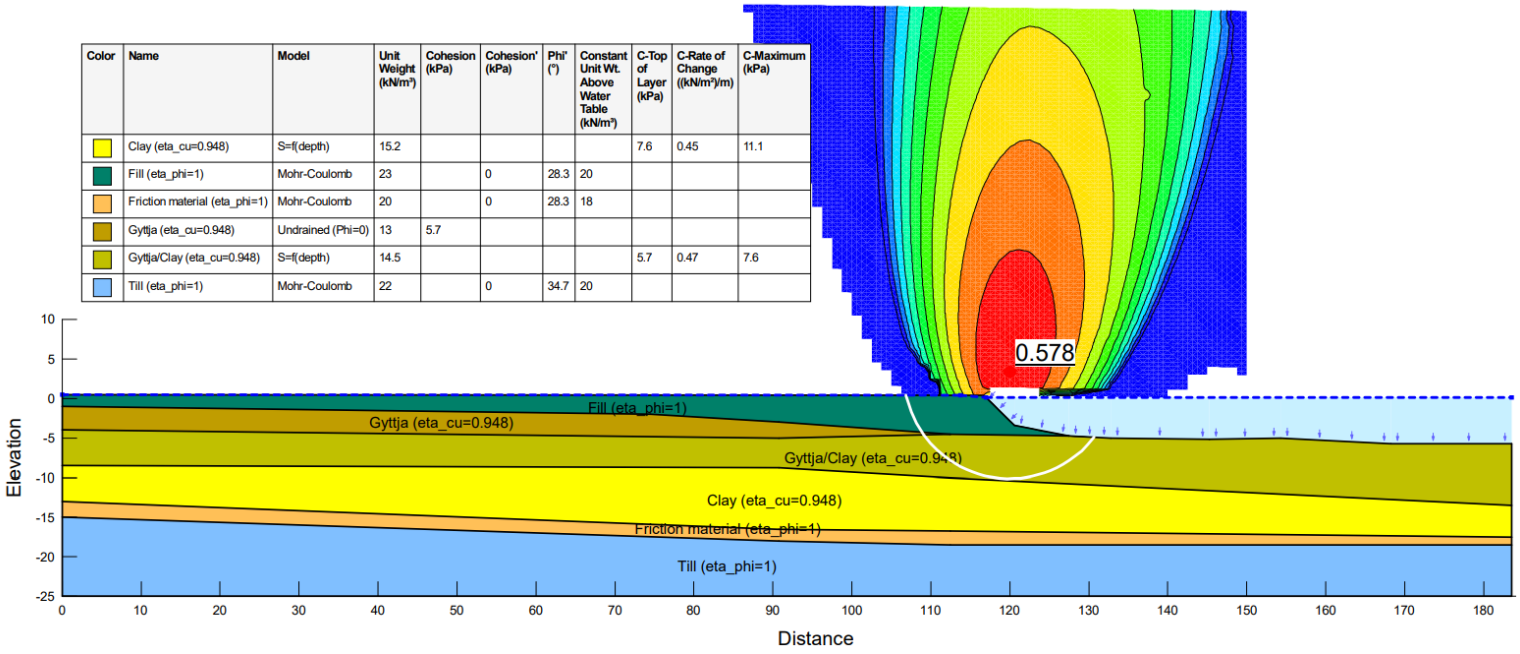

Figure H.3: Undrained analysis in Slope\W with the partial safety factor method, case 3.

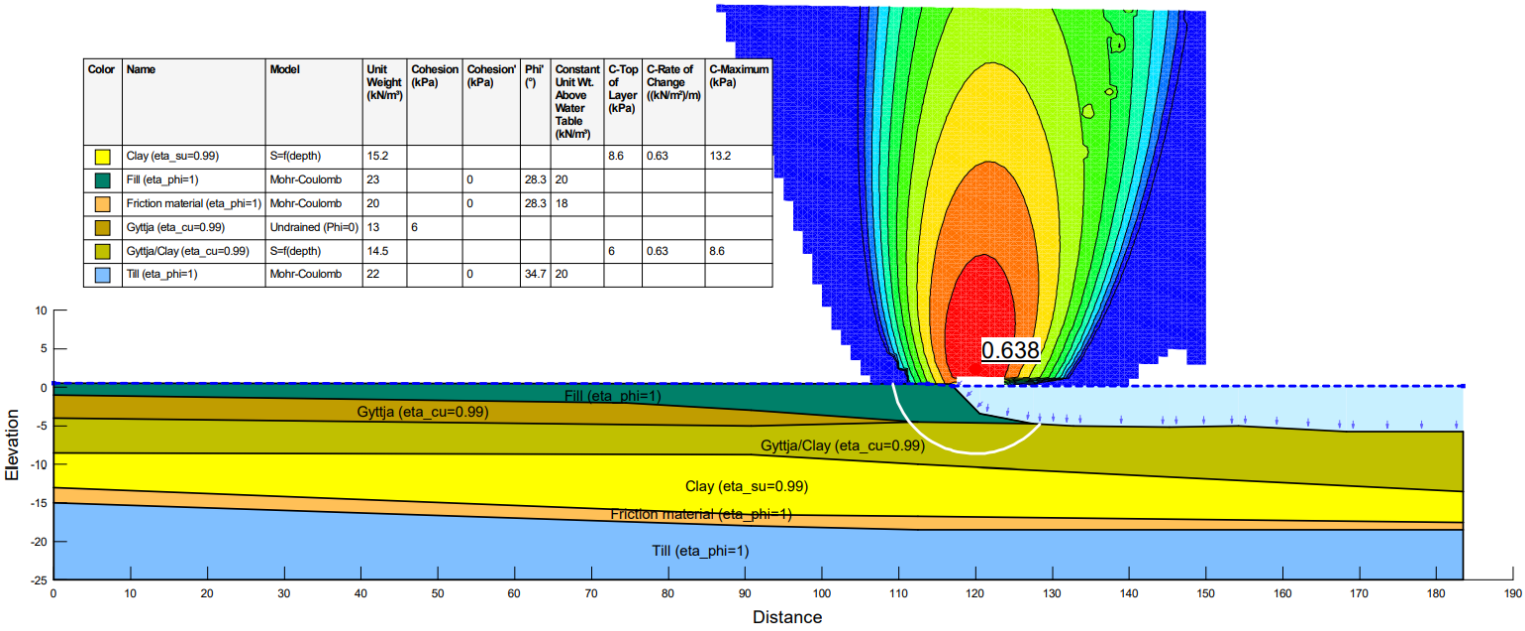

Figure H.4: Undrained analysis in Slope\W with the partial safety factor method, case 4.

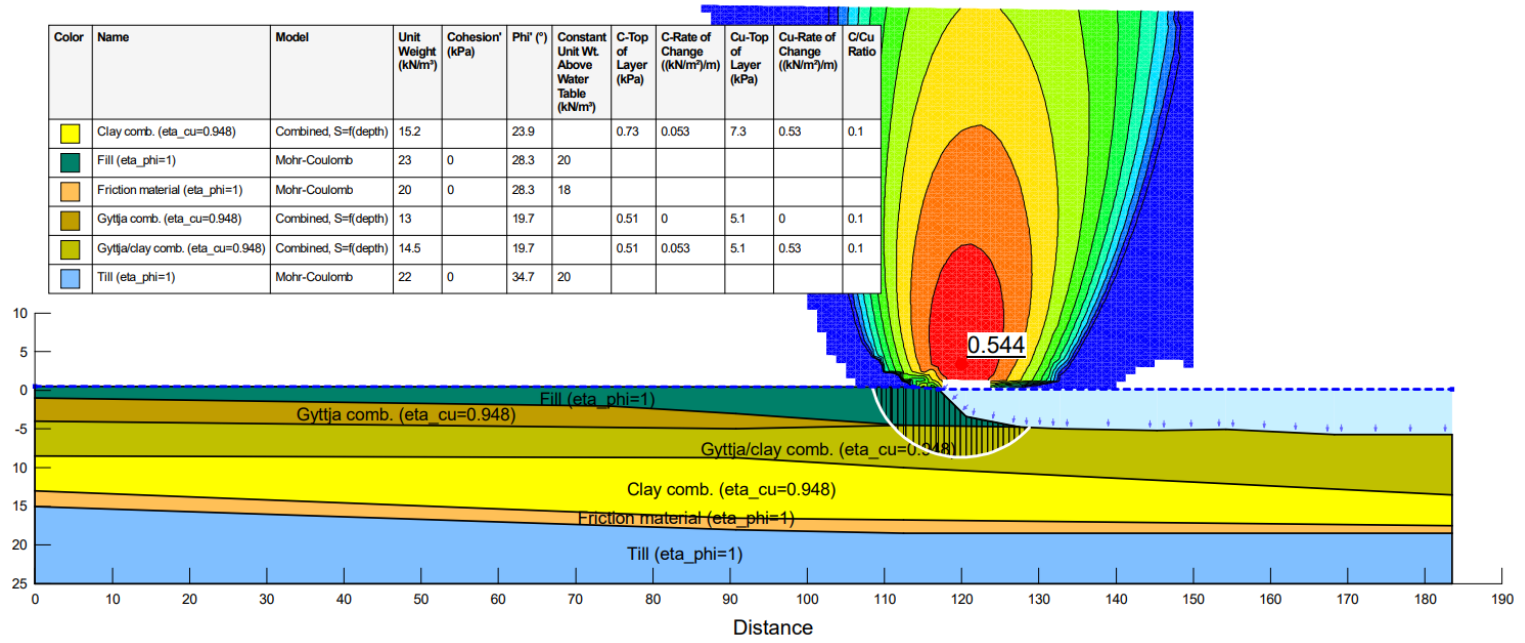

Figure H.5: Combined analysis in Slope\W with the partial safety factor method, case 1.

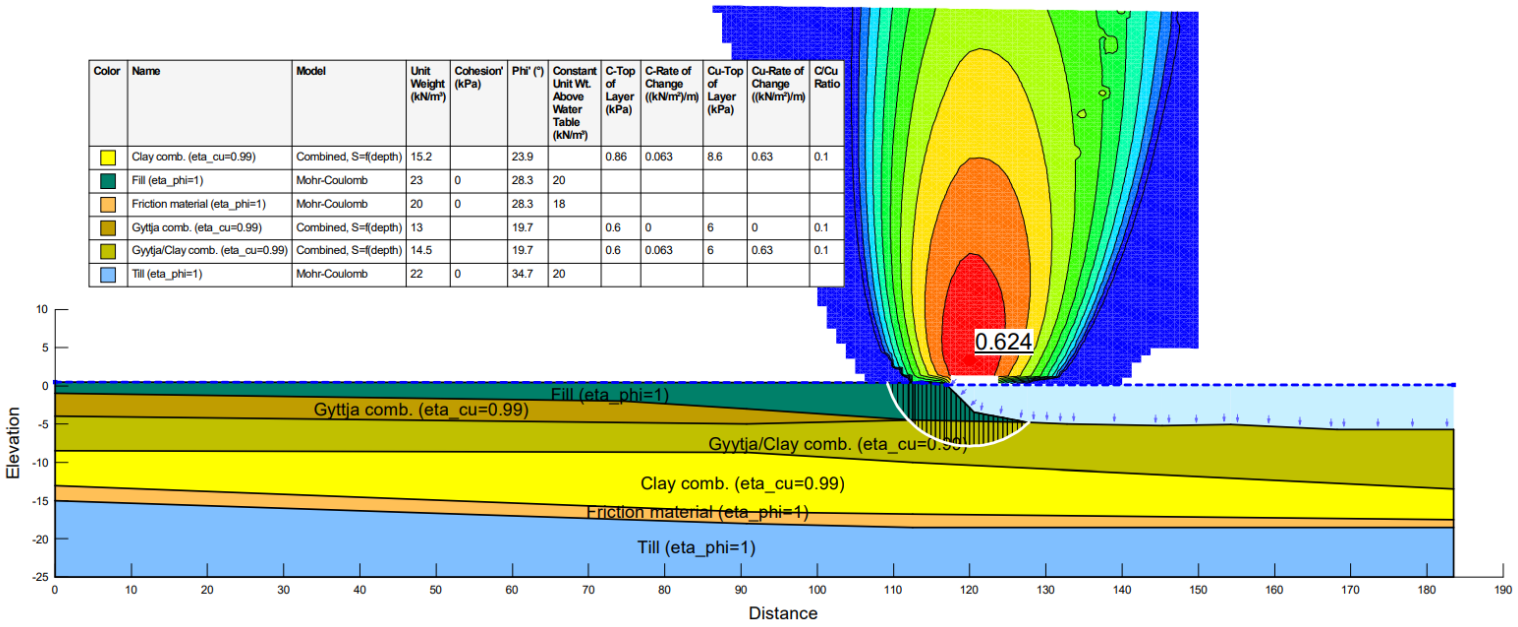

Figure H.6: Combined analysis in Slope\W with the partial safety factor method, case 2.

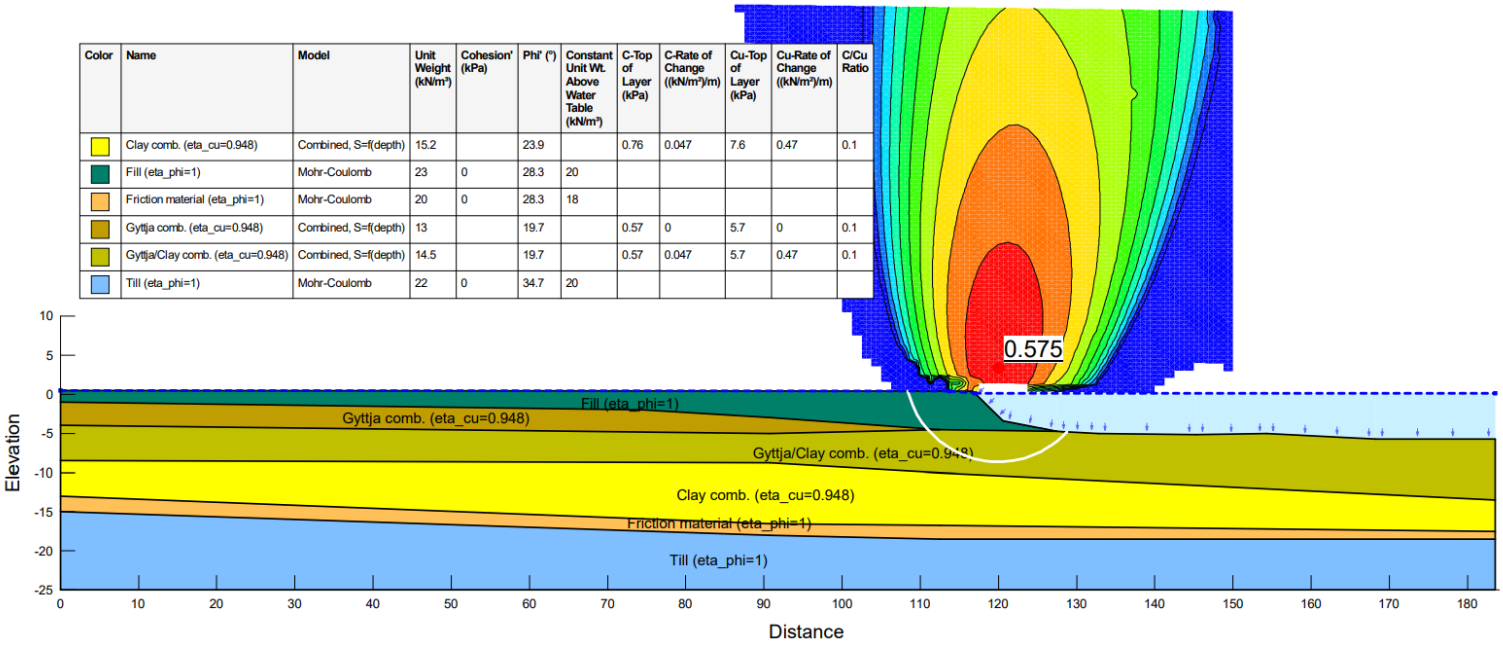

Figure H.7: Combined analysis in Slope\W with the partial safety factor method, case 3.

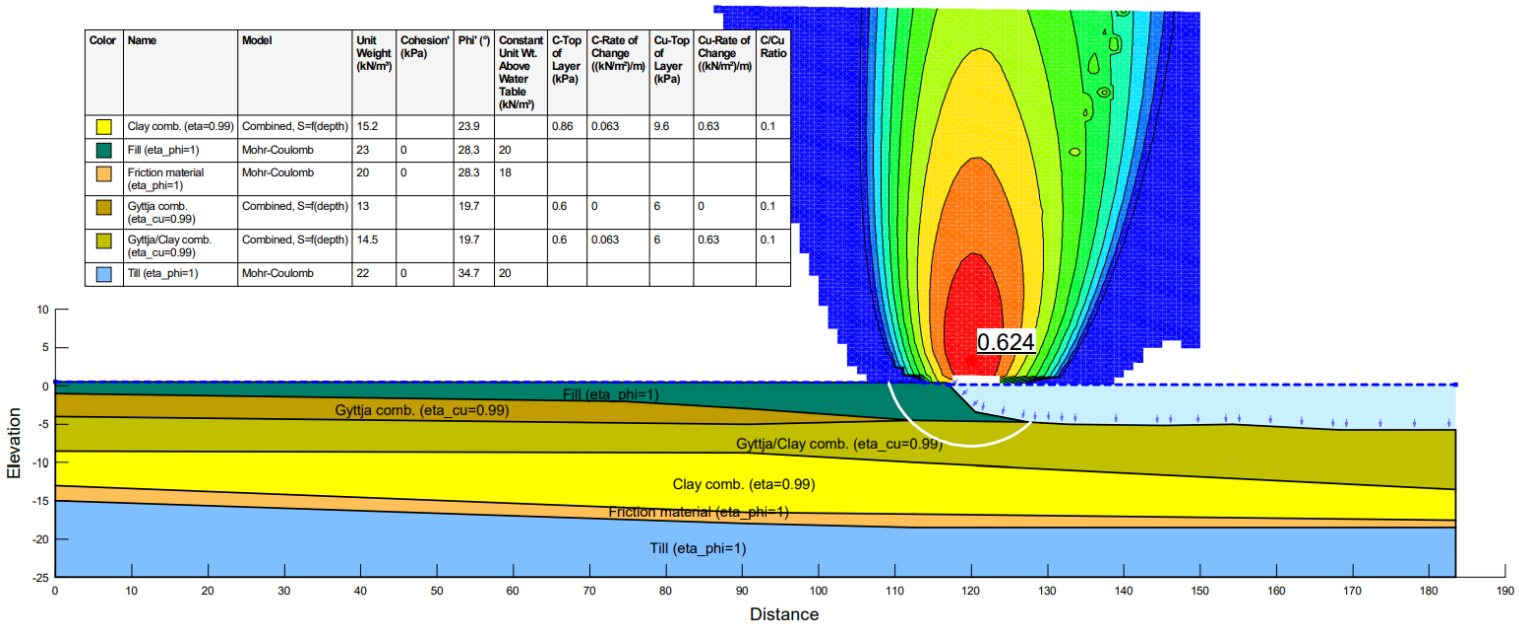

Figure H.8: Combined analysis in Slope\W with the partial safety factor method, case 4.

I

Additional Plaxis results with the MC model.

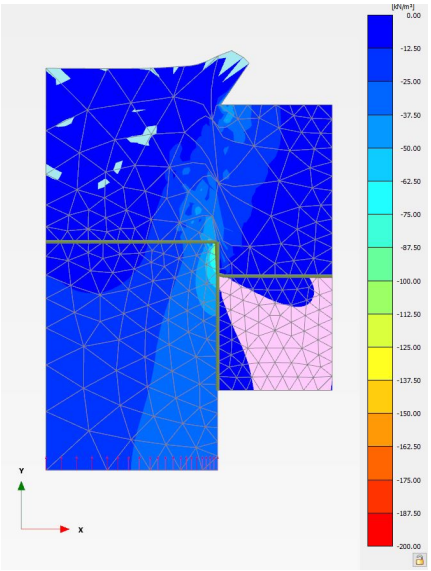

(a) Vertcial total cartesian stress for soil specimen *23AW03 6m*.

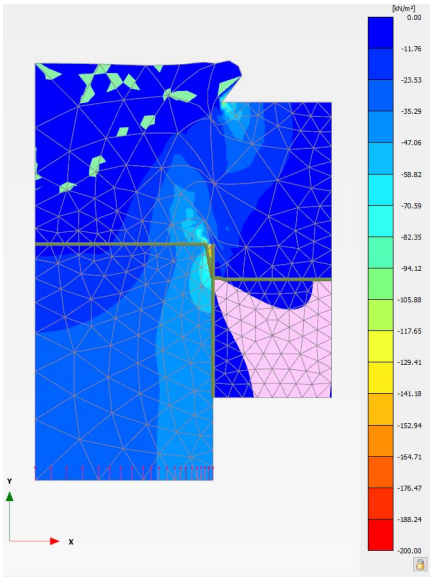

(b) Vertical total cartesian stress for soil specimen *23AW04 3m*.

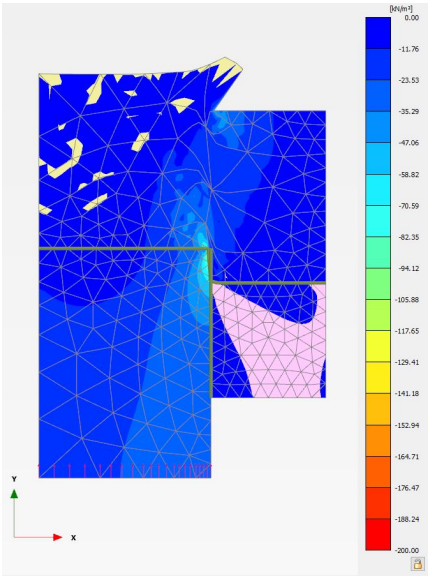

(c) Vertical total cartesian stress for soil specimen *23AW04 5m*.

XXX
Figure I.1: Vertical total cartesian stress, σ_{yy}, in Plaxis 2D after 3 mm deformation.

J

Additional Plaxis results with the SS model.

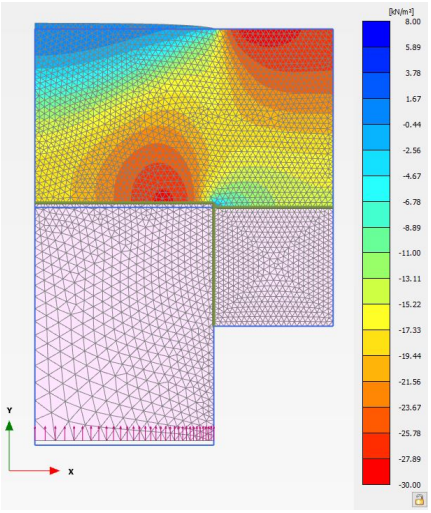

(a) Maximum excess pore pressure for soil specimen *23AW03 6m*, classified as Clsoil (fsa).

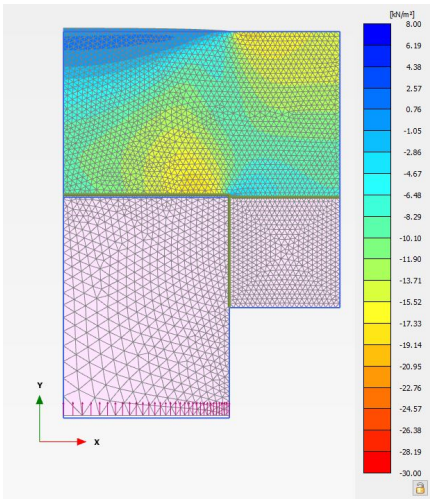

(b) Maximum excess pore pressure for soil specimen *23AW04 3m*, classified as clGy pr.

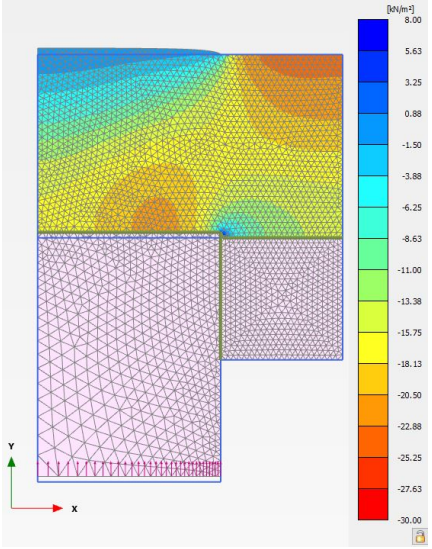

(c) Maximum excess pore pressure for soil specimen *23AW04 5m*, classified as Cl su.

Figure J.1: Maximum excess pore pressure, p_{excess}, in Plaxis 2D for each soil specimen

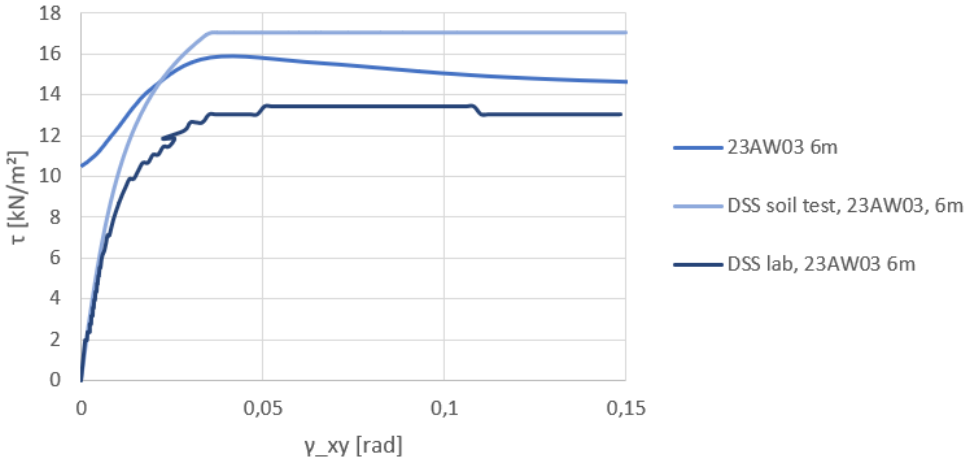

(a) Shear strength and strain for *23AW03 6m*, classified as Cl (fsa).

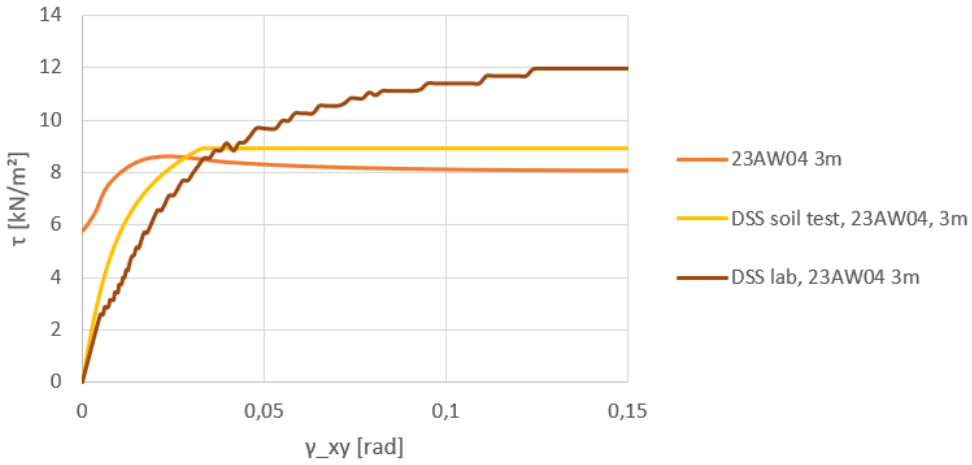

(b) Shear strength and strain for *23AW04 3m*, classified as clGy pr.

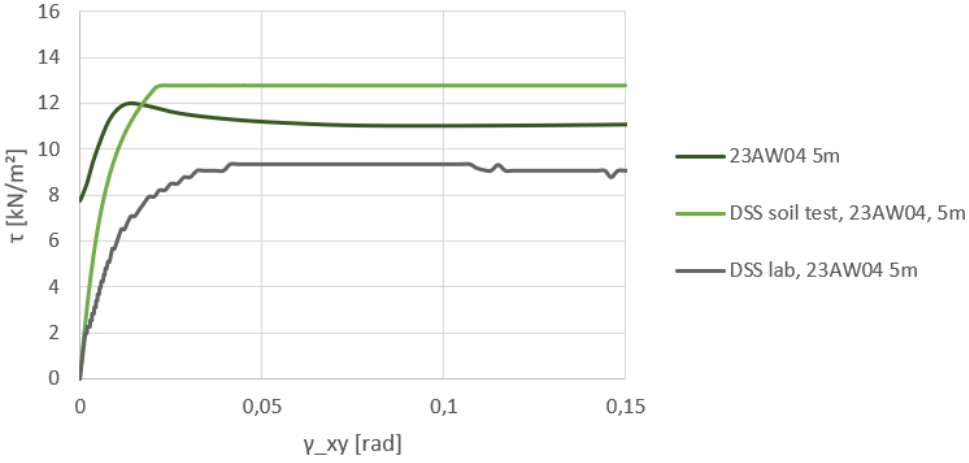

(c) Shear strength and strain for *23AW04 5m*, classified as Cl su.

Figure J.2: Shear strength and strain plotted from a single point in the shear zone in the Plaxis model, from the Plaxis DSS Lab Test tool and from a DSS test conducted in the SGI laboratory.

DEPARTMENT OF ARCHITECTURE AND CIVIL ENGINEERING
CHALMERS UNIVERSITY OF TECHNOLOGY
Gothenburg, Sweden
www.chalmers.se

CHALMERS
UNIVERSITY OF TECHNOLOGY